

## 6. SITE 708<sup>1</sup>

### Shipboard Scientific Party<sup>2</sup>

#### HOLE 708A

**Date occupied:** 0215 L, 3 June 1987

**Date departed:** 0230 L, 4 June 1987

**Time on hole:** 24 hr, 15 min

**Position:** 05°27.35' S, 59°56.63' E

**Water depth (sea level; corrected m, echo-sounding):** 4109.3

**Water depth (rig floor; corrected m, echo-sounding):** 4120.8

**Bottom felt (m, drill pipe):** 4107.0

**Penetration (m):** 236.2

**Number of cores:** 25

**Total length of cored section (m):** 236.2

**Total core recovered (m):** 189.7

**Core recovery (%):** 80.3

**Oldest sediment cored:**

Depth (mbsf): 234.7

Nature: nannofossil chalk

Age: early Oligocene

Measured velocity (km/s): 1.555

**Principal results:** Site 708 is located in the western equatorial Indian Ocean at 5°27.35' S and 59°56.63' E at a water depth of 4096.5 m (Fig. 1). The Seychelles Bank, which forms the northwestern extreme of the Mascarene Plateau, descends from water depths of less than 200 m to just over 4000 m along its eastern rim. The transition from bank to abyssal plain occurs over 60 nmi or less, and Site 708 lies 60 nmi further out on the abyssal plain, toward the Carlsberg Ridge. Sediment completely covers the undulating basement relief, and the present seafloor shows a virtually featureless topography. Total sediment accumulation amounts to about 600 m in the basement depressions and half that figure over the basement highs. Because the ocean crust was formed during Paleocene times in the area of Site 708 (Schlich, 1982), this indicates an average sedimentation rate on the order of 10 m/m.y.

The water depth at Site 708 (4096.5 m) places it toward the deeper end of the carbonate depth profile. Our major objective for drilling at this site was to recover a complete Neogene sequence in order to study the time-dependent dissolution of the slowly accumulating pelagic carbonate as a function of water depth. Biogenic carbonate dissolves when deep waters are undersaturated with respect to calcite, and Site 708 was drilled at a depth approaching two critical chemical boundaries in the water column, namely, the lysocline and the carbonate-compensation depth (CCD). Thus, vertical fluctuations of these boundaries through time reflect changes in the ocean chemistry which (1) are largely driven by climate-induced changes in the deep-ocean circulation, but (2) are also influenced by productivity changes and consequently the rain rate of pelagic carbonate. Because of the proximity of Site 708 to the lysocline and CCD boundaries, we can take advantage of the pronounced time-dependent variability in carbonate preservation here to model the interact-

ing system of carbonate flux/dissolution and climate-induced changes in the deep-ocean circulation.

We drilled Hole 708A to a total depth of 236.2 mbsf, yielding a recovery of 80.3%. Of the 25 cores taken, only the uppermost 8 were retrieved with the advanced hydraulic piston corer (APC), the remaining with the extended core barrel (XCB). Only one hole was drilled because the cored sediments reveal a history of alternating pelagic and turbidite deposition. About 25% of the entire sequence consisted of turbidites, accounting only for those exceeding 0.4 m in thickness. Including all thinner turbidites would increase the turbidite percentage to about 35%. Turbidites occurred in all 25 cores, and the shelf character of the benthic foraminifer assemblages within the turbiditic sediments indicated that the Seychelles Bank is the most likely and prominent source area, located some 120 nmi to the west. Most of the turbidites contained stratigraphically disordered microfossil assemblages, although some turbidites did not show any sign of stratigraphic mixing. For example, one turbidite in Core 115-708A-15X, containing a pure late Paleocene nannofossil assemblage, was sandwiched into a pelagic sequence of middle Miocene age.

Whereas the lower boundaries of the turbidites almost without exception were sharp and easily recognizable, their upper boundaries usually graded into the overlying pelagic oozes. Measurements of whole-core magnetic susceptibility at 5-cm intervals, however, clearly revealed the upper boundaries of most turbidites because of their higher carbonate content (see "Paleomagnetism" section, this chapter). In fact, most of the variability in the magnetic susceptibility record at Site 708 is caused by the alternating modes of turbidite and pelagic deposition.

We recognized three major lithologic units in the pelagic sediments, based on differences in color and lithology:

Unit I (0–111.0 mbsf) is divided into two subunits (IA and IB). Subunit IA (0–56.8 mbsf) is dominated by white to light gray foraminifer-bearing nannofossil ooze. Subunit IB (56.8–111.0 mbsf) contains sediments which are consistently darker than Subunit IA and consists of foraminifer-bearing nannofossil ooze which occasionally is relatively clay rich. Unit I sediments range in age from Pleistocene to late Miocene.

Unit II (111.0–178.2 mbsf) alternates between intervals of nannofossil ooze and dark-brown, clay-rich nannofossil ooze. This unit is characterized by its low carbonate content and ranges in age from late to early Miocene.

Unit III (178.2–236.2 mbsf) is dominated by white to pale brown nannofossil ooze and chalk. The oldest sediment is of early Oligocene age.

The cored stratigraphic sequence is summarized in Figure 2.

#### Summary of Interpretation

The clay-rich (40%–70% carbonate), turbidite-free, pelagic sediments provided measurable paleomagnetic field directions, but severe problems with magnetic overprint resulted in uninterpretable magnetostratigraphic signals. The time control therefore is based on biostratigraphy. On a turbidite-free basis, the biostratigraphy suggests sedimentation rates of approximately 10 m/m.y. from the Pleistocene back to about 9 Ma, followed (going downhole) by a stepwise reduction in rate to values between 1 and 3 m/m.y. for the late early and middle Miocene. The average sedimentation rate for the remaining part of the sequence, lower Miocene through most of the Oligocene, is estimated to be about 5 m/m.y.

Low-resolution analyses of carbonate content (1 sample/0.75 m; see "Geochemistry" section, this chapter) in the pelagic parts of the sequence yield values which oscillate roughly  $\pm 10\%$  around an average content of 70% during late Miocene through Pleistocene times. The middle Miocene is characterized by the most extreme variability,

<sup>1</sup> Backman, J., Duncan, R. A., et al., 1988. *Proc. ODP, Init. Repts.*, 115: College Station, TX (Ocean Drilling Program).

<sup>2</sup> Shipboard Scientific Party is as given in the list of Participants preceding the contents, with the addition of Isabella Premoli Silva and Silvia Spezzaferria, Dipartimento de Scienze della Terra, Università di Milano, Via Mangiagalli 34, I-20129 Milano, Italy.

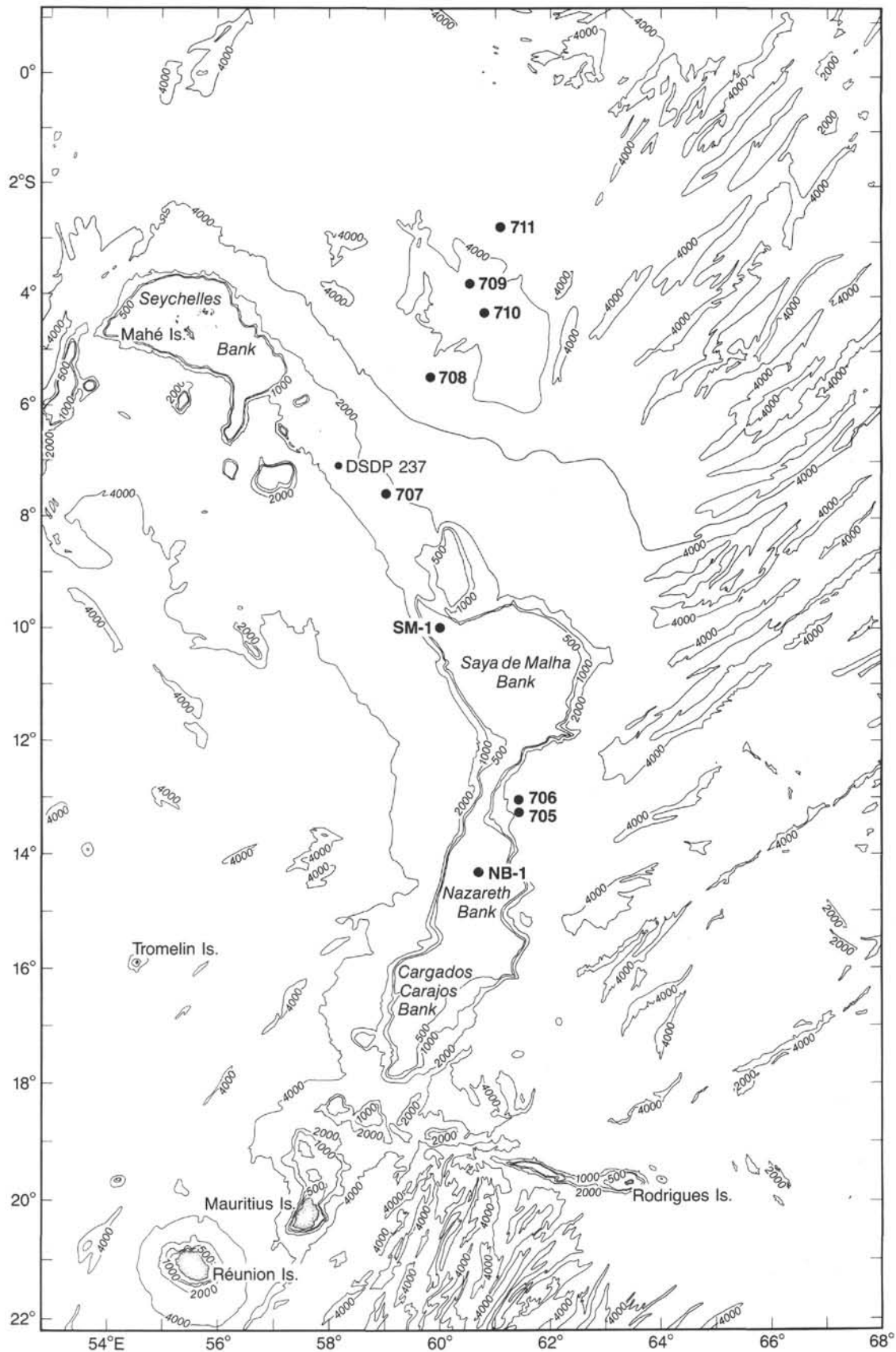


Figure 1. Bathymetric map of the western Indian Ocean (after Fisher et al., 1971) showing the location of Site 708 and other Leg 115 sites. Site 708 was drilled on the abyssal plain separating the Madingley Rise from the Seychelles-Saya de Malha banks. Depth in meters.

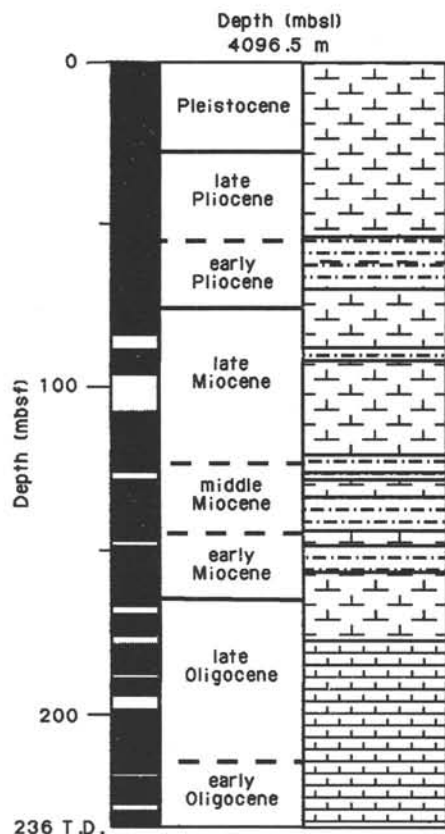


Figure 2. Stratigraphic summary of Site 708. Black column represents recovered section.

with values ranging from <1% to >80%, whereas the Oligocene shows the most stable values (around 90%). These changes in carbonate content also appear clearly in the color variation of the pelagic sediments, from white or gray Pliocene-Pleistocene and Oligocene nannofossil oozes to dark-brown, middle Miocene clays.

The chief causes for this pattern are at least threefold:

1. The thermal relaxation and subsidence of the ocean crust have transported the site with time into progressively deeper and more corrosive waters. Thus, the higher Oligocene carbonate percentages at Site 708 are partly due to the fact that the past location was closer to the ridge crest and therefore shallower.
2. The history of carbonate preservation at Site 708 also reveals a strong influence by another factor that operates on shorter time scales and is superimposed on the subsidence effect. This second, and more pronounced, influence presumably reflects variations in ocean chemistry as induced by changes in the Neogene climate.
3. Time-related variations in the supply of biogenic carbonate from the mixed layer would certainly have contributed to the observed pattern of carbonate preservation.

Preliminary estimates of bulk and carbonate sediment accumulation rates, calculated on a "turbidite-free" basis, are plotted vs. time in Figure 3. One should regard much of the detailed variability with caution because this figure was produced using shipboard biostratigraphic data and has not been updated for the *Initial Reports*. It is clear, however, that the largest differences between bulk and carbonate accumulation rates occurred during late Neogene times, that carbonate accumulation began to approach the bulk figures during early Miocene times, and that the Oligocene carbonate rates made up 90% of the bulk accumulation. The middle Miocene gap is caused partly by minimal recovery in two cores and partly by the very preliminary nature of the biostratigraphic control. We will present a more detailed analysis of sediment accumulation rates at this site in the *Scientific Results* of the ODP *Proceedings*.

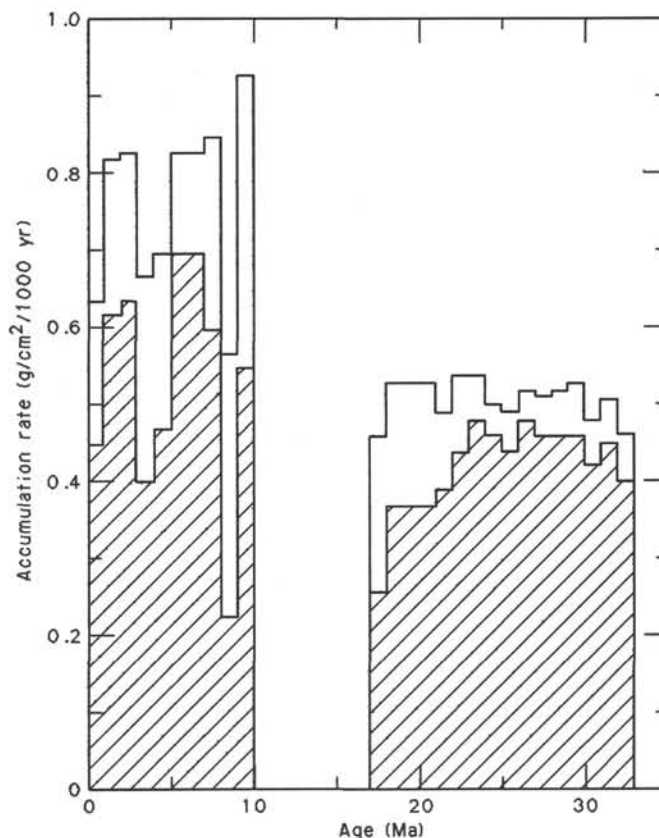


Figure 3. Mass accumulation rates of bulk sediment (unfilled area) and biogenic calcium carbonate (diagonal lines), on a "turbidite-free" basis, plotted vs. age at Site 708. The gap in the center of the graph is caused partly by the combined effects of poor recovery and slumps in this interval (which have been removed from the sequence), and partly by the limits of our preliminary shipboard biostratigraphy. The data represent mean values within 1-m.y. time increments.

## BACKGROUND AND OBJECTIVES

Site 708 is one of five sites in a transect drilled at different water depths from the Mascarene Plateau, the Madingley Rise, and surrounding abyssal plains (Fig. 4). The chapter on Site 707 gives the broader strategy for drilling this bathymetric transect (see "Background and Objectives" section, "Site 707" chapter, this volume). Site 708 is located toward the deeper end of the transect in water depths of 4096.5 m, on the abyssal plain due north of Site 707, and southwest of Madingley Rise, a regional topographic high rising about 1 km above the surrounding plains.

Our primary objective was to retrieve a stratigraphically continuous Neogene sequence so that we could quantify the processes which control the depth-dependent dissolution of biogenic carbonate through Neogene times in the western tropical Indian Ocean. At its present water depth of 4096.5 m, Site 708 lies between the modern foraminiferal lysocline and the carbonate-compensation depth (CCD). Thus, we expected to encounter considerable dissolution of the foraminifer microfossils and a bias of species compositions toward assemblages less susceptible to dissolution. We also expected a similar bias for the nannofossil assemblages, although perhaps not so strongly expressed as among the planktonic foraminiferal assemblages. The Pliocene-Pleistocene lysocline and CCD have anomalously deep positions when viewed with respect to the entire Cenozoic.

In the Indian Ocean, these chemical and depositional boundaries were positioned around 4000-m water depth through most

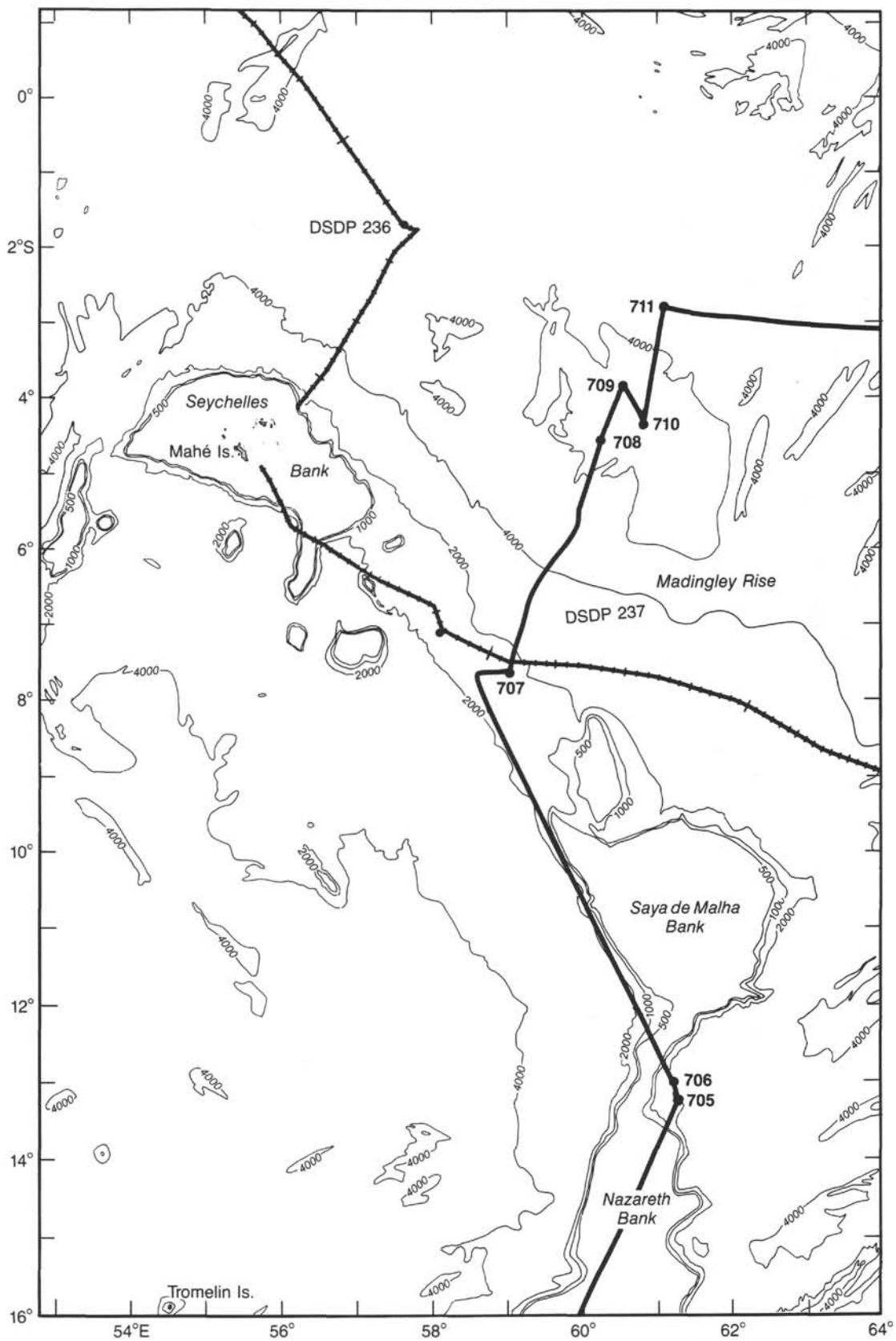


Figure 4. Expanded view of bathymetric conditions and geographic location of Site 708 (after Fisher, Bunce, et al., 1974). Shown for reference is the track line of the *Glomar Challenger* on DSDP Leg 24, as well as that of *JOIDES Resolution* on ODP Leg 115. Depth in meters.

of the Cenozoic, and they deepened during the middle Miocene to their present depths (van Andel, 1975). By correcting for the extent of subsidence through time, we hope to monitor the true variations in lysocline and CCD positions throughout the Neogene. The causal mechanisms for this variability should be found in changes in the Neogene climate and the corresponding effects of these changes on the deep-ocean circulation.

We can achieve these objectives only with precise time controls, without which we cannot establish meaningful cause-and-effect relationships. Other principal objectives of Leg 115, therefore, were (1) to increase the precision in the biostratigraphic correlation between different microfossil groups and (2) to calibrate useful datum events directly to magnetostratigraphy.

## OPERATIONS

### Site 708 Approach

The transit to Site 708 (target site CARB-4) was begun at 0330 hr, 2 June 1987. At 1700 hr, 2 June, we dropped the recallable beacon and established Site 708. The ship was in dynamic-positioning (DP) mode by 1800 hr.

### Hole 708A

A typical 6-drill-collar, APC/XCB bottom-hole assembly (BHA) with 1/2-in. angled jets in the bit and modified for the XCB with shoe-seal system was run to the seafloor. The mud line was established at 4096.5 m drill-pipe measurement (DPM), and eight APC cores were drilled to a depth of 4172.5 m (76 mbsf). Coring with the APC recovered 76.76 m for 100% recovery. On the last APC core, the pull-out force was 60,000 lb, and we decided to switch to the XCB system. The hole was advanced to 4332.7 m (236.2 mbsf), with 17 XCB cores recovering 112.9 m for a 71% recovery rate. At the request of the Co-Chiefs, we abandoned the hole. Total penetration was 236.2 mbsf to 4332.7 m with 189.7 m of core recovered for a total recovery rate of 80.3% (Table 1).

We began using a new "speeded-up coring" procedure with this site. In the new procedure, the sinker bars are left in the

drill string and are pumped down with the core barrel. This procedure reduced XCB-coring wireline trip times by approximately 40% from the time estimates given in the *Preliminary Time Estimates for Coring Operations* for XCB-coring wireline trips.

### Site 708 to Site 709 (CARB-2A)

We recalled the beacon and retrieved it at 0825 hr. The ship was under way for Site CARB-2A at 1200 hr, 4 June 1987.

## LITHOSTRATIGRAPHY

### Introduction

Site 708 is located on the abyssal plain between the Madingley Rise and the Seychelles Bank in water depths of 4096.5 m. In Site 708 sediments, turbidite layers interbedded with pelagic oozes. Components of the pelagic oozes are mainly nannofossils, clays, and radiolarians, whereas turbidites consist of nannofossil oozes containing fragments and whole tests of foraminifers and calcareous lithoclasts. The turbidites generally are normally graded. The minor components of both the turbidites and the pelagic sediments are diatoms, radiolarians, clay, and volcanic ash.

Discontinuous intervals of chalk begin to appear in Core 115-708A-21X, both in the turbidites and in the pelagic parts of the late Oligocene sequence. We identified a total of 197 turbidites, which varied in thickness from 1 to 335 cm. The average frequency of turbidites is one turbidite per meter of sediment and does not change systematically from top to bottom of the hole. Turbidites comprise about 35% of the recovered sediment in Hole 708A.

On the basis of major color and lithologic differences within the pelagic sediments, we differentiated three units. Two subunits further divide Unit I. These are described in detail in the following sections.

**Unit I: Cores 115-708A-1H to -8H and Cores 115-708A-9X to -12X (0-111.0 mbsf); Age: Pleistocene to late Miocene.**

*Subunit IA: Cores 115-708A-1H to -6H (0-56.8 mbsf).*

Subunit IA, 0-56.8 mbsf (Cores 115-708A-1H through -6H), is dominated by white to very light gray (N9 to 5Y 8/1) nannofossil ooze. The sediments at the top of Subunit IA are slightly coarser than the underlying nannofossil oozes and are the only sediments where diatoms are more abundant than 10%. Subunit IA is also unique in containing radiolarian-bearing nannofossil ooze as a minor lithology in Sample 115-708A-4H-6, 100 cm.

*Subunit IB: Cores 115-708A-7H to -8H and 115-708A-9X to -12X (56.8-111.0 mbsf).*

Subunit IB, 56.8-111.0 mbsf (Cores 115-708A-7H to -12X), consists of light greenish gray (5GY 7/1) to light gray (5Y 7/1) nannofossil oozes. Subunit IB contains more foraminifers than IA. Foraminifer-bearing nannofossil ooze occurs between the turbidites in Sections 115-708A-8H-3 through 115-708A-8H-6. This is the thickest interval of foraminifer-bearing nannofossil ooze occurring in the pelagic sediments in Hole 708A. Clay-bearing, foraminifer-bearing nannofossil oozes overlie this layer, and clay-bearing nannofossil oozes underlie it. A brownish stain coats many of the foraminifer tests.

**Unit II: Cores 115-708A-13X through -19X (111.0-178.2 mbsf); Age: late Miocene to early Miocene.**

Brown colors predominate in Unit II sediments. From the bottom to the top of the unit, the colors change from light olive

Table 1. Coring summary, Site 708.

Core no.	Date (June 1987)	Time (local)	Depth (mbsf)	Cored (m)	Recovered (m)	Recovery (%)
115-708A-						
1H	3	0230	0-9.0	9.0	8.93	98.9
2H	3	0345	9.0-18.6	9.6	9.43	98.2
3H	3	0430	18.6-28.1	9.5	9.63	101.0
4H	3	0530	28.1-37.6	9.5	9.90	104.0
5H	3	0630	37.6-47.2	9.6	9.17	95.5
6H	3	0745	47.2-56.8	9.6	10.09	105.1
7H	3	0830	56.8-66.4	9.6	9.86	103.0
8H	3	0915	66.4-76.0	9.6	9.75	101.0
9X	3	1030	76.0-82.1	6.1	3.37	55.2
10X	3	1115	82.1-91.7	9.6	3.62	37.7
11X	3	1200	91.7-101.4	9.7	0.05	0.5
12X	3	1300	101.4-111.0	9.6	8.46	88.1
13X	3	1400	111.0-120.6	9.6	6.57	68.4
14X	3	1615	120.6-130.3	9.7	9.63	99.3
15X	3	1715	130.3-140.0	9.7	8.44	87.0
16X	3	1815	140.0-149.6	9.6	9.73	101.0
17X	3	1915	149.6-159.3	9.7	7.20	74.2
18X	3	2015	159.3-168.6	9.3	5.31	57.1
19X	3	2115	168.6-178.2	9.6	5.48	57.1
20X	3	2200	178.2-187.9	9.7	7.44	76.7
21X	3	2300	187.9-197.5	9.6	3.50	36.4
22X	4	0000	197.5-207.1	9.6	9.18	95.6
23X	4	0045	207.1-216.8	9.7	8.78	90.5
24X	4	0130	216.8-226.5	9.7	7.93	81.7
25X	4	0230	226.5-236.2	9.7	8.27	85.2

brown (2.5Y 5/4) and light gray (2.5Y 7/2) to olive brown (2.5Y 4/4), then to light yellowish brown (2.5Y 6/4) and brown (10YR 5/3) in the top three cores. The lithologies alternate between intervals of pure nannofossil oozes and oozes that contain more clay and foraminifers. Sediments in Sections 115-708A-14X-1 through 115-708A-14X-6 are clay-bearing, foraminifer-bearing nannofossil oozes. This interval coincides with a zone of very low carbonate content (see "Geochemistry" section, this chapter).

**Unit III: Cores 115-708A-20X through -25X (178.2–236.2 mbsf); Age: early Miocene to early Oligocene.**

Unit III sediments are characteristically white (10YR 9/2) to very pale brown (10YR 8/3) nannofossil oozes and chalks. A 5-cm-thick layer of gray (N6) nannofossil chalk is present in Sample 115-708A-23X-4, 130–135 cm.

### Turbidites

The most striking aspect of the sediment in Hole 708A is the large number of turbidites, dominated by white (10YR 8/2, N9) colors, alternating with layers of darker pelagic sediments, dominated by light gray (5Y 7/1), light greenish gray (5GY 7/1), and pale brown (10YR 8/3) colors. We recognized many of the turbidites by the sharp color change at their basal boundary (Fig. 5).

The average thickness of the 197 turbidites we observed is 38 cm, but they range from 1 to 335 cm. The distribution of these turbidites is shown in Figure 6. Estimating turbidite thickness is not easy due to the gradational upper boundary. The thickest turbidite layer is between Sample 115-708A-3H-1, 40 cm, and Sample 115-708A-3H-3, 130 cm, and is a foraminifer-bearing nannofossil ooze, whitish gray (5Y 8/1) at the bottom and grading to white (N8 and N9) toward the top. The bottom 3 cm of the turbidite section consists of foraminifer-nannofossil ooze, light greenish gray (5GY 7/1) in color, and containing limestone fragments and glauconite of sand size to very coarse sand size. A smear slide taken at the bottom of this turbidite layer (Sample 115-708A-3H-3, 25 cm) contains nannofossil ooze with an estimated 20% sand-sized fragments consisting of foraminifers, molluscan fragments, radiolarians, and sponge spicules.

### Minor Constituents in Turbidites and Pelagic Sediments

In the upper six cores of Hole 708A, coarse grains at the base of the turbidites are occasionally (iron sulfide?) stained, light gray (N7) or gray (N6). We counted 17 such thin dark zones in the upper six cores, but none below. Radiolarians were estimated to account for 5% of the sediments throughout most of the hole. In the upper six cores, diatoms comprise about 3% of the sediments.

### Sedimentary Environment

The nearby Madingley Rise probably gave rise to the thick sequences of foraminifer-bearing turbidites. The occurrence of aragonite in 2 of the 10 turbidites analyzed suggests sediment transport from a more distant and shallower water source (see "Geochemistry" section, this chapter). It is possible that these sediments came from shallow carbonate banks, such as the Seychelles Bank 200 km to the west.

## BIOSTRATIGRAPHY

### Introduction

The sedimentary sequence recovered at Site 708 is characterized by the presence of numerous turbidites. Despite the inclusion of much reworked material throughout the sequence, the

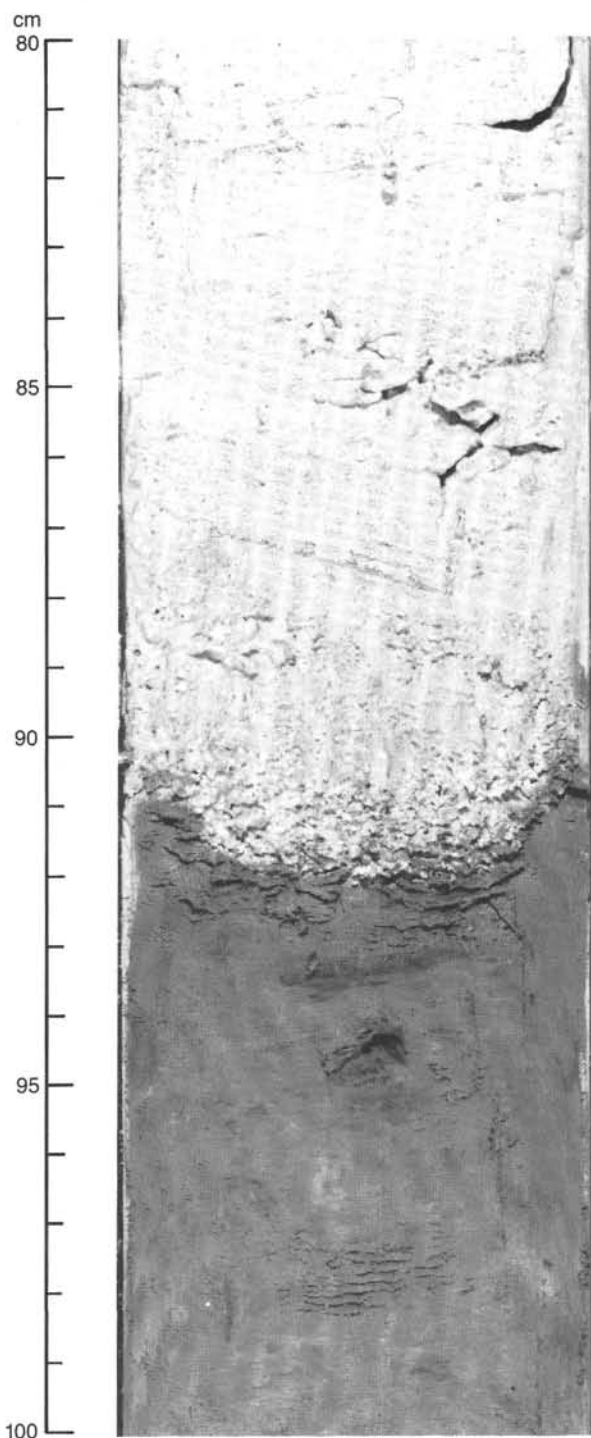


Figure 5. Pelagic/turbidite sediment sequence showing a typical sharp contact between the very light-colored, coarse-grained turbidite and the dark pelagic nannofossil ooze (Section 115-708A-18X-2, 80–100 cm).

biostratigraphy is relatively well ordered, and all of the major microfossil groups are represented with varying degrees of abundance and preservation.

Calcareous nannofossils are abundant and well preserved in the nonturbidite sequences of the Pleistocene. Reworking characterizes the Pliocene-Pleistocene assemblages, especially in turbidite sequences, obscuring the true range of the zonal marker species. The Miocene floras record several intervals in which the

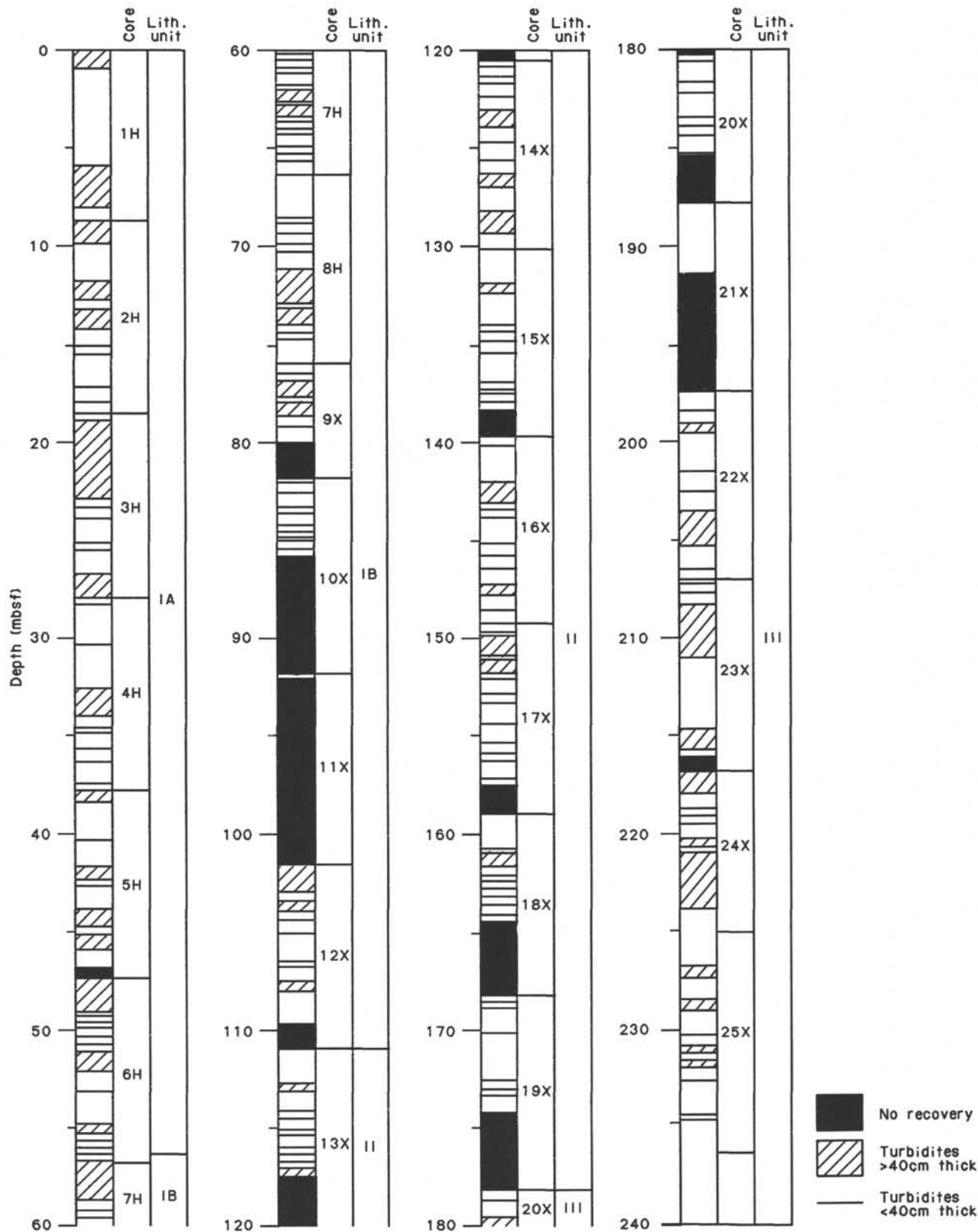


Figure 6. The distribution of turbidites within Hole 708A. Also shown are the lithologic units defined at Site 708.

coccoliths are poorly preserved. The Oligocene coccolith assemblages are diversified and generally well to moderately well preserved.

Planktonic foraminifers show pronounced dissolution throughout the Neogene section, where they are rare and highly

fragmented. In the Paleogene section, only a few, poorly preserved planktonic foraminifers of late Oligocene age are present.

Benthic foraminifers are well to moderately well preserved in the Pliocene-Pleistocene interval. The pre-Pliocene assemblages

are moderately well to poorly preserved; they often have a component of either redeposited shelf-carbonate benthic foraminifers or a fauna from an upper to middle bathyal environment. Several intervals of the Miocene are barren of benthic foraminifers as a result of the proximity to the foraminifer compensation depth. The Oligocene faunas are badly preserved and characterized by small and uncommon specimens.

Radiolarians are common and well preserved in the Pleistocene, few and moderately well preserved in the upper Pliocene, and again common and well preserved in the lower Pliocene and upper Miocene. The lower Miocene and upper Oligocene contain rare and poorly preserved radiolarians, which become common and moderately preserved in the lower Oligocene.

Diatoms are present only in the Pleistocene to upper Miocene interval, where they are common and moderately preserved. They are, however, rare and highly dissolved in the upper Pliocene, with a slight increase in abundance and preservation in the lower Pliocene. The uppermost Miocene flora are poorly preserved. No diatoms are present in the pre-upper Miocene section, except for a scattered distribution in the Paleogene.

A biostratigraphic summary for Hole 708A is presented in Figure 7.

### Calcareous Nannofossils

We recovered Pleistocene to upper Oligocene nannofossil assemblages from Hole 708A. Although the nannofossils are moderately to badly corroded, we were able to identify most age-diagnostic species and almost all zones. Because of the frequent occurrences of turbidites, reworked Paleocene to Pliocene forms are also abundant in some intervals.

#### Pleistocene

The Pleistocene nannofossils suffered relatively little dissolution. Although turbidites contain reworked fossils, sediment between turbidites is relatively free of reworked forms. The uppermost turbidite recovered in Sections 115-708A-1H-1 and 115-708A-1H-2 contains common *Pseudoemiliania lacunosa*, but *Emiliania huxleyi* was not observed. Moderately dissolved coccoliths recognized as *E. huxleyi* are common in Samples 115-708A-1H-2, 110 cm, and 115-707A-1H-3, 42–43 cm. We tentatively assigned these two samples, therefore, to the uppermost Quaternary Zone CN15.

We can assign the interval between Samples 115-708A-1H-3, 120 cm, and 115-708A-1H-4, 110 cm, to Subzone CN14b. Due to the heavy reworking, the last occurrence (LO) of *P. lacunosa* (base of Subzone CN14b) is difficult to locate. Samples 115-708A-1H-5, 40 cm, and 115-708A-1H-5, 140 cm, yielded abundant *P. lacunosa*, but the presence of such abundant reworked fossils as *Calcidiscus macintyreii*, *Cyclicargolithus floridanus*, *Discoaster brouweri*, *D. pentaradiatus*, and *Reticulofenestra pseudoumbilica* was also recognized in these two samples. Sample 115-708A-1H-6, 90 cm, which yielded common *P. lacunosa* but no reworked specimens, is referred to Subzone CN14a. The base of Subzone CN14b, therefore, is likely to be located within or very close to Section 115-708A-1H-5.

The top of the small *Gephyrocapsa* Zone of Gartner (1977) can be placed between Samples 115-708A-2H-6, 42 cm, and 115-708A-2H-6, 120 cm. Due to the common occurrence of reworked specimens, however, the LOs of *Helicosphaera sellii* and *C. macintyreii* were difficult to locate. We observed the first occurrence (FO) of *Gephyrocapsa oceanica*, which defines the base of Subzone CN14a, in Sample 115-708A-3H-4, 42–43 cm.

#### Pliocene

It was difficult to recognize upper Pliocene zonal boundaries with precision because of reworking. We used the horizons where the abundance of the marker species were significantly reduced

as LO levels. Thus, the upper boundaries of Subzone CN12d (NN18) and CN12c were identified in Sample 115-708A-4H-6, 130 cm, and the LO of common and continuous *Discoaster pentaradiatus* was recognized in Sample 115-708A-5H-4, 55 cm. Due to the generally rare occurrence of *Discoaster tamalis* and *Discoaster surculus*, however, we did not attempt to identify the boundaries between CN12a, CN12b, and CN12c.

The interval between Samples 115-708A-7H-2, 90–91 cm, and 115-708A-9X-3, 40 cm, is assigned to the lower Pliocene Zones CN10 and CN11. We did not identify zones and subzones because of the low abundances of ceratoliths, which are used for zonal boundary definitions in this interval. However, the FO of *Ceratolithus rugosus* was recorded in Sample 115-708A-8H-3, 40 cm.

#### Miocene

Although placoliths are badly dissolved, discoasters are generally well preserved in the Miocene sequence. The LO (top of CN9) and FO (base of CN9) of *Discoaster quinquerramus* are easy to identify in Samples 115-708A-9X-1, 30 cm, and 115-708A-13X-2, 76–77 cm, respectively. We detected the FO of *Ceratolithus primus* (base of CN9b) in Sample 115-708A-12X-2, 130 cm. In Core 115-708A-13X, *Discoaster neohamatus* is one of the major components of the nannoflora, and Sections 115-708A-13X-3 to 115-708A-13X, CC, are assigned to Zone CN8 (NN10).

The presence of *Discoaster hamatus* is easy to recognize, and the interval between Samples 115-708A-14X-1, 42–43 cm, and 115-708A-14X-4, 42–43 cm, is assigned to Zone CN7 (NN9). We observed well-preserved specimens of *Catinaster calyculus* in Samples 115-708A-14X-1, 42–43 cm, and 115-708A-14X-2, 42–43 cm, justifying the placement of these two samples in Subzone CN7b. The FO of *Catinaster coalitus*, which defines the base of Zone CN6 (NN8), was detected in Sample 115-708A-14X-5, 130 cm.

Some samples in Core 115-708A-14X are barren of nannofossils, whereas other samples show advanced states of nannofossil dissolution. This evidence is interpreted as an indication of significant shoaling of the CCD in the middle Miocene sequence at this site during the CN6–CN7 interval. In the underlying Section 115-708A-14X-6, nannofossils are badly dissolved or missing. Section 115-708A-14X, CC, contains moderately dissolved nannofossils in which *C. coalitus* is absent and *Discoaster kugleri* is present. We assigned this assemblage to the upper middle Miocene Subzone CN5b (10.8–11.5 Ma). Despite the relatively long duration of Subzone CN5b, this is the only examined sample within Subzone CN5b. This evidence suggests that CCD shoaling occurred within the earlier Subzone CN5b time interval as well.

The top 80 cm of sediment recovered in Section 115-708A-15X-1 contains abundant nannofossils of upper Paleocene age. Particularly in Samples 115-708A-15X-1, 52–53 cm, and 115-708A-15X-1, 80 cm, the flora consists almost entirely of well-preserved and diversified representatives of the lower upper Paleocene. *Discoaster multiradiatus*, *Heliolithus kleinpellii*, *Toweius emimens*, and *T. tovae* are predominant taxa of this assemblage. In Sample 115-708A-15X-1, 64–65 cm, we observed a mixed Paleocene–middle Miocene assemblage. This anomalous sequence, which is interpreted as a debris flow by the shipboard sedimentologists, was redeposited here during the early middle Miocene.

We did not observe Subzone CN5a (NN6). This is probably the result of a hiatus caused by either extensive carbonate dissolution (CCD shoaling) or by erosion associated with debris flows. The interval between Samples 115-708A-15X-1, 110 cm, and 115-708A-16X-3, 42–43 cm, is assigned to Zone CN4.

Samples 115-708A-16X-4, 42–43 cm, and 115-708A-16X-5, 130 cm, yielded a species composition typical of Zone CN3.

Preservation of nannofossils in Sample 115-708A-16X-6, 51–52 cm, is poor due to the extensive dissolution. Since the underlying Sample 115-708A-16X-7, 31–32 cm, yields moderately preserved nannoflora from Zone CN2, we interpreted the extensive dissolution observed in Section 115-708A-16X-5 as evidence of the first temporal shoaling of the CCD at this site during the Neogene.

Cores 115-708A-17X and 115-708A-18X yielded abundant and moderately well preserved nannofossils indicative of Zones NN2 and NN3 (CN1c and CN2) (early Miocene in age). The most common species are *Cyclicargolithus floridanus*, *C. abisectus*, *Discoaster deflandrei*, *D. drugii*, *Triquetrorhabdulus carinatus*, and *Sphenolithus dissimilis*. Core 115-708A-19X yielded a nannofossil assemblage consisting of abundant *T. carinatus* and *Sphenolithus delphix*, indicative of the lowest Miocene Zone NN1 (CN1a–CN1b).

### Oligocene

The Oligocene/Miocene boundary is located between Samples 115-708A-20X-1, 74 cm, and 115-708A-20X-2, 112 cm, on the basis of the LOs of *Discoaster bisectus* and *Sphenolithus ciperensis*.

Calcareous nannofossils are abundant and moderately well preserved in the Oligocene interval. Discoasters and *Triquetrorhabdulus* are overgrown, and helicoliths are missing or are severely etched. Sphenoliths and placoliths are well preserved and easily recognized. Reworking is minimal in the pelagic sediments but high in the turbidite beds. Obviously reworked species of mainly Eocene age and species restricted to the Oligocene represent the nannofossil assemblages in the turbidites analyzed in the Oligocene interval. Evidently, the turbidites were formed from the mixing of sediments either older and/or penecontemporaneous (within the time resolution possible with nannofossils) with the depositional event itself.

The presence of abundant sphenoliths determines the base of Subzone CN19b (NP25), such as *Sphenolithus distentus* (LO) in Sample 115-708A-22X-3, 140 cm, as well as the base of Subzone CN19a (NP24), in this case, *S. ciperensis* (FO) in Sample 115-708A-24X-5, 130 cm. We detected the FO of *S. distentus* (base of Zone CP18) in Sample 115-708A-25X-4, 122–124 cm. Since we did not observe *Reticulofenestra umbilica* or *Ericsonia formosa*, the lower two sections of the basal Core 115-708A-25X belong to Zone CP17, which is early Oligocene in age.

### Planktonic Foraminifers

#### Neogene

Planktonic foraminiferal assemblages show pronounced dissolution throughout the Neogene sequence. Planktonic foraminifers are rare and highly fragmented. Radiolarians and sponge spicules are common to abundant in the residues.

Pleistocene and Pliocene assemblages are dominated by the solution-resistant species *Globorotalia tumida*. Other solution-resistant species include rare *Neogloboquadrina dutertrei* and *Pulleniatina obliquiloculata*. *Globigerinoides sacculifer* occurs sporadically.

We assigned Sections 115-708A-1H, CC, and 115-708A-2H, CC, to Zone N22 based on the presence of rare *Globorotalia truncatulinoides*. No zonal assignment is made for Section 115-708A-3H, CC, in which this species was absent. Sections 115-708A-4H, CC, and 115-708A-5H, CC, belong to the upper Pliocene Zone N21. Section 115-708A-5H, CC, contains very rare *Globigerinoides fistulosus* and *Dentoglobigerina altispira*, giving this sample an age of approximately 2.9 Ma. Sections 115-708A-6H, CC, and 115-708A-7H, CC, show slightly better preservation, foraminiferal fragments being less abundant, whereas Sections 115-708A-8H, CC, to 115-708A-10H, CC, show in-

creased dissolution, the residue consisting almost entirely of radiolarians and foraminiferal fragments. The LO of *Sphaeroidinellopsis* spp. (3.0 Ma) occurs in Section 115-708A-6H, CC, and the FO of *G. tumida* (5.2 Ma) in Section 115-708A-8H, CC. We assigned Sections 115-708A-6H, CC, and 115-708A-7H, CC, to Zone N21 and Section 115-708A-8H, CC, to the lower Pliocene zonal interval N20–N19 to N18.

The presence of rare *Pulleniatina* placed Sections 115-707A-9X, CC, to 115-708A-11X, CC, in the upper Miocene Zone N17b. No zonal assignment was possible for Sections 115-708A-12X, CC, and 115-708A-13X, CC, in which the fauna were poorly preserved and dominated by the two resistant forms *Globoquadrina venezuelana* and *Sphaeroidinellopsis*.

From Section 115-708A-14X, CC, down through the remainder of the Neogene (Core 115-708A-19X), planktonic foraminifers are very rare. The residue greater than 63  $\mu$ m consists almost entirely of sponge spicules, radiolarians, and clayey aggregates. Only a few solution-resistant forms (*G. venezuelana* and *Globoquadrina dehiscens*) occur in the prevailing zonal assignment.

### Paleogene

We located a few, badly dissolved planktonic foraminiferal faunas in Oligocene Sections 115-708A-20X, CC, to 115-708A-25X, CC. The solution-resistant forms, *Globoquadrina tripartita* group, *Globoquadrina sellii*, *Catapsydrax unicavus*, and *Paragloborotalia siakensis*, indicate a late Oligocene age. Faunas indicative of Zone P22 were found in Sample 115-708A-20X-3, 38 cm, and indices for Zone P21 in Sample 115-708A-22X-2, 38 cm. We assigned Sample 115-708A-23X-6, 38 cm, to Zone P20. No age-diagnostic forms were found in core catchers from Cores 115-708A-24X or 115-708A-25X, which were badly dissolved and composed of over 90% sponge spicules.

### Benthic Foraminifers

Well- to moderately well-preserved benthic foraminifers were found in all Pleistocene and Pliocene core catchers (Sections 115-708A-1H, CC, to 115-708A-13X, CC); rare and poorly preserved to barren samples occurred through the Miocene (Cores 115-708A-14X to -19X); and badly preserved, dissolved, small, and uncommon faunas were typical of the Oligocene (Cores 115-708A-20X to -25X). All benthic faunas contain redeposited shallow-carbonate-platform benthic foraminifers. Reworked Eocene planktonic foraminifers became common in early Miocene size-sorted, spicule-juvenile foraminifer oozes (Sections 115-708A-17X, CC, to 115-708A-19X, CC) and were present in the Oligocene (Sections 115-708A-20X, CC, to 115-708A-22X, CC), and common in Section 115-708A-24X, CC, as well.

Most core catchers contained three benthic components: (1) the *in-situ* abyssal benthic foraminifers, (2) redeposited shelf-carbonate benthic foraminifers and bryozoans, and (3) redeposited upper and middle bathyal benthic foraminifers. These components occur in varying percentages in each sample. Only in early Pliocene Section 115-708A-12X, CC, does the *in-situ* benthic fraction predominate. The shelf-carbonate fraction comprises more than 50% of some Miocene turbidite layers and of late Oligocene samples in Sections 115-708A-21X, CC, and 115-708A-23X, CC.

Pliocene-Pleistocene *in-situ* benthic faunas contain frequent *Nuttalides umbonifera*, *Eggerella bradyi*, *Melonis pompilioides*, *Laticarinina halophora*, *Globocassidulina subglobosa*, and *Cibicides kullenbergi*. Only in Section 115-708A-12X, CC, where there was very little siliceous component, did *N. umbonifera* reach high numbers, as would be expected in an abyssal fauna.

Redeposited upper or middle bathyal benthic foraminifers included *Uvigerina spinulosa*, large nodosariids and stilostomel-

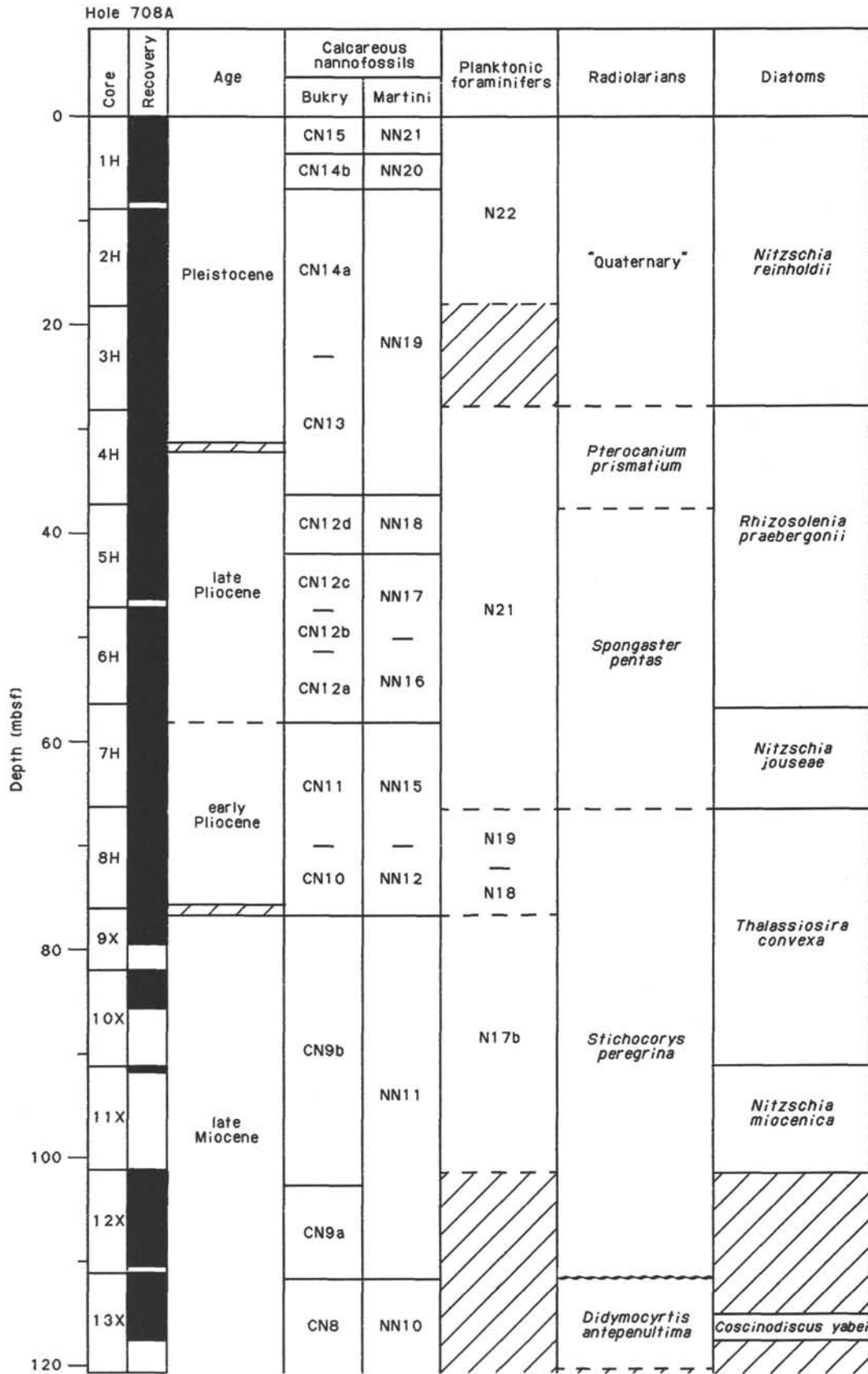


Figure 7. Biostratigraphic summary for Site 708. Black bars represent recovery in Hole 708A.

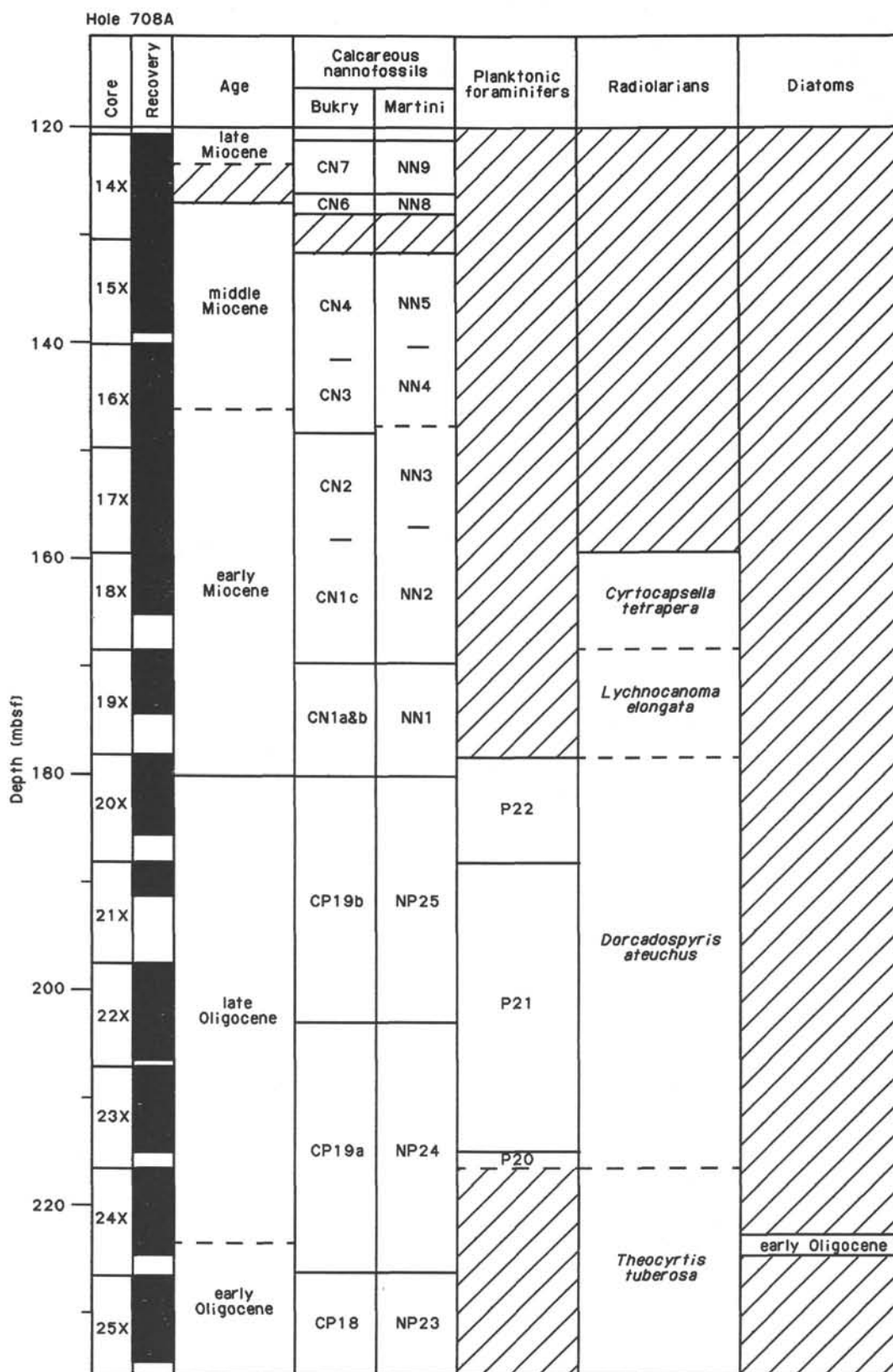


Figure 7 (continued).

lids, *Osangularia bengalensis*, and several miliolids. Most of the bathyal element was very large in size. Shelf-depth redeposited material contained *Elphidium*, other members of the Elphidiidae, and various orbitoidal foraminifers, all highly ornamented, large genera reported from shallow carbonate platforms and reefs.

In core catchers from Cores 115-708A-14X to -17X, the brown clays contained few benthic foraminifers and were presumably deposited near the foraminiferal lysocline. Only the solution-resistant forms, *N. umbonifera*, *Oridorsalis umbonatus*, and *Cibicoides kullenbergi* remained in these samples. Most benthic foraminifers of Miocene age were juveniles or babies and occurred in apparently size-sorted, fine-fraction, turbiditic sediments. Included were *O. umbonatus*, *Stilostomella lepidula*, *C. kullenbergi*, *Uvigerina auberiana*, *Gyroidinoides planulatus*, and *N. umbonifera*. The redeposited fraction was dominated by the shelf-rotaloid benthic foraminifers, and the upper-middle bathyal element was uncommon to indistinguishable (Section 115-708A-15X, CC).

*In-situ* benthic foraminifers were rare in the very dissolved Oligocene levels not considered to be turbiditic (Sample 115-708A-20X-3, 100 cm). Oligocene benthic foraminifers seem to represent a different paleodepth, thus suggesting that the site was receiving deep-water input by the Oligocene. Forms included *Stilostomella nuttalli*, *S. abyssorum*, *Heterolepa mexicana* (a deep-water form), *Vulvulina spinosa*, and only rare *N. umbonifera*. The fauna suggest deep- rather than bottom-water depths. As in the early Miocene, the redeposited component (e.g., *Pararotalia*, *Rotalia*, and the larger foraminifers) is derived primarily from shallow platform depths rather than from upper or middle bathyal depths.

### Radiolarians

Radiolarian assemblages at Site 708 are generally common and moderately to well preserved for the entire stratigraphic interval recovered. However, the assemblages are of doubtful stratigraphic value because of the dominance of reworked sediment throughout the entire interval cored. Calcareous turbidites, generally between 10 cm and 1 m in thickness, occur at an average spacing of five to eight turbidites per 9.5 m of core. As a result of the reworked nature of the entire core, random samples examined from the core catchers vary greatly in the degree of reworking. Some samples are dominated by reworked components, whereas a few show no evidence at all for reworking.

Because of the physiographic setting of Site 708 and the resulting dominance of reworked components, we only examined core-catcher samples in shipboard analyses. Subsequent detailed studies by nannofossil specialists indicating the presence of significant unreworked intervals at this site may justify more detailed follow-up studies of radiolarians.

In the following discussion, we summarize the results of our core-catcher analyses.

Sections 115-708A-1H, CC, through 115-708A-3H, CC, are of Pleistocene age, and assemblages of radiolarians are common and well preserved. Diagnostic taxa include *Pterocorys hertwigii*, *Theocorythium trachelium*, and *Amphirhopalum ypsilon*. No attempt was made to subdivide the Pleistocene into its various zones due to the low abundances of diagnostic species required for making such a division.

Section 115-708A-4H, CC, is of late Pliocene age, belonging to the *Pterocanium prismatium* Zone. Diagnostic taxa include *P. prismatium*, *Theocorythium vetulum*, and *A. ypsilon*. Radiolarians are few and moderately preserved.

Sections 115-708A-5H, CC, through 115-708A-7H, CC, are of early Pliocene age, belonging to the *Spongaster pentas* Zone. Diagnostic taxa include *Anthocyrthidium jenghisi*, *A. micheli-*

*nae*, *Stichocorys peregrina*, and *P. prismatium*. Radiolarians in this interval are common and well preserved.

Sections 115-708A-8H, CC, through 115-708A-12X, CC, belong to the *Stichocorys peregrina* Zone, of earliest Pliocene and latest Miocene age. Diagnostic taxa include *Solenosphaera omnitubus*, *Phormostichoartus doliolum*, *Didymocyrtis penultima*, *Anthocyrthidium nosicae*, *A. michelinae*, *A. jenghisi*, and *S. peregrina*. Radiolarians are common and well preserved throughout this interval. All samples contain trace amounts of reworked Eocene species, generally of middle and late Eocene age.

The *Didymocyrtis penultima* Zone is evidently missing from the core-catcher samples, perhaps indicating the presence of a short hiatus in this interval of the hole.

Section 115-708A-13X, CC, is of late Miocene age, belonging to the *Didymocyrtis antepenultima* Zone. Diagnostic taxa include *D. antepenultima*, *Diartus hughesi*, and *Stichocorys delmontensis*. Radiolarians are few and moderately well preserved.

Sections 115-708A-14X, CC, through 115-708A-17X, CC, contain rare and poorly preserved radiolarian fragments which could not be assigned to a particular biostratigraphic zone. Reworked Eocene radiolarian specimens are rare to common throughout this interval.

Section 115-708A-18X, CC, belongs to the *Cyrtocapsella tetrapera* Zone of early Miocene age. Radiolarians are few and poorly preserved. Diagnostic taxa include *Calocycletta virginis*, *C. serrata*, and *Didymocyrtis prismatica*.

Section 115-708A-19X, CC, belongs to the *Lychnocanoma elongata* Zone of earliest Miocene age. Radiolarians are rare and poorly preserved. Diagnostic taxa include only *L. elongata* and *Calocycletta robusta*.

Sections 115-708A-20X, CC, through 115-708A-23X, CC, are of late Oligocene age and belong to the *Dorcadospyrus atechus* Zone. Radiolarians are few and poorly preserved. Diagnostic taxa include only *D. atechus*, *Cyclampterium pegetrum*, and *Dorcadospyrus pseudopapilio*.

Sections 115-708A-24X, CC, and 115-708A-25X, CC, are of early Oligocene age and belong to the *Theocyrthium tuberosa* Zone. Radiolarians are common and moderately preserved. Diagnostic taxa include *Lithocyclia angusta* and *Artophormis gracilis*.

### Diatoms

Diatom assemblages recovered at Site 708 have a restricted stratigraphic range. Of the 25 cores recovered, only the 13 uppermost cores contained diatoms. These are of Pleistocene through late Miocene age. The abundance of diatoms is generally low, except in the Pleistocene. All the recovered assemblages are moderately to poorly preserved.

We recorded turbidites in all cores. This explains why many of the planktonic diatom assemblages are mixed with reworked specimens of older ages and with specimens of neritic origin.

The Pleistocene *in-situ* flora contains a diversified assemblage with moderately preserved diatoms. *Pseudoenotia doliolum*, *Thalassiosira oestrupii*, *T. leptopus*, and *Coscinodiscus africanus* occur frequently. Sections 115-708A-1H, CC, through 115-708A-3H, CC, belong to the lower Pleistocene *Nitzschia reinholdii* Zone.

Sections 115-708A-4H, CC, through 115-708A-6H, CC, belong to the late Pliocene *Rhizosolenia praebergonii* Zone. The poorly preserved assemblages include *R. praebergonii*, *Nitzschia jouseae*, and *T. oestrupii*.

The amount of opaline silica increases in sediments from the lower Pliocene and uppermost part of the upper Miocene sequences. Section 115-708A-7H, CC, which contains abundant but fairly poorly preserved diatoms, including *N. jouseae* and *Thalassiosira convexa* var. *aspinosa*, belongs to the *N. jouseae* Zone.

Sections 115-708A-8H, CC, through 115-708A-10X, CC, are of earliest Pliocene to latest Miocene age. They are characterized by a relatively high abundance of *Thalassionema* spp. and by the presence of diagnostic taxa like *Thalassiosira praeconvexa*, *Thalassiosira miocenica*, and *N. reinholdii*, representing the *Thalassiosira convexa* Zone.

The abundance of diatoms decreases significantly in Sections 115-708A-11X, CC, through 115-708A-13X, CC, and the preservation of the opaline silica is poor. A few age-diagnostic specimens, including *T. praeconvexa*, places Section 115-708A-11X, CC, in the *N. miocenica* Zone. No age-diagnostic taxa are present in Section 115-708A-12X, CC. In the sparse assemblage of Section 115-708A-13X, CC, the presence of *Coscinodiscus yabei* indicates the *C. yabei* Zone.

No well-preserved diatom assemblages are found in the Paleogene section of Hole 708A except for some early Oligocene specimens of *Cestodiscus* sp. and *Hemiaulus* sp. in Section 115-708A-24X, CC.

### PALEOMAGNETICS

The paleomagnetic data acquired at this site were generally quite poor, and we can offer no magnetostratigraphic interpretation. The exact cause of the erratic paleomagnetic signature of the sediments recovered here is unknown. We suspect, however, that the poor results may be caused, at least in part, by the remagnetization effect, which was more clearly displayed at Site 709 (see "Paleomagnetism" section, "Site 709" chapter, this volume, for a discussion of this effect).

The natural remanent magnetization (NRM) of Cores 115-708A-1H through -23X, measured both before and after demagnetization using the pass-through magnetometer system, provides little data that we can readily interpret. Pass-through records typically display highly variable directions and a general lack of serial correlation between data points. Since we cannot reasonably ascribe the large amount of scatter to geomagnetic field behavior, we believe these results must reflect only a recent disturbance or remagnetization. From the pass-through results, it seems unlikely that paleolatitudes or polarity stratigraphy of the sediments from this site can be determined with any reasonable degree of confidence; however, we have not yet analyzed discrete samples taken at this site.

### Magnetic Susceptibility

We measured the low-frequency (0.47 kHz), volume-magnetic susceptibility of all sections of cores recovered from Hole 708A at intervals of 5 cm, using a Bartington Susceptibility Meter (Model MS1) and a whole-core, pass-through sensor coil of 80-mm inner diameter (Model MS2C). Figure 8 illustrates the results of these measurements.

We did not experience problems with artifact contamination from drilling at Site 708. Magnetic susceptibility values range from approximately  $1-2 \times 10^{-6}$  cgs in carbonate-rich (calc-turbidite) horizons, to over  $6 \times 10^{-5}$  cgs in volcanic-ash-rich horizons. Intermediate susceptibility values fall into three general groupings, as follows.

1. Between  $2$  and  $5 \times 10^{-6}$  cgs: This group corresponds to gray or greenish gray (suggesting a reduction of Fe(III) to Fe(II) in the lattice of clay minerals in the sediment; e.g., see Lyle, 1983), clay-bearing nanofossil ooze and volcanogenic-muddy ooze. In these sediments any magnetic (i.e., NRM-carrying minerals such as Fe(II)/Fe(III) oxides and Fe(III) oxides and oxyhydroxides) originally present are likely to have been severely dissolved (i.e., bacterially dissociated), either during suboxic diagenesis of organic matter in the sediment (Froelich et al., 1979) or perhaps during halmyrolysis of sulfide-rich volcanic ash (Bonatti, 1981). In reduced horizons, therefore, only the more weakly

magnetic, non-NRM-carrying (paramagnetic), ferrous-iron-bearing phases remain in the sediment to contribute to susceptibility values.

2. Between  $5$  and  $20 \times 10^{-6}$  cgs: This group corresponds to all oxidized (i.e., light brown or buff colored) or only weakly reduced (i.e., grayish brown) clay-bearing nanofossil ooze horizons (except those of Group 3, below), in which the principal contribution to susceptibility is most probably made by ferric-oxyhydroxides (e.g., goethite) and clay minerals (plus volcanic ash, when present).

3. Between  $10$  and  $40 \times 10^{-6}$  cgs: This group corresponds to moderately well-oxidized to weakly reduced, clay-bearing and clayey nanofossil oozes and nanofossil clays containing a lower proportion of carbonate and higher concentration of lithogenic clay (in which magnetizable components chiefly reside) than Group 1-type sediments, which may possibly be due to these sediments having undergone more intense dissolution of biogenic (carbonate and silica) constituents than Group 1-type sediments.

The three generalized groupings of susceptibility values noted above, together with superimposed peaks due to volcanic-ash-rich horizons and troughs due to calc-turbidites, effectively subdivides the susceptibility profile of Hole 708A into five distinct intervals, as follows:

1. From  $0$  to  $20$  mbsf: Group 2-type, presumably well-oxidized to weakly reduced (with depth), clay-bearing nanofossil oozes of Pleistocene age, sandwiched between calc-turbidite horizons. Oscillations in susceptibility values between turbidite horizons reflect changes in carbonate content of the sediment which may possibly be related to dissolution.

2. From  $20$  to  $48$  mbsf: Group 1-type, strongly reduced clay-bearing nanofossil ooze and volcanogenic-muddy ooze with degraded volcanic-ash horizons and intercalated calc-turbidites (also reduced), mainly of middle to late Pliocene and early Pleistocene age.

3. From  $48$  to  $120$  mbsf: Group 1-type weakly reduced oozes and volcanogenic-muddy oozes of late Miocene to late Pliocene age, containing a larger number of fresh or mildly altered volcanic-ash horizons than does the overlying, more strongly reduced interval.

4. From  $120$  to  $170$  mbsf: Group 3-type moderately oxidized to weakly reduced, clayey nanofossil oozes and nanofossil clays of early to middle Miocene age, where high-frequency ( $>1$  cycle/m) oscillations in susceptibility values between turbidite horizons reflect changes in the carbonate content of the sediment which may possibly be dissolution controlled.

5. From  $170$  to  $234$  mbsf: Group 2-type strongly oxidized, clay-bearing nanofossil oozes of early Oligocene to early Miocene age, containing frequent volcanic-ash horizons, many fresh to only mildly altered, which probably contain a high proportion of primary titanomagnetite (e.g., up to 10%; Kennett, 1981).

The combination of (1) large variations in carbonate content, possibly due to dissolution, between calc-turbidite horizons; (2) frequent degraded and unaltered volcanic-ash horizons; (3) moderately to strongly reduced intervals of the sequence, regardless of lithology; and (4) a large number of calc-turbidite horizons at Site 708 has resulted in a sequence which very clearly demonstrates the strong lithologic control of magnetic susceptibility variations in deep-sea sediments. Figure 9 shows three selected subsections of the susceptibility profile of Hole 708 plotted alongside a log of turbidite horizons in the sequence, taken from visual core description data. Clearly, the main control on susceptibility variations at this site is the presence or absence of calc-turbidite horizons. Between calc-turbidites, however, varia-

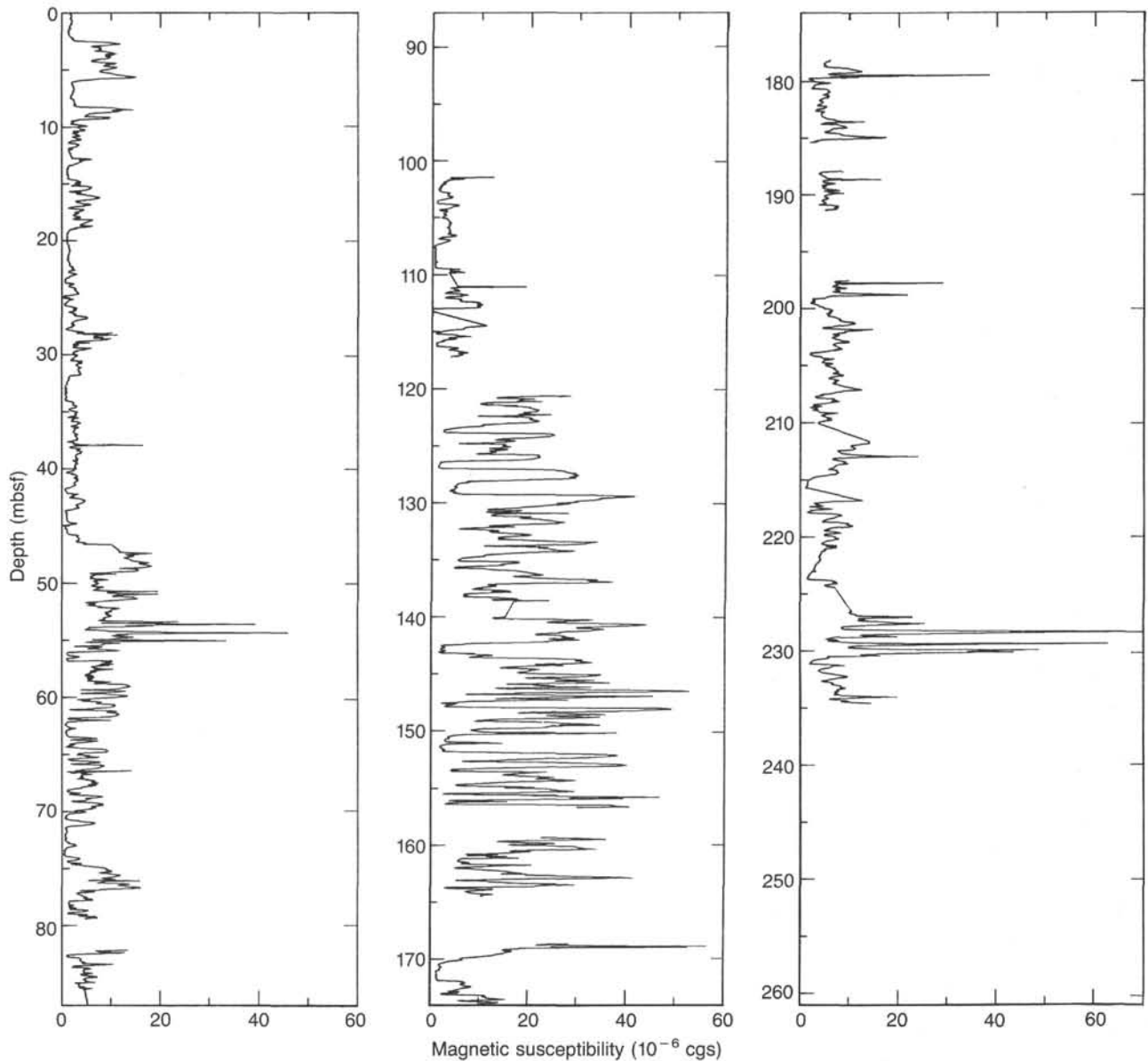


Figure 8. Whole-core magnetic susceptibility profile of Hole 708A.

tions in susceptibility values appear to be modulated by oscillations in carbonate content of the sediment which may be related tentatively to dissolution.

### SEDIMENTATION RATES

The presence of numerous turbidites characterizes the sedimentary sequence recovered at Site 708. The turbidites range in thickness from a few centimeters up to 3.4 m and comprise up to 35% of the recovered section. The turbidites are coarsely textured and consist primarily of a nannofossil-bearing foraminiferal ooze with abundant reworked material.

Sedimentation-rate curves for Hole 708A (Figs. 10 and 11) are based on the biostratigraphic data given in Tables 2 and 3. The biostratigraphic resolution for nannofossil events is more precise than for any other fossil group, since the nannofossil events are determined at closely spaced intervals in the core.

Figure 10 presents the sedimentation-rate curve for the entire sequence of Hole 708A; Figure 11 shows the "pelagic" section only. In this latter "turbidite-free" curve, we have subtracted the accumulated thicknesses of all turbidites exceeding 40 cm in

thickness. All curves are drawn to the best fit by eye, without making corrections for compaction or dissolution, and without considering short-term fluctuations. This report discusses only the "turbidite-free" sedimentation-rate curves.

The oldest sediment recovered at Site 708 is of early Oligocene age. The average sedimentation rate for the Paleogene section is fairly low: 4–7 m/m.y. (Fig. 11). The sedimentation rate remains low during the late early and middle Miocene (approximately 1–3 m/m.y.). A pronounced increase in the sedimentation rate takes place around 9 Ma; the Neogene rate averages 10 m/m.y.

### GEOCHEMISTRY

#### Interstitial Water Studies

Table 4 and Figure 12 present data from interstitial water analyses.

#### Calcium and Magnesium

Calcium and magnesium exhibit very weak downhole gradients, changing from seawater values of 10.25 and 53.72 mmol/L

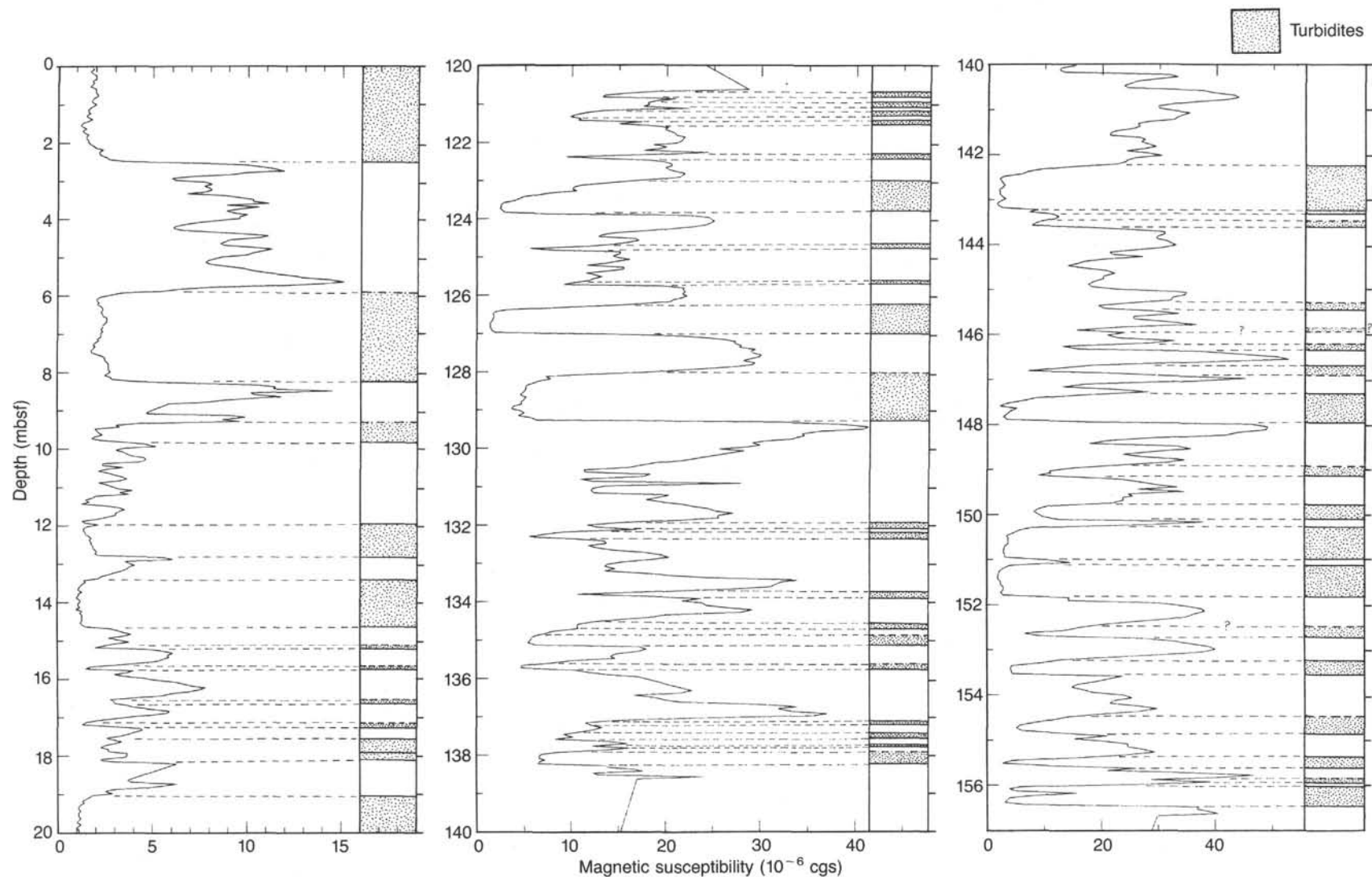


Figure 9. Whole-core magnetic susceptibility profiles of selected intervals from Hole 708A. Left: 0–20 mbsf (Cores 115-708A-1H and -2H); center: 120–140 mbsf (Cores 115-708A-14X and -15X); right: 140–157 mbsf (Cores 115-708A-16X and -17X). Note the sharp negative deflections in the susceptibility profiles in response to calc-turbidite horizons. Variations in susceptibility values between calc-turbidite horizons may possibly be related to carbonate-dissolution cycles in the sediment. Logs of turbidite horizons are taken from visual core description data.

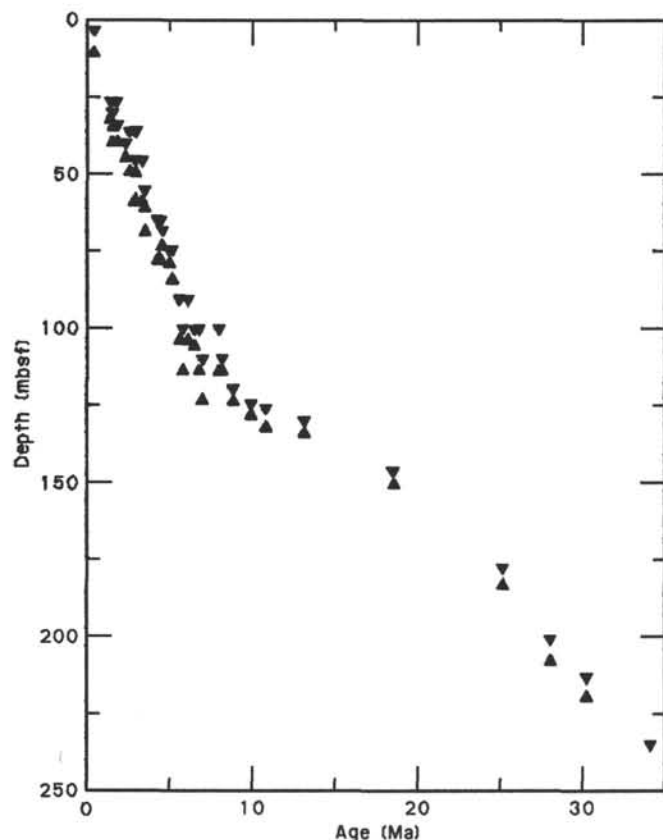


Figure 10. Average sedimentation-rate curve for the total sedimentary sequence in Hole 708A.

to 14.24 and 48.99 mmol/L, respectively. These variations correspond to an overall  $\text{Ca}^{2+}$  gradient of 0.016 mmol/L/m and a  $\text{Mg}^{2+}$  gradient of  $-0.0212$  mmol/L/m. However, while small gradients do exist in these elements, the changes are not uniform. Furthermore, between 34.05 and 203.45 mbsf, the down-hole  $\text{Ca}^{2+}$  gradient falls as low as 0.006 mmol/L/m. The absence of predictable changes in the concentration gradients of  $\text{Ca}^{2+}$  and  $\text{Mg}^{2+}$  strongly suggests that trace element profiles are controlled by factors other than simple diffusion.

#### Alkalinity and Sulfate

Alkalinity and sulfate concentrations show the largest change with depth observed in any of the sites studied thus far. Alkalinity rises rapidly from a value of 3.93 mmol/L at 5.95 mbsf to 4.95 mmol/L at 34.05 mbsf, and is accompanied by a slight decrease in the concentration of sulfate, suggesting that organic material is being oxidized.

#### Chlorinity and Salinity

Chlorinity and salinity rise with increasing sub-bottom depth, reaching high and relatively constant values between 14.95 and 136.0 mbsf and then decreasing slightly further downhole.

#### Silica

Concentrations of silica rise rapidly with increasing sub-bottom depth, reaching a maximum concentration of 1037  $\mu\text{mol/L}$  near the bottom of the hole.

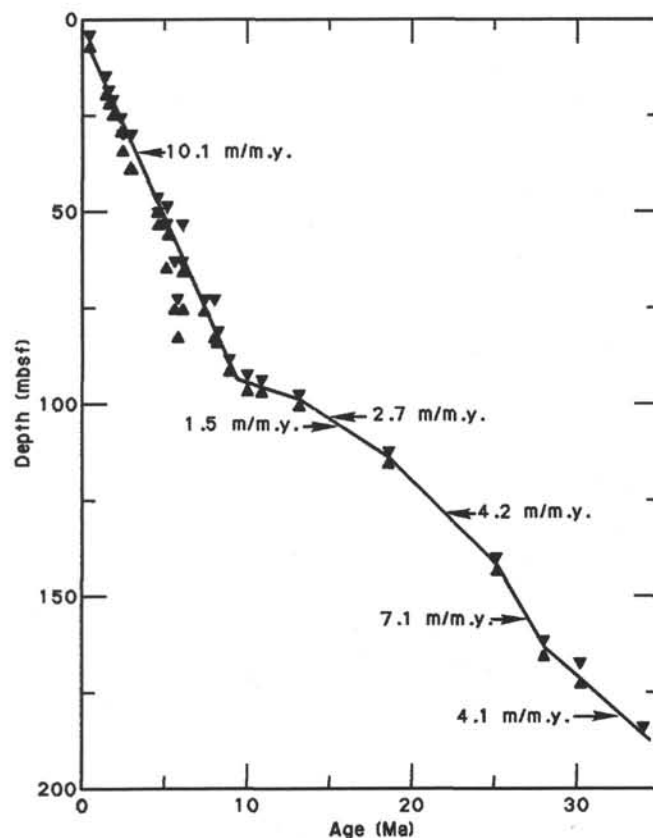


Figure 11. Average sedimentation-rate curve for the "turbidite-free" sequence in Hole 708A.

### X-ray Mineralogy, Carbonate, and Organic Carbon Analyses

#### X-ray Mineralogy

X-ray analyses performed on 64 samples from Hole 708A detected significant quantities of aragonite, quartz, and dolomite in the interstitial water/sediment samples. The occurrence of aragonite in these deep deposits is probably related to the abundance of turbidites (shallow-water sediments) seen in the core (see "Lithostratigraphy" section, this chapter). These data are shown in Table 5 and Figure 13. Dolomite and quartz are ubiquitous throughout the upper Pliocene and Pleistocene, with concentrations never exceeding 2%–4%. Although there is one isolated occurrence of dolomite at 145 mbsf, dolomite ceases to be a regular component at 75 mbsf (early Pliocene age). In upper Miocene sediments, quartz increases in concentration and in some cases during the middle Miocene exceeds 30%. This interval has an extremely low carbonate content, the remainder of the sample being composed of clay minerals such as smectite and chlorite. Near the Oligocene/Miocene boundary the concentration of quartz decreases and is no longer detectable by 205 mbsf.

#### Carbonate Content

The carbonate content mirrors the trends seen in the X-ray analyses. This can be observed by means of a running mean (Figs. 14 and 15); the mean carbonate content for the entire hole is 72.2% ( $\pm 18.98$ ; Table 6). Using this approach, we can identify three minima: the first occurs in the Pleistocene be-

Table 2. Biostratigraphic datum levels, Hole 708A.

	Species event	Depth (mbsf)	Age (Ma)
LO	<i>P. lacunosa</i> (N)	5.6–8.4	0.46
LO	<i>C. macintyreii</i> (N)	28.0–30.0	1.45
LO	<i>P. prismatium</i> (R)	28.1–37.6	1.55
FO	<i>G. oceanica</i> (N)	31.5–32.4	1.60
FO	<i>P. doliolus</i> (D)	28.1–37.6	1.80
LO	<i>D. brouweri</i> (N)	35.4–36.9	1.89
LO	<i>D. pentaradiatus</i> (N)	41.4–42.5	2.35
LO	<i>S. peregrina</i> (R)	37.6–47.2	2.60
LO	<i>N. jouseae</i> (D)	37.6–47.2	2.60
LO	<i>D. altispira</i> (F)	37.6–47.2	2.90
FO	<i>G. fistulosus</i> (F)	47.2–56.8	2.90
LO	<i>Sphaerodinellopsis</i> (F)	47.2–56.8	3.00
FO	<i>R. praebergonii</i> (D)	37.6–47.2	3.00
LO	<i>L. audax</i> (R)	47.2–56.8	3.35
LO	<i>P. doliolum</i> (R)	56.8–66.4	3.53
LO	<i>R. pseudoubilica</i> (N)	56.8–58.7	3.56
LO	<i>S. omnitubus</i> (R)	66.4–76.0	4.30
FO	<i>N. jouseae</i> (D)	66.4–76.0	4.50
FO	<i>C. rugosus</i> (N)	69.8–71.1	4.60
LO	<i>D. quinqueramus</i> (N)	77.9–82.0	5.00
FO	<i>G. tumida</i> (F)	76.0–82.1	5.20
FO	<i>N. miocenica</i> (D)	91.7–101.4	5.60
FO	<i>Pulleniatina</i> (F)	101.4–111.0	5.80
FO	<i>T. convexa</i> var. <i>aspinosa</i> (D)	82.1–91.7	6.10
FO	<i>T. miocenica</i> (D)	91.7–101.4	6.10
FO	<i>S. omnitubus</i> (R)	101.4–111.0	6.80
LO	<i>D. hughesi</i> (R)	111.0–120.6	7.00
FO	<i>A. primus</i> (N)	101.4–103.3	6.50
FO	<i>N. reinholdii</i> (D)	101.4–111.0	8.00
FO	<i>D. quinqueramus</i> (N)	111.0–111.25	8.20
LO	<i>D. hamatus</i> (N)	120.6–121.2	8.90
FO	<i>D. hamatus</i> (N)	125.5–127.0	10.00
FO	<i>C. coalitus</i> (N)	127.0–129.4	10.90
LO	<i>S. heteromorphus</i> (N)	131.1–131.6	13.20
FO	<i>S. heteromorphus</i> (N)	147.3–147.9	18.60
LO	<i>S. ciperoensis</i> (N)	178.9–180.8	25.20
LO	<i>S. distentus</i> (N)	201.9–205.3	28.10
FO	<i>S. ciperoensis</i> (N)	214.0–216.8	30.30
Presence	<i>S. distentus</i> (N)	236.6–230.0	34.10

Note: FO = first occurrence, LO = last occurrence, N = nanno-fossil, F = foraminifer, D = diatom, and R = radiolarian.

tween 5 and 10 mbsf, the second between 40 and 60 mbsf in lower Pliocene sediments, and the third between 105 and 125 mbsf. The carbonate minimum between 105 and 125 mbsf exhibits extremely low values and is middle to late Miocene in age. It appears to be slightly older than the Messinian carbonate minimum seen in Hole 707A, perhaps equivalent to one of the three Miocene minima seen at that site. Average carbonate concentrations at both carbonate minima and maxima are statistically lower than those at Site 707, in accord with deeper water depths and, hence, more corrosive waters.

### Organic Carbon

The concentration of organic carbon in Hole 708A attains values as high as 0.75 wt% and then gradually decreases with depth. The reduction in organic matter is accompanied by a decrease in  $\text{SO}_4^{2-}$  and a rise in alkalinity. These sediments produced no detectable amounts of hydrocarbons.

## PHYSICAL PROPERTIES

### Index Properties

The index properties (wet-bulk density, porosity, water content, and grain density) determined on discrete samples from Site 708 (Table 7) reflect the inhomogeneity of the sediments. The only reasonably constant parameter is the grain density (Fig. 16), which ranges between 2.5 and 2.75 g/cm<sup>3</sup> with the ex-

Table 3. Biostratigraphic datum levels, Hole 708A (turbidites removed).

	Species event	Depth (mbsf)	Age (Ma)
LO	<i>P. lacunosa</i> (N)	5.6–6.0	0.46
LO	<i>C. macintyreii</i> (N)	16.3–18.3	1.45
FO	<i>G. oceanica</i> (N)	19.8–20.8	1.60
LO	<i>D. brouweri</i> (N)	19.8–20.8	1.89
LO	<i>D. pentaradiatus</i> (N)	27.1–28.2	2.35
LO	<i>D. surculus</i> (N)	31.4–32.9	2.45
FO	<i>G. fistulosus</i> (F)	31.3–37.7	2.90
LO	<i>Sphaerodinellopsis</i> (F)	31.3–37.9	3.00
FO	<i>C. rugosus</i> (N)	47.7–49.0	4.60
LO	<i>D. quinqueramus</i> (N)	51.7–52.2	5.00
LO	<i>T. miocenica</i> (D)	54.7–64.3	5.10
FO	<i>G. tumida</i> (F)	49.9–54.7	5.20
FO	<i>N. miocenica</i> (D)	64.3–74.0	5.60
FO	<i>Pulleniatina</i> (F)	74.0–81.2	5.80
FO	<i>T. convexa</i> var. <i>aspinosa</i> (D)	54.7–64.3	6.10
FO	<i>T. miocenica</i> (D)	64.3–74.0	6.10
FO	<i>A. primus</i> (N)	74.0–74.4	7.40
FO	<i>N. reinholdii</i> (D)	74.0–81.2	8.00
FO	<i>D. quinqueramus</i> (N)	82.2–82.5	8.20
LO	<i>D. hamatus</i> (N)	89.4–90.0	8.90
FO	<i>D. hamatus</i> (N)	93.3–94.8	10.00
FO	<i>C. coalitus</i> (N)	94.8–95.5	10.90
LO	<i>S. heteromorphus</i> (N)	98.6–99.1	13.20
FO	<i>S. heteromorphus</i> (N)	113.4–114.5	18.60
LO	<i>S. ciperoensis</i> (N)	141.0–141.9	25.20
LO	<i>S. distentus</i> (N)	162.2–163.9	28.10
FO	<i>S. ciperoensis</i> (N)	168.3–171.1	30.30
Presence	<i>S. distentus</i> (N)	185.1–180.0	34.10

Note: FO = first occurrence, LO = last occurrence, N = nanno-fossil, F = foraminifer, and D = diatom.

ception of two extreme values (2.41 and 3.27 g/cm<sup>3</sup>; Table 7). The grain-density curve (Fig. 16) is similar to the carbonate curve shown in Figure 17. Carbonate data plotted in this latter figure were measured on physical properties samples and represent a subset of data plotted in Figure 13. In sections where the carbonate content decreases from more than 90% to less than 20%, the carbonate is replaced by clay minerals and, to a minor degree, biogenic silica. The combination of these two components produces almost the same grain density as pure carbonate. No grain-density gradient is observed downhole.

Figure 16 demonstrates that variations in wet-bulk density are more dependent upon variations in porosity than on variations in grain density at this site. High porosity values are reflected by low wet-bulk densities (e.g., from 25 to 76 mbsf); low porosities coincide with higher wet-bulk densities. The wet-bulk densities vary between 1.28 and 2.37 g/cm<sup>3</sup>; however, wet-bulk densities greater than 1.80 g/cm<sup>3</sup> are considered erroneous. A slight increase in the wet-bulk density with sub-bottom depth, from 1.28 to 1.62 g/cm<sup>3</sup>, corresponds to decreases in water content and porosity from 57.12 to 43.23% and 78.52% to 66.87%, respectively (Fig. 16 and Table 7).

Index properties reflect the variation in sediment types at Site 708, but measurements are spaced too widely to resolve the alternating layers. The downhole gradient of wet-bulk density, water content, and porosity are characteristic of a pelagic depositional environment with high carbonate and clay sedimentation and only minor biogenic silica, as indicated by the mean grain density of 2.73 g/cm<sup>3</sup>, which lies slightly below the grain density of pure carbonate (2.76 g/cm<sup>3</sup>).

### Compressional-Wave Velocity and Acoustic Impedance

The *P*-wave logger provided high-quality data for compressional velocity ( $V_p$ ) throughout the length of the hole. Discrete measurements using the Hamilton Frame were less successful because many samples were too brittle to insert into the device.

Table 4. Interstitial water analyses, Hole 708A.

Sample interval (cm)	Depth (mbsf)	Ca (mmol/L)	Mg (mmol/L)	Cl (mmol/L)	Al (mmol/L)	pH	Salinity (‰)	Si (μmol/L)	SO <sub>4</sub> (mmol/L)
Seawater	0	10.25	53.72	556.03	2.58	8.4	34.4	5.5	28.74
115-708A-									
1H-4, 145-150	5.95	10.41	55.36	568.91	3.93	7.7	35.0	671.0	28.93
2H-4, 145-150	14.95	11.25	53.86	588.73	3.81	7.6	35.4	805.0	27.84
3H-4, 145-150	24.55	11.71	52.42	584.77	4.10	7.6	35.2	907.0	28.43
4H-4, 145-150	34.05	12.62	52.91	587.74	4.95	7.6	35.2	801.0	27.09
5H-4, 145-150	43.55	12.41	52.38	590.72	4.63	7.5	35.0	962.0	27.45
6H-3, 145-150	51.65	13.05	52.56	587.74	4.58	7.4	35.2	846.0	26.72
9X-1, 145-150	77.45	13.46	51.90	593.69	4.79	7.4	35.2	860.0	26.0
12X-4, 120-125	107.10	13.05	50.91	589.73	4.45	7.4	35.0	1000.0	25.45
15X-4, 120-125	136.00	13.19	50.03	581.80	4.71	7.3	34.8	847.0	24.18
18X-2, 120-125	162.00	13.65	49.91	566.93	4.60	7.4	34.8	860.0	24.91
22X-4, 145-150	203.45	13.72	49.59	567.92	4.56	7.4	34.5	901.0	23.64
24X-4, 145-150	222.75	14.24	48.99	582.79	4.96	7.5	34.5	1037.0	28.36

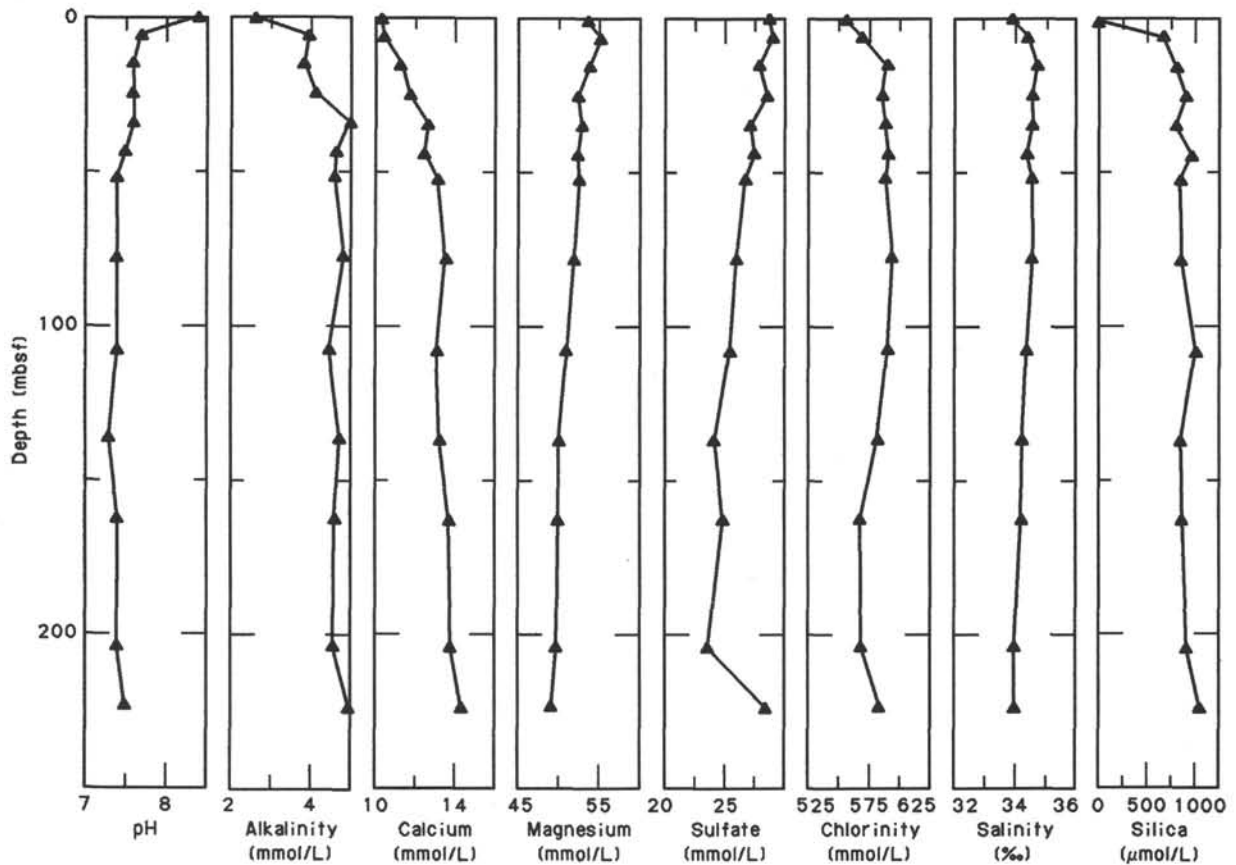


Figure 12. Summary of interstitial water analyses, Hole 708A, as a function of sub-bottom depth. Surface seawater is plotted at 0 mbsf.

The results of the discrete measurements of  $V_p$  vs. depth are given in Table 8 and displayed in Figure 18. The  $P$ -wave logger data are illustrated in Figure 19. On average, the results from both techniques are in good agreement, with the discrete measurements being slightly lower than the continuous log. This discrepancy was due to fracturing within the discrete samples. The high-frequency variation of the  $P$ -wave logger results with depth (Fig. 19), and is due to the many alternating turbidite-pelecagic ooze layers.

The interface between two media of differing impedances will cause reflection of acoustic waves. This is the principle be-

hind seismic-reflection profiling. The impedance of a sediment is an intrinsic property that will vary for different lithologies. One can use the measured impedances of a series of beds in two simple ways: (1) to identify seismic (e.g., 90 Hz) and higher-frequency (e.g., 3.5 kHz) "reflectors" and (2) to resolve and characterize lithologies.

We combined the discrete measurements for wet-bulk density and  $V_p$  given in Tables 7 and 8 to yield the downhole impedance profile shown in Figure 18. It shows the general trend of increasing impedance with depth, in addition to three significant "apparent horizons." The first is a positive peak at 30 mbsf, which

Table 5. Mineralogy determined by using X-ray diffraction.

Sample interval (cm)	Depth (mbsf)	Parameters			
		Calcite (%)	Quartz (%)	Aragonite (%)	Dolomite (%)
115-708A-					
1H-2, 76-77	2.26	66.0	2.6	30.7	0.7
1H-4, 58-59	5.08	98.0	2.0	0	0
1H-4, 125-130	5.75	100.0	0	0	0
2H-2, 109-110	11.59	98.3	1.7	0	0
2H-4, 125-130	14.75	98.0	2.0	0	0
2H-5, 35-36	15.35	97.2	2.8	0	0
2H-6, 124-125	17.74	99.3	0.7	0	0
3H-4, 125-130	24.35	98.5	1.5	0	0
3H-5, 66-67	25.26	96.4	0.4	4.2	0
3H-6, 33-34	26.43	98.5	1.5	0	0
4H-2, 55-57	30.15	98.7	1.3	0	0
4H-3, 32-33	31.42	97.2	2.8	0	0
4H-3, 111-112	32.21	99.9	0.1	0	0
4H-4, 107-109	33.67	71.9	0.4	27.6	0.1
4H-4, 125-130	33.85	75.6	8.8	13.8	1.8
4H-5, 32-33	34.42	98.8	1.2	0	0
4H-5, 111-112	35.21	97.1	0.5	2.7	0
4H-7, 61-62	37.71	98.7	0.9	0	0.5
5H-3, 39-40	40.99	98.1	1.4	0	0.5
5H-4, 125-130	43.35	100.0	0	0	0
5H-4, 135-136	43.45	98.3	1.3	0	0
5H-6, 135-136	46.45	96.5	0.7	0	2.8
5H-6, 144-145	46.54	95.5	2.4	0	2.1
6H-2, 27-28	48.97	97.5	2.0	0	0.5
6H-2, 136-137	50.06	97.3	1.9	0	0.8
6H-3, 25-27	50.45	99.0	1.0	0	0
6H-3, 27-28	50.47	98.3	2.7	0	0
6H-3, 70-71	50.90	98.0	2.0	0	0
6H-3, 125-130	51.45	100.0	0	0	0
6H-5, 25-26	52.35	97.9	0	0	0.4
6H-5, 113-114	53.23	89.0	6.0	0	5.0
6H-7, 117-119	55.77	98.3	1.6	0	0.1
7H-2, 60-61	58.90	95.4	4.2	0	0.4
7H-2, 117-118	59.47	94.6	4.6	0	0.8
7H-3, 25-26	60.05	98.0	0.8	0	1.2
7H-3, 137-138	61.17	97.3	2.7	0	0
7H-4, 26-27	61.56	96.2	3.1	0	0.7
7H-4, 141-142	62.71	99.5	0.5	0	0
8H-2, 135-136	69.25	98.3	1.4	0	0.3
8H-4, 25-26	71.15	96.6	2.4	0	1.0
8H-6, 25-26	74.15	99.8	0.8	0	0
9X-1, 125-130	77.25	97.0	0	0	3.0
13X-1, 22-23	11.22	98.8	1.2	0	0
13X-2, 11-12	111.57	95.6	4.4	0	0
13X-2, 126-127	112.72	97.0	3.0	0	0
13X-3, 12-13	113.08	97.3	2.7	0	0
13X-5, 11-12	116.07	97.5	2.5	0	0
14X-1, 135-137	121.95	90.0	10.0	0	0
14X-2, 25-27	122.35	99.7	0.3	0	0
14X-2, 135-137	123.45	99.6	0.2	0	0.2
14X-3, 13-14	123.73	98.0	2.0	0	0
14X-3, 135-137	124.95	98.0	2.0	0	0
15X-2, 40-41	132.20	98.7	1.3	0	0
15X-5, 58-59	136.88	95.0	5.0	0	0
16X-2, 68-69	142.18	96.8	3.2	0	0
16X-5, 53-55	146.53	87.0	12.0	0	1.0
17X-3, 137-38	153.97	98.6	1.4	0	0
18X-2, 5-52	160.85	99.8	0.2	0	0
22X-1, 118-119	198.68	100.0	0	0	0
22X-3, 43-44	200.93	100.0	0	0	0
22X-4, 66-67	202.66	100.0	0	0	0
22X-4, 120-122	203.20	100.0	0	0	0
22X-6, 55-57	205.55	100.0	0	0	0
24X-4, 120-122	222.50	100.0	0	0	0

Note: We are assuming that the sample is composed solely of calcite, quartz, aragonite, and dolomite.

extends vertically over 20 m. The second is a small step which occurs at 105 mbsf. The third feature, at 210 mbsf, is the possible onset of another "step," occurring at the base of the hole. The evidence for the definition of the latter two horizons is weak, due to the large discrete sampling intervals.

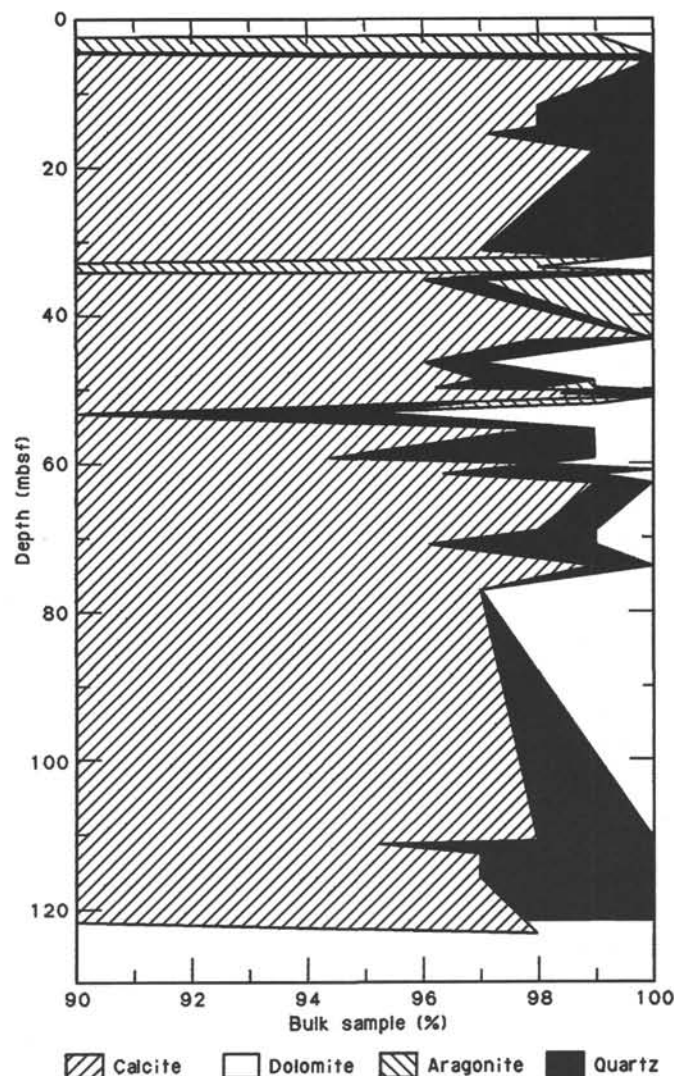


Figure 13. Percent mineralogy as determined by X-ray diffraction. Patterns are defined on diagram.

In order to increase the vertical depth resolution, we created an impedance profile from a combination of the continuous *P*-wave logger and GRAPE wet-bulk density data. These data did not match, point for point, due to differences in data collection rates and uncertainties in the intervals over which we collected the data. In addition, the density of measurements (over 30,000 downhole GRAPE density values!) required that some statistical averaging or smoothing be employed. A simple windowed averaging procedure was applied to these data in order to produce a quick unrefined impedance profile.

Figure 19 illustrates the *P*-wave velocity and GRAPE density logs for Site 708. Each data set was divided into windows of 0.5 m in core length downhole. We averaged the windowed values for both wet-bulk density and velocity and used the product of these averages to evaluate an impedance profile, which is also shown in Figure 19. Intervals greater than 10 m, where no impedance data occur, are not connected by a solid line. The continuous impedance profile allows resolution of the higher-frequency (thicker than 1 m) turbidite beds, in addition to lower-frequency contrasts. The existence of apparent horizons obtained from the discrete data set (shown in Fig. 18) is not supported by the continuous impedance data; only the "step" feature occurring between 100 and 125 mbsf is present in both

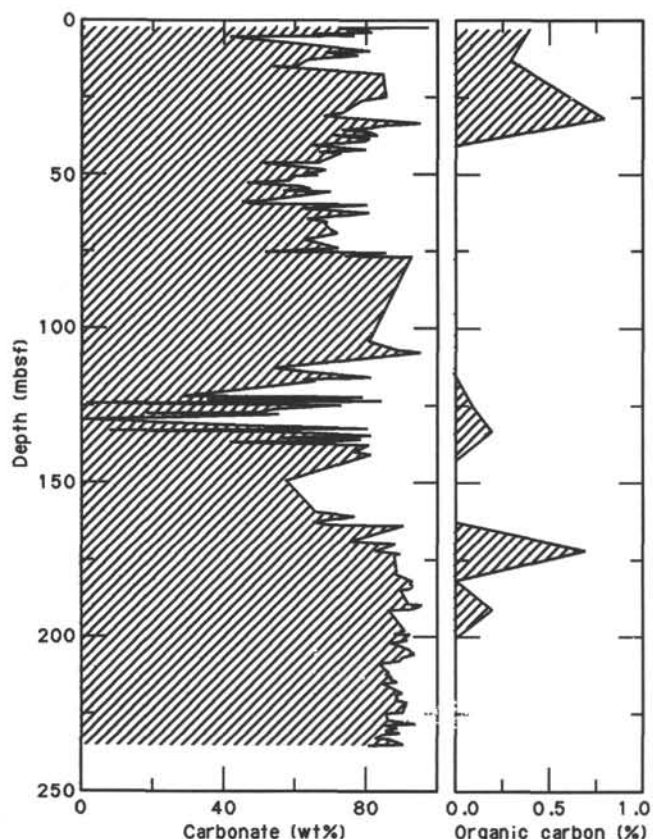


Figure 14. Carbonate and organic carbon content of samples from Hole 708A plotted against increasing sub-bottom depth.

records. These observations show the importance of closely spaced measurements, relative to the scale of the features requiring resolution.

Another application of the impedance data calculated for Hole 708A was to produce a high-resolution profile over the length of one core. We selected Core 115-708A-25X as an example, using a window length of 10 cm; plots of impedance,  $V_p$ , and wet-bulk density are shown in Figure 20. A plot of the impedance for this core is shown beside a simplified lithologic description in Figure 21. One can see that the peaks in the impedance curve correlate well with the turbidite layers. Within the turbidites, the impedance increases from the top to the base, with a sudden decrease at the transition to the underlying pelagic ooze. The impedance gradient at these interfaces is dependent on the sharpness of the boundary: immediate lithologic changes produce a sharp impedance contrast, whereas gradual changes create gradual impedance differences. The distinct peaks toward the base of the turbidite layers (e.g., at 231.1 mbsf) are due to graded bedding. Interbedded ash layers also create impedance increases but on a much smaller scale than the turbidites. The pelagic nannofossil oozes and chalks have a relatively constant impedance of  $2750 \text{ g/cm}^2 \cdot \text{s} \cdot 10^2$ .

#### Shear-Wave Velocity and Shear Strength

The variation of shear-wave velocity ( $V_s$ ) with depth is shown in Figure 22 and is given in Table 9. These data show a slow increase in  $V_s$  from 50 to 100 m/s over the first 50 mbsf, between 100 and 250 m/s to 175 mbsf, and then a decrease to between 50 and 150 m/s for the remainder of the hole. The fluctuations in  $V_s$  appear to be superimposed upon an underlying increasing velocity gradient, although we restricted testing to the less stiff units at depths greater than 175 mbsf.

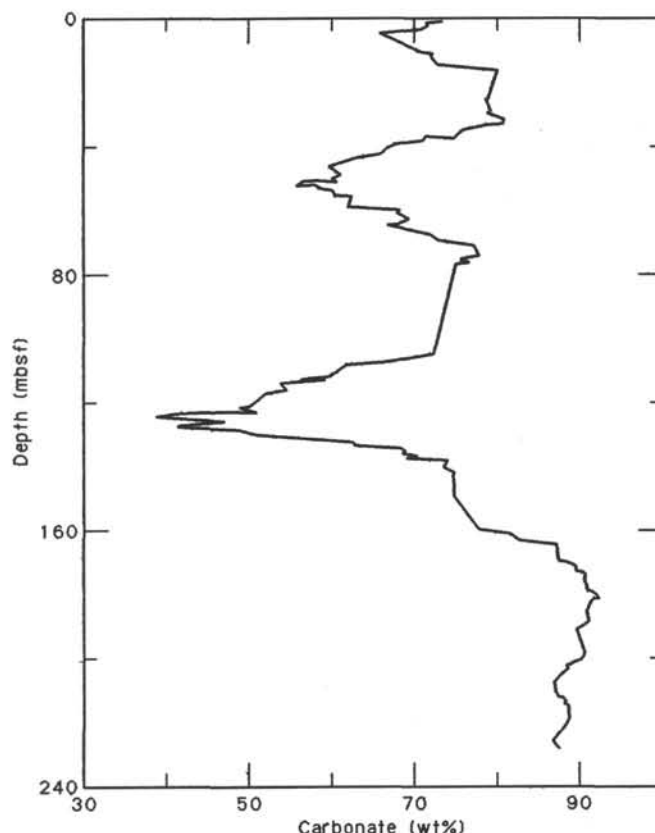


Figure 15. Ten-sample running mean of carbonate data shown in Table 6, plotted as a function of sub-bottom depth.

Two broad categories define the shear velocities: (1) a velocity of 50–100 m/s, which was characteristic of “sticky” clay-bearing nannofossil oozes, soft nannofossil oozes, and nannofossil-bearing foraminiferal sands and silts; and (2) a velocity of 150–250 m/s, which was measured in stiff clay-bearing nannofossil oozes showing various degrees of consolidation.

The results for (maximum) shear strength for the pelagic-turbidite sequence of sediments at Hole 708A are given in Table 10 and are plotted together with  $V_s$  in Figure 22. The average shear strength increases steadily from 15 kPa at the seafloor to 100 kPa at a depth of 150 mbsf and then decreases slowly to 50 kPa at 225 mbsf. The fluctuations in shear strength correlate fairly well with the variations of  $V_s$  with depth.

#### Thermal Conductivity

We measured thermal conductivity in Hole 708A at intervals of at least once per section (1.5 m). This was part of the ongoing effort to obtain a large number of conductivity measurements in carbonate-rich sediments and to correlate these data with the accompanying physical property and composition data. The conductivity data are shown in Figure 23 and presented in Table 11. The data show a general increase with depth, from approximately  $1.1 \text{ W} \cdot \text{m}^{-1} \cdot \text{K}^{-1}$  at the surface, to  $1.5 \text{ W} \cdot \text{m}^{-1} \cdot \text{K}^{-1}$  at 225 mbsf. High local variability is again present, as at Site 707. There are sections of the hole where the variability is reduced, such as from 65 to 80 mbsf and from 185 to 210 mbsf. We observed no “extreme” values in these sediments, and the overall amplitude of local variability is less than at Site 707.

#### Summary

Site 708 provided an alternating series of over 200 turbidite beds interbedded within pelagic oozes and chalks. Discrete mea-

Table 6. Carbonate content of samples from Hole 708A.

Sample interval (cm)	Depth (mbsf)	Carbonate (wt%)
115-708A-		
1H-2, 76-78	2.26	97.39
1H-2, 111-112	2.61	71.95
1H-3, 32-33	3.32	78.53
1H-3, 111-112	4.11	81.53
1H-4, 32-33	4.82	64.56
1H-4, 58-60	5.08	76.35
1H-4, 111-112	5.61	41.43
1H-6, 86-88	8.36	71.18
2H-1, 111-112	10.11	81.06
2H-2, 32-33	10.82	68.29
2H-2, 109-111	11.59	77.77
2H-2, 111-112	11.61	76.6
2H-3, 111-112	13.11	63.57
2H-5, 32-33	15.32	59.79
2H-5, 35-38	15.35	53.71
2H-5, 111-112	16.11	60.83
2H-6, 32-33	16.82	74.51
2H-6, 111-112	17.61	83.94
2H-6, 124-125	17.74	84.70
3H-5, 66-69	25.26	85.65
3H-6, 33-36	26.43	78.71
3H-6, 55-58	30.15	73.12
4H-2, 111-112	30.71	70.12
4H-3, 32-33	31.42	67.7
4H-3, 111-112	32.21	81.69
4H-4, 107-109	33.67	95.11
4H-5, 32-33	34.42	84.26
4H-5, 111-112	35.21	81.14
4H-6, 32-33	35.92	72.54
4H-6, 111-112	36.71	81.22
4H-7, 61-64	37.71	83.00
4H-7, 32-33	37.42	70.68
5H-1, 135-136	38.95	81.19
5H-2, 25-26	39.35	79.38
5H-2, 39-42	39.49	79.41
5H-3, 25-26	40.85	64.70
5H-4, 25-26	42.35	79.93
5H-4, 91-94	43.01	66.65
5H-4, 135-136	43.45	72.85
5H-6, 135-136	46.45	66.74
5H-6, 144-147	46.54	50.83
6H-2, 27-28	48.97	68.71
6H-2, 136-137	50.06	63.29
6H-3, 25-26	50.45	65.27
6H-3, 27-31	50.47	66.31
6H-3, 70-71	50.90	59.90
6H-5, 25-26	52.35	58.27
6H-5, 27-31	52.37	57.63
6H-5, 113-114	53.23	46.40
6H-6, 60-61	54.20	61.94
6H-7, 25-26	54.85	64.36
6H-7, 99-102	55.59	56.77
6H-7, 117-118	55.77	69.92
7H-2, 60-61	58.90	50.25
7H-2, 71-74	59.01	45.09
7H-2, 117-118	59.47	47.99
7H-3, 25-26	60.05	80.44
7H-3, 137-138	61.17	61.69
7H-4, 15-18	61.45	62.17
7H-4, 26-27	61.56	64.13
7H-4, 141-142	62.71	80.85
7H-6, 25-26	64.55	63.46
7H-6, 45-48	64.75	63.46
7H-6, 135-136	65.65	68.94
7H-7, 21-22	66.01	68.26
8H-1, 135-136	67.75	69.71
8H-2, 135-136	69.25	71.91
8H-3, 25-26	69.65	72.17
8H-4, 25-26	71.15	62.72
8H-6, 25-26	74.15	72.17
8H-6, 90-94	74.80	64.63
8H-6, 135-136	75.25	51.67
8H-7, 25-26	75.65	85.93
9X-1, 72-75	76.72	74.24

Table 6 (continued).

Sample interval (cm)	Depth (mbsf)	Carbonate (wt%)
115-708A-(cont.)		
9X-1, 89-92	76.89	93.06
12X-2, 137-139	104.27	80.98
12X-4, 92-94	106.82	88.73
12X-5, 56-58	107.96	95.41
13X-1, 22-23	111.22	71.25
13X-2, 126-128	112.72	56.25
13X-2, 110-111	112.56	54.58
13X-3, 120-121	114.16	65.07
13X-4, 124-126	115.70	81.63
13X-5, 80-82	116.76	62.35
13X-5, 115-116	117.11	65.88
14X-1, 25-26	120.85	37.15
14X-1, 135-136	121.95	28.15
14X-2, 25-26	122.35	78.93
14X-2, 88-90	122.98	35.26
14X-2, 135-136	123.45	84.31
14X-3, 52-53	124.12	1.24
14X-3, 135-136	124.95	73.04
14X-4, 25-26	125.35	62.11
14X-4, 112-113	126.22	54.03
14X-5, 53-54	127.13	49.62
14X-5, 85-87	127.45	18.28
14X-5, 135-136	127.95	55.59
14X-6, 145-146	129.55	0.70
15X-1, 25-26	130.55	22.48
15X-1, 135-136	131.65	50.53
15X-2, 40-42	132.20	78.58
15X-2, 64-65	132.44	80.31
15X-2, 135-136	133.15	7.58
15X-3, 25-26	133.55	51.80
15X-3, 137-138	134.67	81.45
15X-4, 49-50	135.29	56.14
15X-4, 110-112	135.90	78.48
15X-5, 25-26	136.55	70.7
15X-5, 58-60	136.88	41.77
15X-5, 136-137	137.66	80.86
15X-6, 50-51	140.00	76.71
15X-7, 24-25	141.00	81.42
16X-7, 25-26	149.25	57.46
18X-1, 25-26	159.55	66.12
18X-1, 135-136	160.65	72.79
18X-2, 25-26	161.05	76.75
18X-3, 25-26	162.55	65.05
18X-3, 135-136	163.65	70.48
18X-4, 25-26	164.05	90.58
19X-1, 16-17	168.76	75.40
19X-1, 128-129	169.88	88.46
19X-3, 44-45	172.04	82.70
19X-3, 128-129	172.88	89.62
19X-4, 24-25	173.34	88.05
20X-1, 38-39	178.58	88.84
20X-1, 122-123	179.42	88.58
20X-2, 42-43	180.12	89.67
20X-2, 135-136	181.05	91.72
20X-3, 38-40	181.58	93.24
20X-3, 120-121	182.40	92.26
20X-4, 38-39	183.08	93.20
20X-4, 134-135	184.04	92.26
20X-5, 34-35	184.54	89.79
21X-1, 25-26	188.15	91.88
21X-1, 135-136	189.25	92.56
21X-2, 25-26	189.65	95.73
21X-2, 135-136	190.75	92.33
21X-3, 25-26	191.15	86.26
22X-1, 135-136	198.85	87.93
22X-2, 11-12	199.11	92.38
22X-2, 135-136	200.35	90.77
22X-3, 25-26	200.75	91.60
22X-3, 135-136	201.85	86.93
22X-4, 25-26	202.25	88.49
22X-4, 119-120	203.19	90.23
22X-5, 25-26	203.75	92.21
22X-6, 27-28	205.27	93.79
22X-6, 135-136	206.35	90.28
23X-1, 25-26	207.35	89.47

Table 6 (continued).

Sample interval (cm)	Depth (mbsf)	Carbonate (wt%)
115-708A-(cont.)		
23X-1, 135-136	208.45	83.75
23X-3, 135-136	211.45	86.69
23X-4, 25-26	211.85	85.48
23X-4, 135-136	212.95	87.49
23X-5, 25-26	213.35	86.49
23X-5, 135-136	214.45	88.87
23X-6, 25-26	214.85	84.67
24X-1, 133-134	218.13	89.90
24X-2, 25-26	218.55	88.44
24X-2, 133-134	219.63	88.97
24X-3, 25-26	220.05	88.13
24X-3, 135-136	221.15	91.51
24X-5, 133-134	224.13	90.35
24X-6, 14-15	224.44	85.50
25X-1, 25-26	226.75	86.0
25X-1, 135-136	227.85	93.78
25X-2, 25-26	228.25	85.15
25X-2, 134-135	229.34	88.73
25X-3, 25-26	229.75	85.33
25X-3, 134-135	230.84	89.37
25X-4, 25-26	231.25	84.95
25X-4, 134-135	232.34	82.89
25X-5, 30-31	232.80	86.8
25X-5, 134-135	233.84	89.65
25X-6, 25-26	234.25	90.57
25X-6, 59-60	234.59	80.98

measurements of the physical properties of this series were determined at intervals too large to resolve the fluctuations of each variable with depth. Continuous logging techniques such as the GRAPE and the *P*-wave logger allowed resolution of adjacent beds.

One can distinguish the pelagic nannofossil oozes and nannofossil chinks from the coarser-grained turbidites using the well-resolved impedance profiles obtained from GRAPE and *P*-wave logger results. The nannofossil oozes and chinks have impedances typically ranging between 2300 and 2800 g/cm<sup>2</sup>·s·10<sup>2</sup>. The coarse turbidites are characterized by sharp impedance peaks of 2400 to 3500 g/cm<sup>2</sup>·s·10<sup>2</sup>; the fine-grained turbidites are of similar impedance as the pelagic oozes.

The index property measurements do not show a marked difference between the turbidites and the pelagic sediments, except that the more clay-rich pelagic sediments have a higher water content. The water contents vary from 60% at the top of the hole to 40% at the base, and porosities vary from 80% to 60% over the same interval. The carbonate content ranges between 20% to 98% (in those samples selected for index property measurements), which allows one to distinguish the clay-bearing pelagic oozes from the CaCO<sub>3</sub>-rich turbidites. The shear strengths and shear-wave velocities of the coarse-grained turbidites are lower than those for the clay-rich pelagic sediments.

### SEISMIC STRATIGRAPHY

Site 708 is located on the abyssal plain between the northern part of the Mascarene Plateau and the Madingley Rise, a re-

gional topographic high south of the Carlsberg Ridge. This ocean crust was formed by seafloor spreading between India and the northwestern Mascarene Plateau (Seychelles Bank to Saya de Malha Bank) during Paleocene times (Patriat, 1983). Two near-parallel seismic reflection lines (RC17-07 and V34-06) run in a northeast-southwest direction across the region, and these are crossed obliquely by a third reflection line (Wilkes 1719; Fig. 24). We placed Site 708 on the RC17-07 line (22 May 1974, 0715 hr) just north of the Wilkes 1719 crossing.

The basement reflector reveals an undulating relief with an amplitude up to 200–300 m, creating a large number of minor, sediment-filled depressions. Many of these troughs are only a few miles wide, occasionally intersected by even narrower basement highs ("pinnacles"). The RC17-07 line shows moderately strong reflective layers down to the basement, mostly arranged in an orderly fashion with some disturbances in the sediment lying directly above the basement "pinnacles" (Fig. 25). The sediment thickness varies between about 300 and 600 m, and Site 708 was located over a local basement depression holding an estimated 600-m-thick sediment pile (0.64 s, two-way traveltime).

The final seismic survey began 9 nmi prior to arrival at the projected target and overlapped with the RC17-07 line. The *JOIDES Resolution* line (115-3) shows considerably more detail than the RC17-07 line, emphasizing the acoustic disturbance in the sediment deposited on the basement highs (Figs. 25 and 26). However, we dropped the beacon in the target basin because of the coherent appearance of the internal reflectors. From the drilling results, we know that this layered appearance is due to numerous thin turbidites, probably derived from elevated regions 120 nmi to the south (vicinity of Site 707) and 90 nmi to the north (Madingley Rise).

### REFERENCES

- Bonatti, E., 1981. Metal deposits in the oceanic lithosphere. In Emiliani, C. (Ed.), *The Sea* (Vol. 7): New York (Wiley), 639–686.
- Fisher, R. L., Bunce, E. T., et al., 1974. *Init. Repts. DSDP*, 24: Washington (U.S. Govt. Printing Office).
- Fisher, R. L., Sclater, J. G., and McKenzie, D. P., 1971. Evolution of the Central Indian Ridge, western Indian Ocean. *Geol. Soc. Am. Bull.*, 82:553–562.
- Froelich, P. N., Klinkhammer, G. P., Bender, M. L., Luedtke, N. A., Heath, G. R., Cullen, D., Dauphin, P., Hartman, B., Hammond, D., and Maynard, V., 1979. Early oxidation of organic matter in pelagic sediments of the eastern Equatorial Atlantic: suboxic diagenesis. *Geochim. Cosmochim. Acta*, 43:1075–1090.
- Kennett, J. P., 1981. Marine tephrochronology. In Emiliani, C. (Ed), *The Sea* (Vol. 7): New York (Wiley), 1373–1436.
- Lyle, M., 1983. The brown-green color transition in marine sediments: a marker of the Fe(III)-Fe(II) redox boundary. *Limnol. Oceanogr.*, 28: 1026–1033.
- Patriat, P., 1983. Evolution du système de dorsales de l'Océan Indien [Ph.D. thesis]. Université Paris VI.
- Schlich, R., 1982. The Indian Ocean: aseismic ridges, spreading centers, and oceanic basins. In Nairn, A.E.M., and Stehli, F. G. (Eds.), *The Ocean Basins and Margins* (Vol. 6): New York (Plenum), 51–147.
- van Andel, T. H., 1975. Mesozoic-Cenozoic calcite compensation depth and the global distribution of calcareous sediments. *Earth Planet. Sci. Lett.*, 26:187–194.

Ms 115A-107

Table 7. Index-properties data, Site 708.

Section interval (cm)	Depth (mbsf)	Water content (%)	Porosity (%)	Wet-bulk density (g/cm <sup>3</sup> )	Dry-bulk density (g/cm <sup>3</sup> )	Grain density (g/cm <sup>3</sup> )	Carbonate content (wt%)
115-708A-							
1H-2, 76	2.26	26.94	50.03	1.93	1.41	2.75	97.39
1H-4, 58	5.08	57.12	78.52	1.28	0.55	2.77	76.35
1H-6, 86	8.36	54.24	75.61	1.53	0.70	2.64	71.18
2H-2, 109	11.59	50.66	73.18	1.50	0.74	2.68	77.77
2H-5, 35	15.35	56.87	77.02	1.34	0.58	2.56	53.61
2H-6, 124	17.74	35.25	59.35	1.44	0.93	2.72	84.70
3H-3, 133	22.93	51.78	73.56	1.46	0.70	2.61	92.22
3H-3, 59	22.19	47.57	70.42	1.59	0.83	2.65	75.31
3H-5, 66	25.26	44.44	67.78	1.58	0.88	2.66	85.65
3H-6, 33	26.43	48.50	73.18	1.52	0.78	2.93	78.71
4H-2, 53	30.13	52.40	73.59	2.37	1.13	2.55	73.12
4H-4, 107	33.67	34.73	58.58	1.77	1.15	2.69	95.11
4H-7, 61	37.71	42.82	66.51	1.63	0.93	2.68	83.00
5H-2, 39	39.49	44.99	67.06	1.55	0.85	2.51	79.41
5H-4, 91	43.01	51.13	73.51	1.46	0.72	2.68	66.65
5H-6, 144	46.54	53.12	75.88	1.47	0.69	2.80	50.83
6H-3, 27	50.47	51.90	74.22	1.49	0.71	2.69	66.31
6H-5, 27	52.37	54.10	75.44	1.48	0.68	2.63	57.63
6H-7, 99	55.59	55.95	80.44	1.40	0.62	3.27	56.77
7H-2, 71	59.01	55.83	77.17	1.47	0.65	2.69	45.09
7H-3, 96	60.76	53.62	75.75	1.48	0.69	2.72	61.44
7H-4, 15	61.45	51.09	73.84	1.50	0.73	2.73	62.17
7H-6, 45	64.75	52.24	74.81	1.47	0.70	2.74	63.40
7H-7, 45	66.25	57.17	77.12	1.40	0.60	2.54	62.95
8H-2, 84	68.74	54.77	77.19	1.45	0.65	2.82	64.96
8H-3, 36	69.76	50.23	74.06	1.52	0.76	2.86	70.80
8H-6, 90	74.80	53.19	74.87	1.47	0.69	2.64	64.63
9X-1, 72	76.72	49.17	71.45	1.50	0.76	2.61	74.24
9X-1, 89	76.89	44.93	68.84	1.57	0.86	2.74	93.06
10X-2, 83	84.43	58.70	77.28	1.40	0.58	2.41	54.53
12X-2, 137	104.27	44.04	67.71	1.58	0.88	2.69	80.98
12X-4, 92	106.82	39.79	64.40	1.68	1.01	2.77	88.73
12X-5, 56	107.96	40.61	64.60	1.68	1.00	2.70	95.41
13X-2, 126	112.72	56.17	77.16	1.42	0.62	2.65	56.25
13X-4, 124	115.70	42.73	66.59	1.60	0.92	2.70	81.63
13X-5, 80	116.76	46.45	70.15	1.58	0.85	2.74	62.35
14X-2, 88	122.98	57.78	78.15	1.38	0.58	2.63	35.26
14X-5, 85	127.45	59.82	79.63	1.37	0.55	2.64	18.28
15X-2, 40	132.20	39.87	64.72	1.64	0.98	2.80	78.58
15X-5, 58	136.88	42.19	65.76	1.60	0.93	2.66	41.77
16X-2, 68	142.18	35.94	59.69	1.69	1.09	2.67	62.07
16X-5, 53	146.53	44.06	66.57	1.59	0.89	2.56	16.74
17X-3, 137	153.97	36.28	59.57	1.69	1.07	2.62	71.63
17X-5, 18	155.78	34.90	58.48	1.71	1.11	2.66	51.97
18X-2, 50	161.30	40.38	64.69	1.67	0.99	2.74	93.84
18X-4, 31	164.11	40.56	65.46	1.64	0.97	2.81	89.78
19X-2, 69	170.79	29.19	52.62	1.86	1.32	2.73	92.42
19X-4, 14	173.24	39.73	64.08	1.66	1.00	2.74	85.10
20X-1, 94	179.14	43.58	67.81	1.61	0.91	2.76	82.79
20X-2, 126	180.96	41.83	66.39	1.66	0.97	2.78	91.46
20X-4, 46	183.16	39.25	63.38	1.68	1.02	2.71	93.67
20X-5, 71	184.91	41.86	66.04	1.64	0.95	2.73	86.56
21X-1, 97	188.87	41.09	65.58	1.66	0.98	2.76	88.83
21X-2, 87	190.27	38.92	63.04	1.70	1.04	2.71	92.26
22X-1, 118	198.68	39.07	62.84	1.66	1.01	2.67	81.02
22X-3, 43	200.93	38.38	61.60	1.66	1.02	2.61	88.93
22X-6, 55	205.55	38.92	63.37	1.69	1.03	2.75	90.97
23X-2, 26	208.86	34.12	57.75	1.74	1.15	2.67	95.91
23X-4, 60	212.20	43.30	67.32	1.81	1.03	2.73	85.89
23X-6, 14	214.74	36.41	60.86	1.68	1.07	2.75	86.97
24X-1, 135	218.15	42.50	66.97	1.63	0.94	2.78	85.84
24X-3, 47	220.27	42.21	65.61	1.64	0.95	2.64	88.09
24X-4, 66	221.96	34.10	57.14	1.75	1.16	2.61	91.03
25X-1, 76	227.26	44.59	70.05	1.60	0.89	2.94	80.94
25X-4, 118	232.18	43.23	66.87	1.62	0.92	2.68	84.07

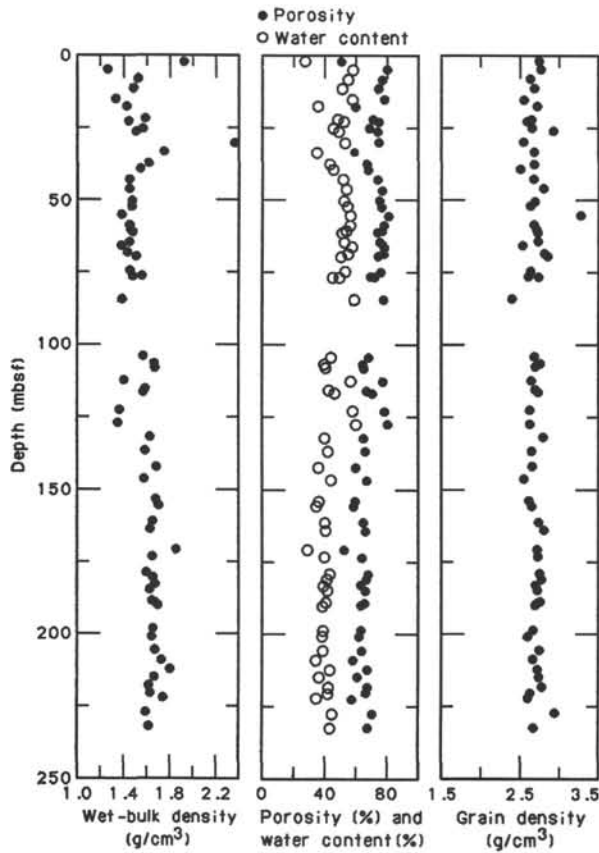


Figure 16. Index properties (wet-bulk density, water content, porosity, and grain density) at Site 708.

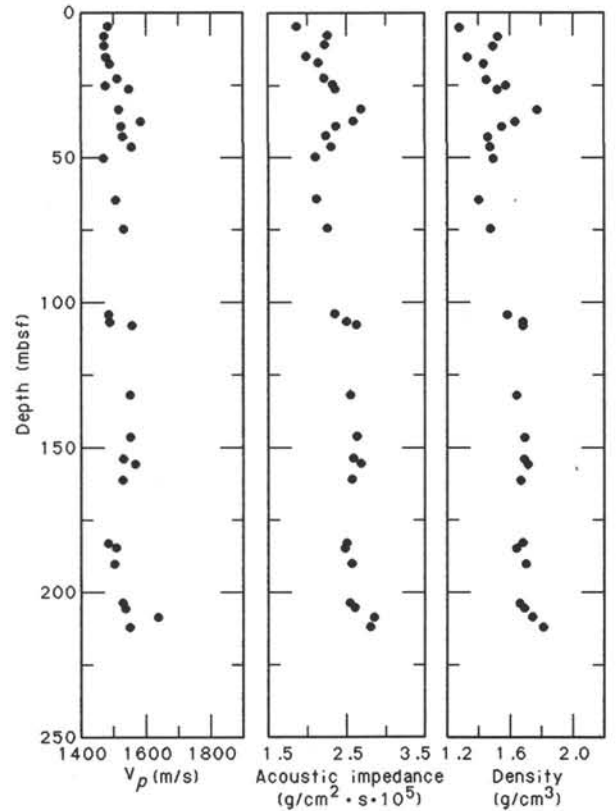


Figure 18. Compressional-wave velocity ( $V_p$ ), acoustic impedance, and wet-bulk density of discrete samples at Site 708.

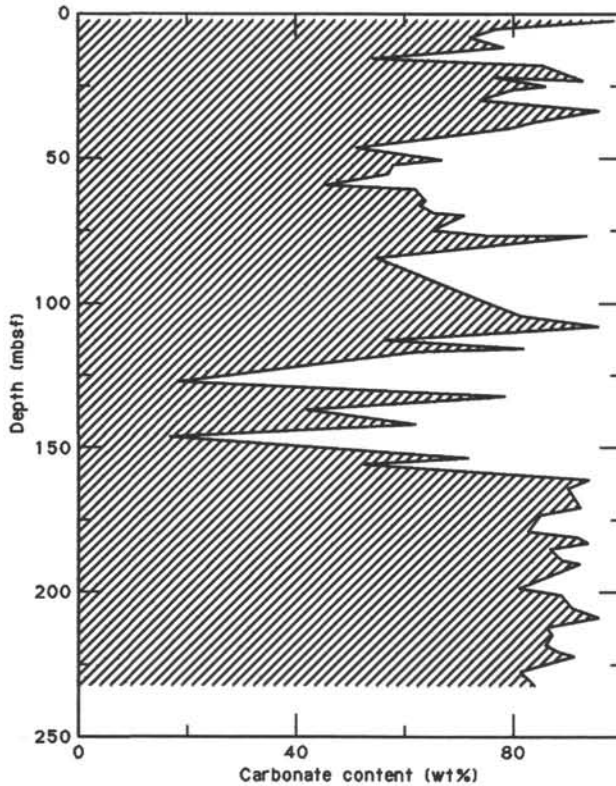


Figure 17. Carbonate content of samples for which the index properties were measured at Site 708.

Table 8. Compressional-wave velocity and acoustic impedance data, Site 708.

Section interval (cm)	Depth (mbsf)	$V_p$ (m/s)	Acoustic impedance ( $g/cm^2 \cdot s \cdot 10^5$ )
115-708A-			
1H-4, 58	5.08	1485	1.86
1H-6, 86	8.36	1473	2.25
2H-2, 109	11.59	1474	2.21
2H-5, 35	15.35	1479	1.98
2H-6, 120	17.70	1492	2.14
3H-3, 133	22.93	1516	2.21
3H-5, 66	25.26	1478	2.33
3H-6, 33	26.43	1551	2.35
4H-4, 107	33.67	1519	2.68
4H-7, 61	37.71	1587	2.58
5H-2, 39	39.49	1527	2.36
5H-4, 91	43.01	1532	2.24
5H-6, 144	46.54	1558	2.30
6H-3, 27	50.47	1472	2.10
7H-7, 45	64.75	1510	2.11
8H-6, 90	74.80	1534	2.25
12X-2, 137	104.27	1488	2.35
12X-4, 92	106.82	1490	2.50
12X-5, 56	107.96	1560	2.62
15X-2, 40	132.20	1555	2.55
16X-5, 53	146.53	1558	2.63
17X-3, 137	153.97	1535	2.59
17X-5, 18	155.78	1571	2.68
18X-2, 50	161.30	1534	2.56
20X-4, 46	183.16	1489	2.50
20X-5, 71	184.91	1513	2.48
21X-2, 87	190.27	1508	2.56
22X-5, 43	203.93	1534	2.54
22X-6, 55	205.55	1541	2.60
23X-2, 26	208.86	1640	2.85
23X-4, 60	212.20	1555	2.81

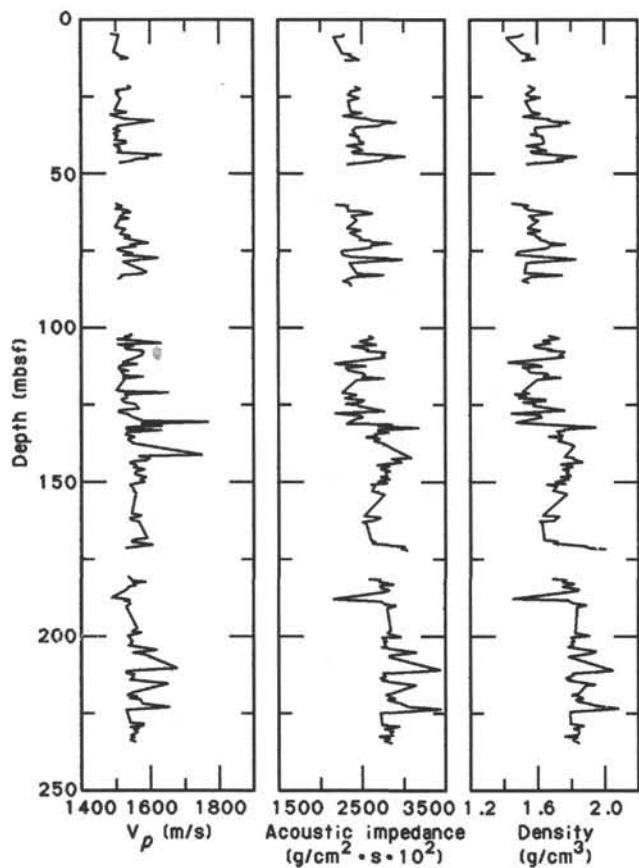


Figure 19. Continuous  $V_p$  record ( $P$ -wave logger), the calculated impedance profile, and the wet-bulk density record (GRAPE) at Site 708.

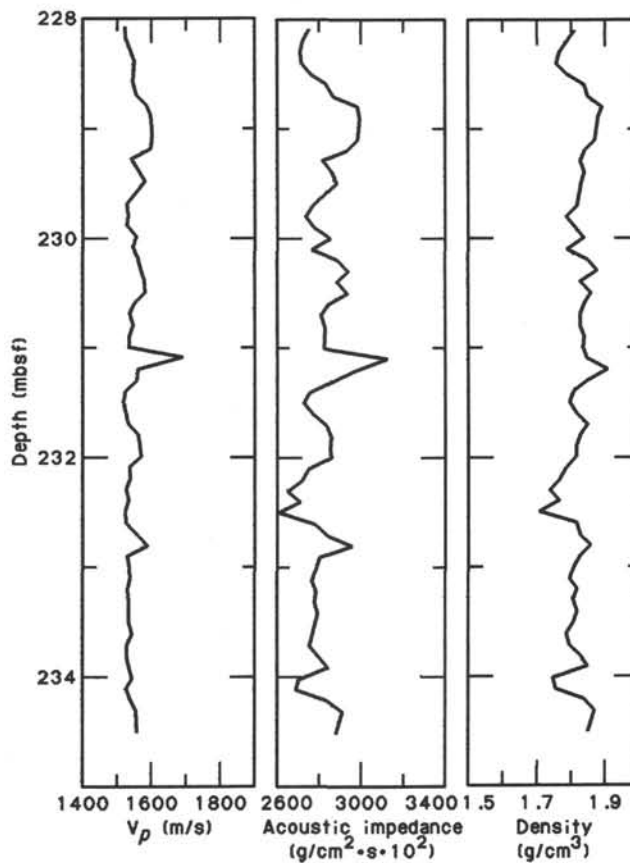


Figure 20. Continuous  $P$ -wave logger, the calculated impedance profile, and the wet-bulk density record (GRAPE) of Core 115-708A-25X at Site 708.

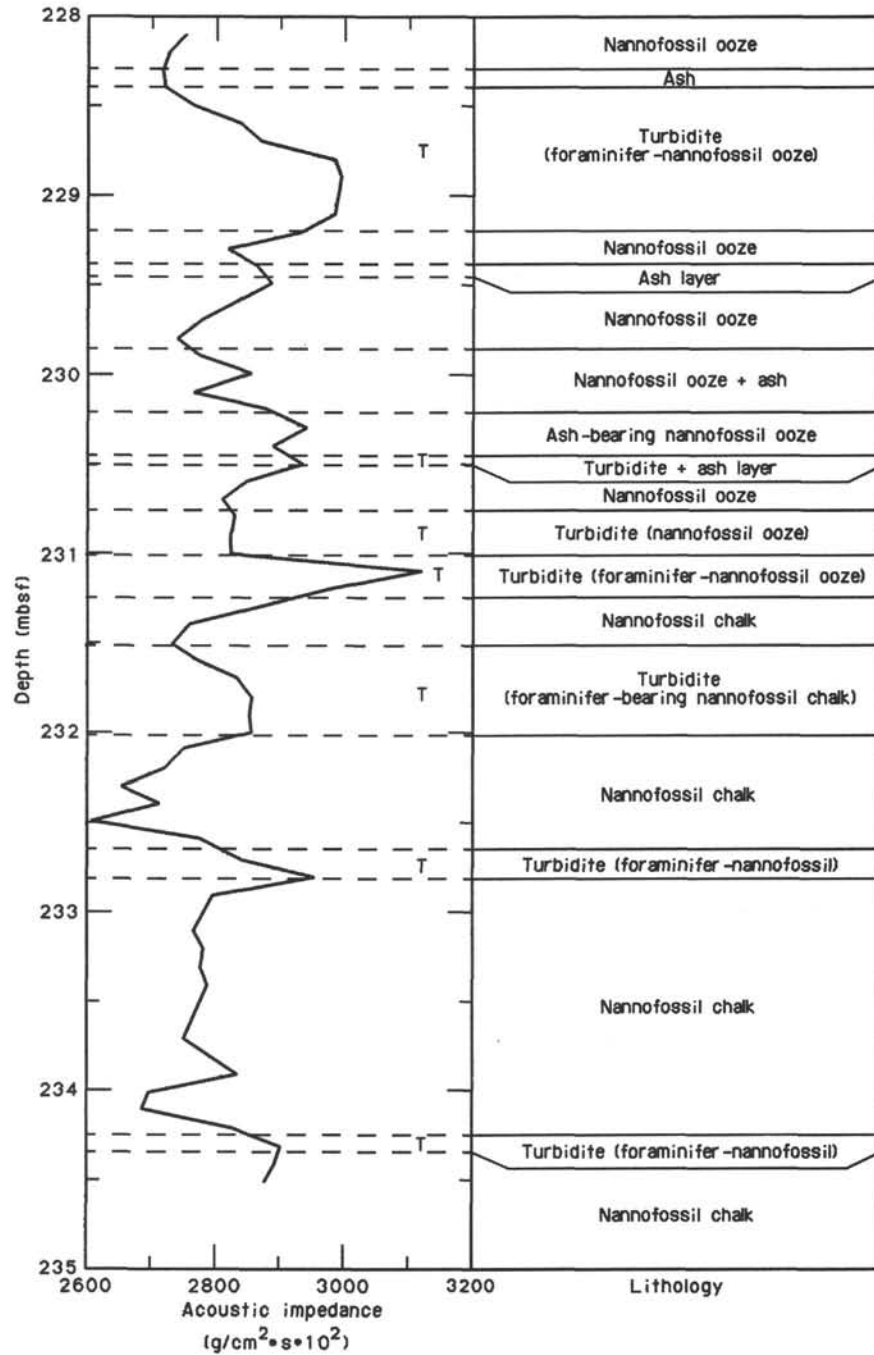


Figure 21. Correlation of the impedance profile with the lithology of Core 115-708A-25X at Site 708. T = turbidite layer.

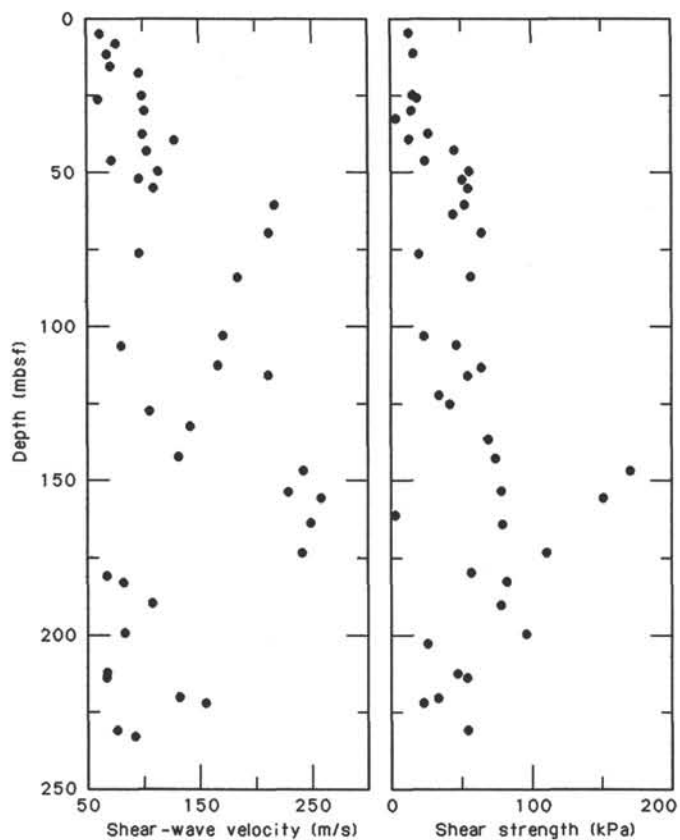


Figure 22. Shear-wave velocity and shear strength at Site 708.

Table 9. Shear-wave velocity data, Site 708.

Section interval (cm)	Depth (mbsf)	$V_s$ (m/s)
115-708A-		
1H-4, 58	5.08	63
1H-6, 86	8.36	76
2H-2, 110	11.60	69
2H-5, 34	15.34	71
2H-6, 124	17.74	96
3H-5, 65	25.25	99
3H-6, 32	26.42	62
4H-2, 55	30.15	102
4H-7, 60	37.70	101
5H-2, 41	39.51	128
5H-4, 95	43.05	104
5H-6, 102	46.12	73
6H-2, 115	49.85	113
6H-5, 52	52.62	97
6H-7, 84	55.44	110
7H-3, 84	60.64	217
8H-3, 40	69.80	212
9X-1, 20	76.20	98
10X-2, 49	84.09	183
12X-2, 32	103.22	172
12X-4, 61	106.51	82
13X-2, 127	112.73	167
13X-4, 125	115.71	212
14X-5, 86	127.46	108
15X-2, 75	132.55	143
16X-2, 70	142.20	133
16X-5, 64	146.64	244
17X-3, 140	154.00	232
17X-5, 18	155.78	260
18X-4, 34	164.14	252
19X-4, 15	173.25	244
20X-2, 121	180.91	71
20X-4, 27	182.97	86
21X-2, 34	189.74	110
22X-2, 27	199.27	86
23X-4, 50	212.10	71
23X-5, 64	213.74	70
24X-3, 57	220.37	135
24X-4, 76	222.06	158
25X-3, 138	230.88	80
25X-5, 55	233.05	94

**Table 10. Motorized shear strength data, Site 708.**

Sample interval (cm)	Depth (mbsf)	Peak (kPa)
115-708A-		
1H-4, 70	5.20	6.5
2H-2, 115	11.65	8.3
3H-5, 58	25.18	7.9
3H-6, 27	26.37	9.5
4H-2, 49	30.09	7.4
4H-4, 38	32.98	1.8
4H-7, 64	37.74	13.6
5H-2, 47	39.57	7.1
5H-4, 98	43.08	23.1
5H-6, 139	46.49	12.4
6H-2, 140	50.10	28.5
6H-5, 64	52.74	25.5
6H-7, 112	55.72	27.9
7H-3, 96	60.76	26.6
7H-5, 85	63.65	22.5
8H-3, 48	69.88	32.6
9X-1, 81	76.81	10.6
10X-2, 66	84.26	29.0
12X-2, 49	103.39	12.4
12X-4, 52	106.36	23.7
13X-2, 121	113.71	32.6
13X-4, 121	116.20	27.9
14X-2, 61	122.71	17.8
14X-5, 92	125.41	22.0
15X-5, 64	136.94	35.5
16X-2, 107	142.75	38.0
16X-5, 64	147.07	85.3
17X-3, 135	153.95	40.3
17X-5, 23	155.83	75.9
18X-2, 60	161.41	2.3
18X-4, 15	164.06	40.5
19X-4, 35	173.45	55.7
20X-2, 47	180.17	29.6
20X-4, 61	182.97	41.5
21X-2, 69	190.09	39.7
22X-2, 62	199.62	48.6
22X-4, 66	202.66	13.1
23X-4, 100	212.60	23.7
23X-5, 65	213.65	27.3
24X-3, 63	220.43	16.6
24X-4, 81	222.11	11.9
25X-3, 145	230.95	27.3

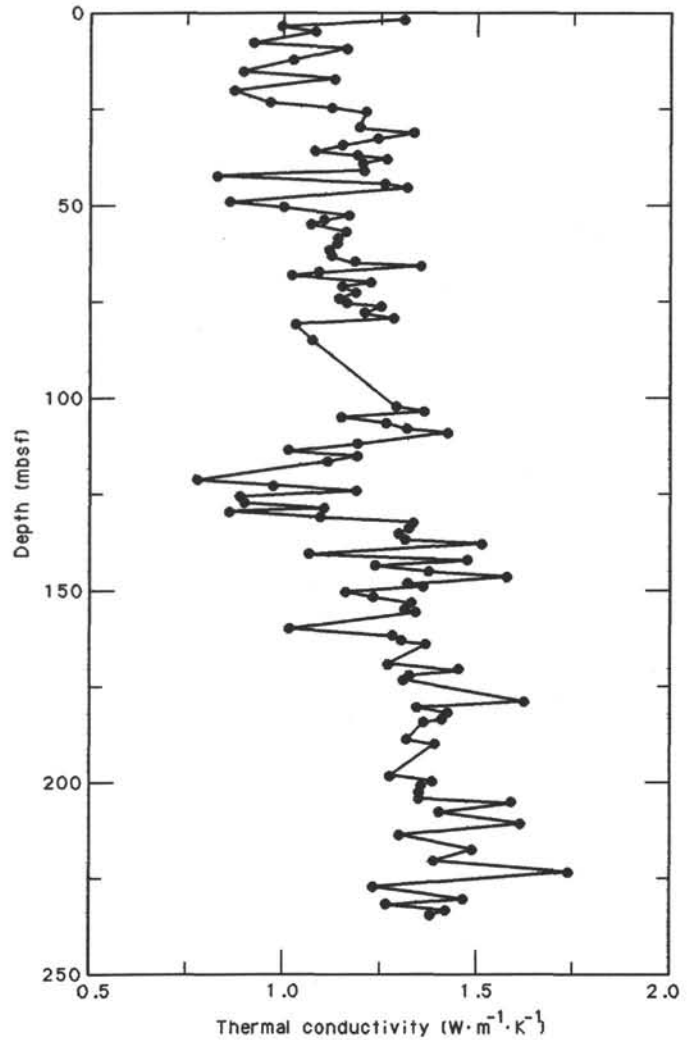


Figure 23. Thermal conductivity at Site 708.

Table 11. Thermal conductivity data, Site 708.

Section interval (cm)	Depth (mbsf)	Thermal conductivity ( $W \cdot m^{-1} \cdot K^{-1}$ )
115-708A-		
1H-2, 80	2.30	1.318
1H-3, 80	3.80	1.003
1H-4, 80	5.30	1.085
1H-6, 80	8.30	0.930
2H-1, 80	9.80	1.167
2H-3, 80	12.80	1.031
2H-5, 80	15.80	0.902
2H-6, 100	17.50	1.137
3H-2, 80	20.90	0.881
3H-4, 60	23.70	0.971
3H-5, 70	25.30	1.132
3H-6, 50	26.60	1.219
4H-2, 80	30.40	1.202
4H-3, 80	31.90	1.342
4H-4, 80	33.40	1.248
4H-5, 80	34.90	1.158
4H-6, 70	36.30	1.089
4H-7, 40	37.50	1.196
5H-1, 80	38.40	1.272
5H-2, 80	39.90	1.211
5H-3, 80	41.40	1.214
5H-4, 80	41.90	0.838
5H-5, 120	44.80	1.268
5H-6, 80	45.90	1.325
6H-2, 80	49.50	0.871
6H-3, 60	50.80	1.007
6H-5, 80	52.90	1.176
6H-6, 60	54.20	1.112
6H-7, 80	55.40	1.078
7H-1, 60	57.40	1.168
7H-2, 90	59.20	1.147
7H-3, 70	60.50	1.145
7H-4, 80	62.10	1.125
7H-5, 80	63.60	1.131
7H-6, 80	65.10	1.190
7H-7, 40	66.20	1.361
8H-1, 125	67.65	1.100
8H-2, 80	68.70	1.031
8H-3, 80	70.20	1.235
8H-4, 80	71.70	1.160
8H-5, 80	73.20	1.194
8H-6, 80	74.70	1.151
8H-7, 40	75.80	1.172
9X-1, 80	76.80	1.258
9X-2, 80	78.30	1.217
9X-3, 80	79.60	1.292
9X-4, 80	81.30	1.039
10X-3, 25	85.35	1.081
12X-1, 100	102.40	1.301
12X-2, 80	103.70	1.373
12X-3, 80	105.20	1.160
12X-4, 80	106.70	1.273
12X-5, 80	108.20	1.328
12X-6, 40	109.30	1.432
13X-2, 80	112.26	1.200
13X-3, 80	113.76	1.022
13X-4, 80	115.26	1.196
13X-5, 80	116.76	1.124
14X-1, 80	121.40	0.787
14X-2, 80	122.90	0.982
14X-3, 80	124.40	1.196
14X-4, 80	125.90	0.898
14X-5, 80	127.40	0.910
14X-6, 80	128.90	1.114
14X-7, 15	129.75	0.873
15X-1, 80	131.10	1.104
15X-2, 80	132.60	1.346
15X-3, 80	134.10	1.335
15X-4, 80	135.60	1.308
15X-5, 80	137.10	1.326
15X-6, 30	138.10	1.526
16X-1, 80	140.80	1.077
16X-2, 80	142.30	1.485
16X-3, 80	143.80	1.249

Table 11 (continued).

Section interval (cm)	Depth (mbsf)	Thermal conductivity ( $W \cdot m^{-1} \cdot K^{-1}$ )
115-708A- (Cont.)		
16X-4, 80	145.30	1.386
16X-5, 80	146.80	1.587
16X-6, 80	148.30	1.334
16X-7, 15	149.15	1.371
17X-1, 80	150.40	1.172
17X-2, 80	151.90	1.240
17X-3, 80	153.40	1.340
17X-4, 80	154.90	1.324
17X-5, 40	156.00	1.349
18X-1, 80	160.10	1.029
18X-2, 80	161.60	1.293
18X-3, 90	163.20	1.317
18X-4, 40	164.20	1.379
19X-1, 80	169.40	1.283
19X-2, 80	170.90	1.462
19X-3, 80	172.40	1.338
19X-4, 40	173.50	1.322
20X-1, 80	179.00	1.631
20X-2, 80	180.50	1.357
20X-3, 80	182.00	1.434
20X-4, 80	183.50	1.420
20X-5, 40	184.60	1.373
21X-1, 80	188.70	1.331
21X-2, 80	190.20	1.401
22X-1, 80	198.30	1.290
22X-2, 80	199.80	1.398
22X-3, 80	201.30	1.369
22X-4, 80	202.80	1.364
22X-5, 80	204.30	1.364
22X-6, 70	205.70	1.599
23X-1, 80	207.90	1.416
23X-3, 80	210.90	1.627
23X-5, 80	213.90	1.315
24X-1, 80	217.60	1.501
24X-3, 80	220.60	1.400
24X-5, 80	223.60	1.749
25X-1, 80	227.30	1.247
25X-3, 80	230.30	1.477
25X-4, 80	231.80	1.282
25X-5, 80	233.30	1.432
25X-6, 40	234.40	1.392

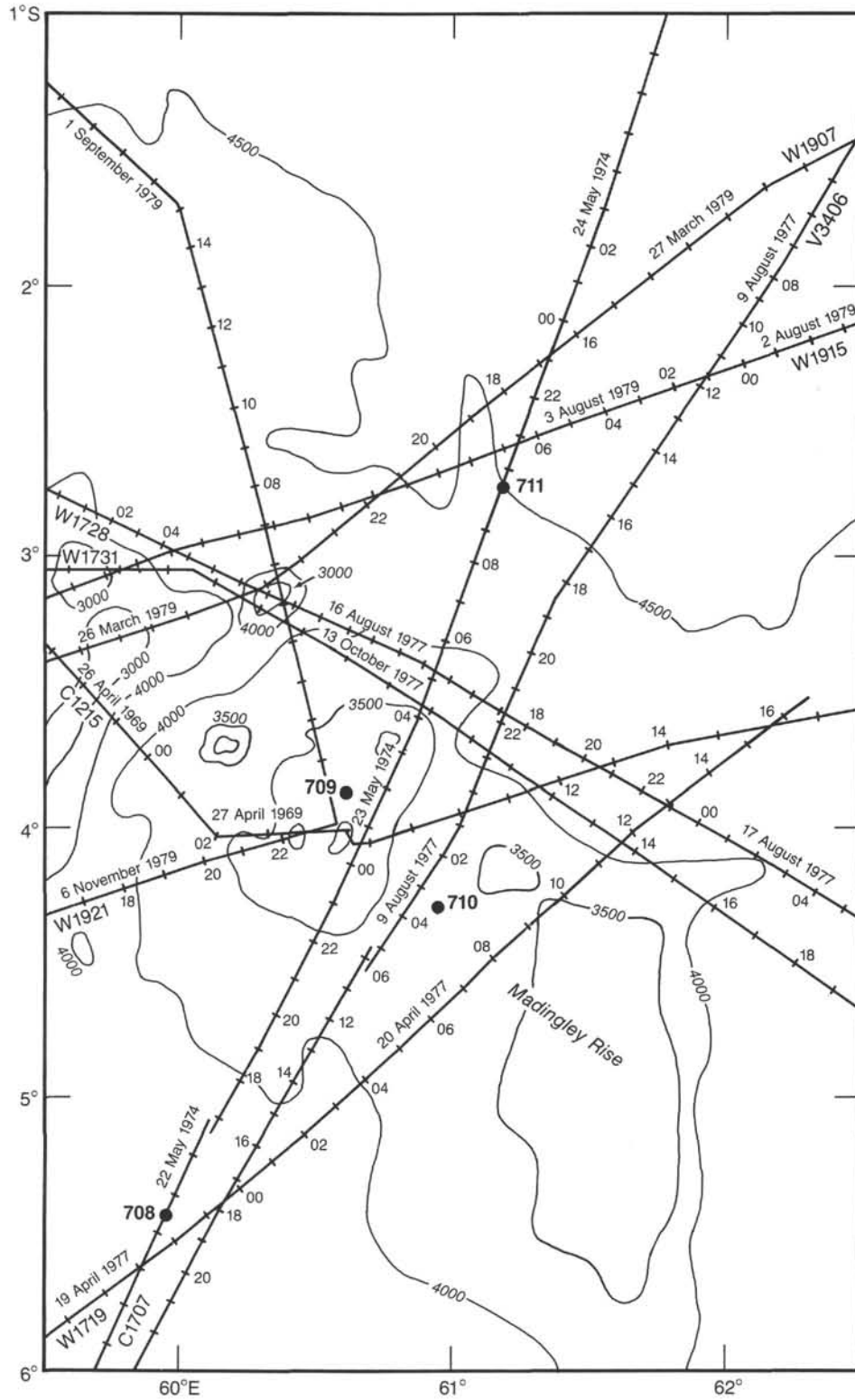


Figure 24. Bathymetric map of the seafloor near Site 708 showing the location of single-channel seismic (SCS) profiles used to select the site. Depth in meters.

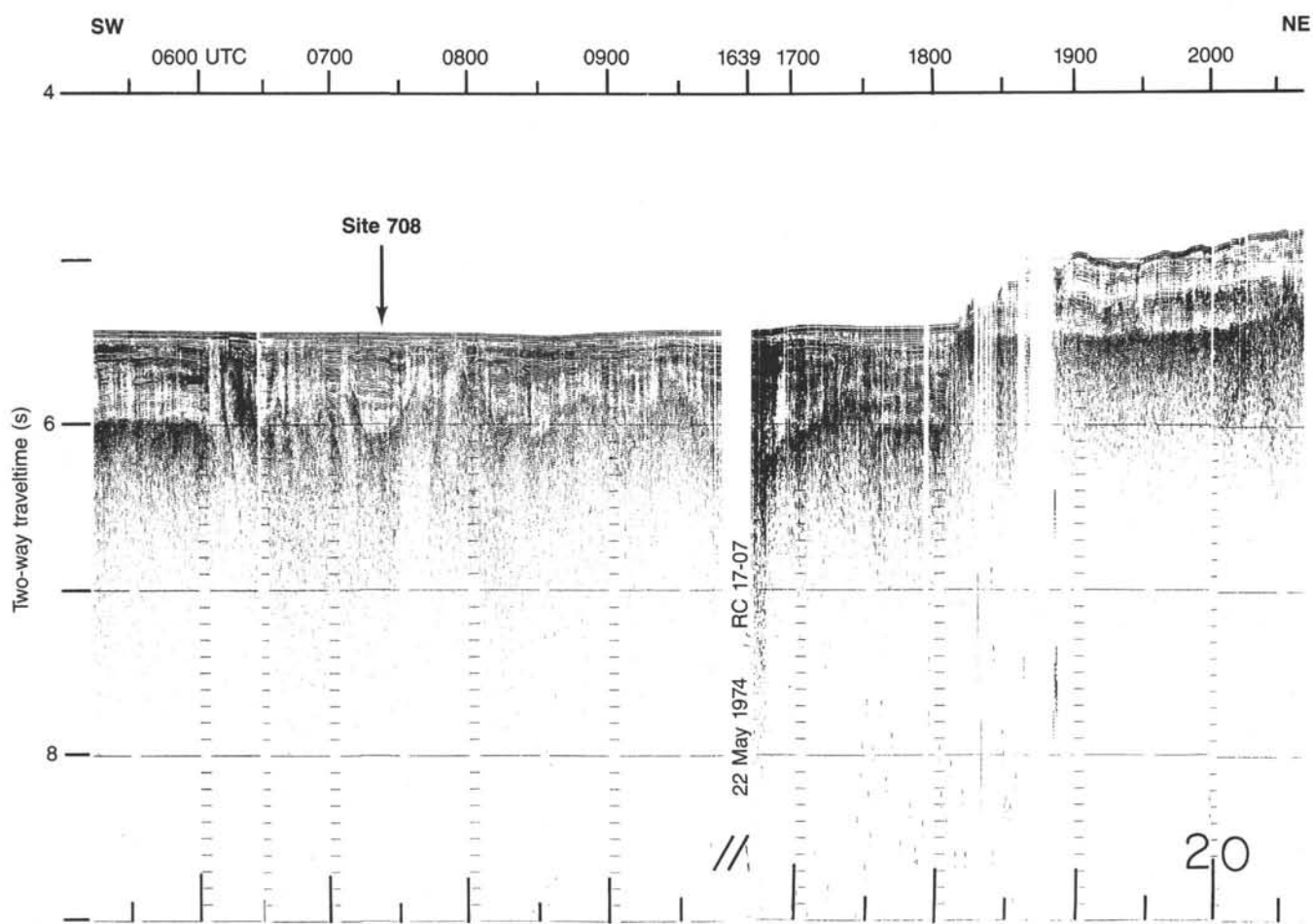


Figure 25. The RC17-07 cruise SCS line (22 May 1974) in the vicinity of Site 708. The basement reflector shows a typical irregular topography produced by seafloor spreading at the Paleocene ridge separating India from the Seychelles-Saya de Malha Banks.

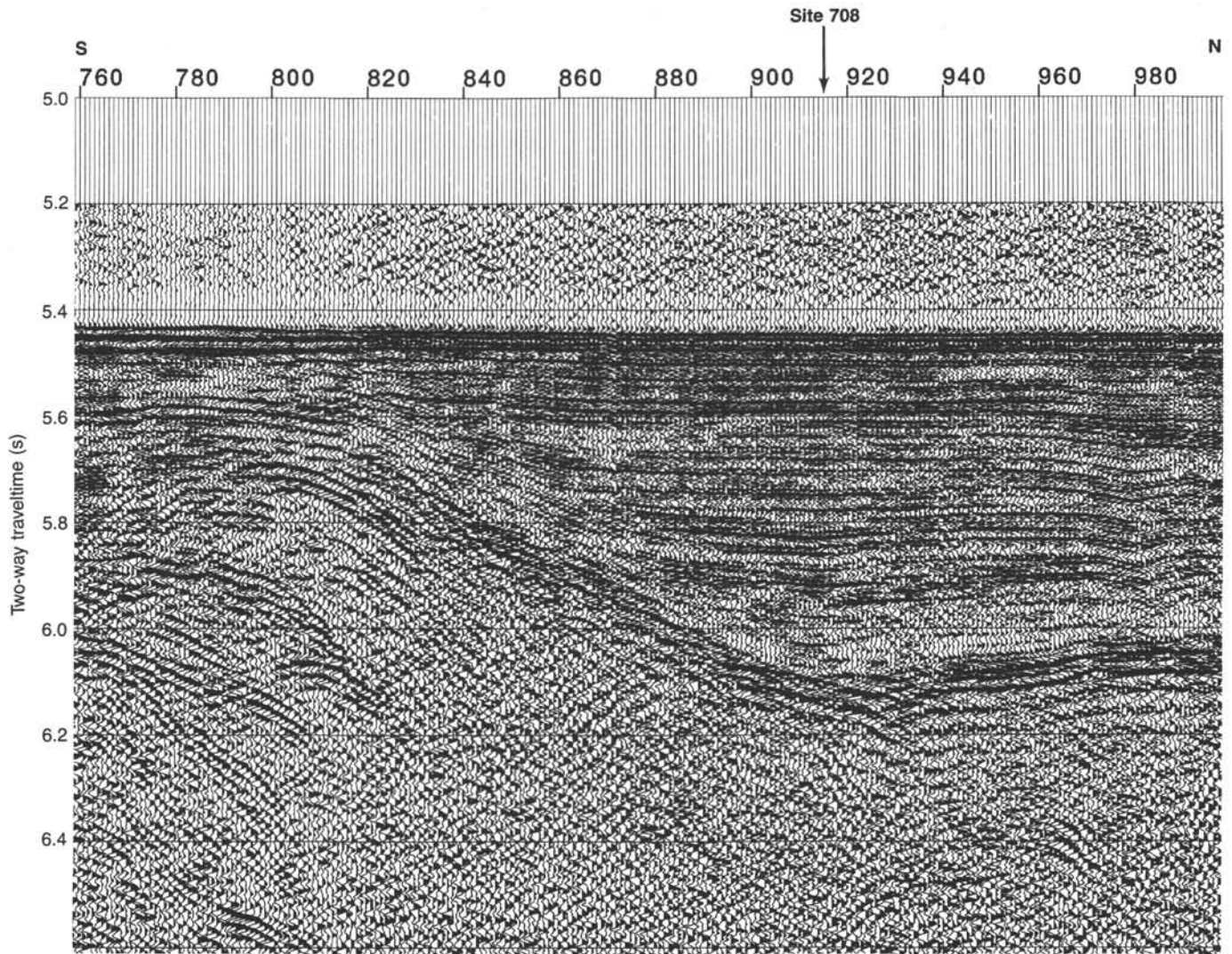
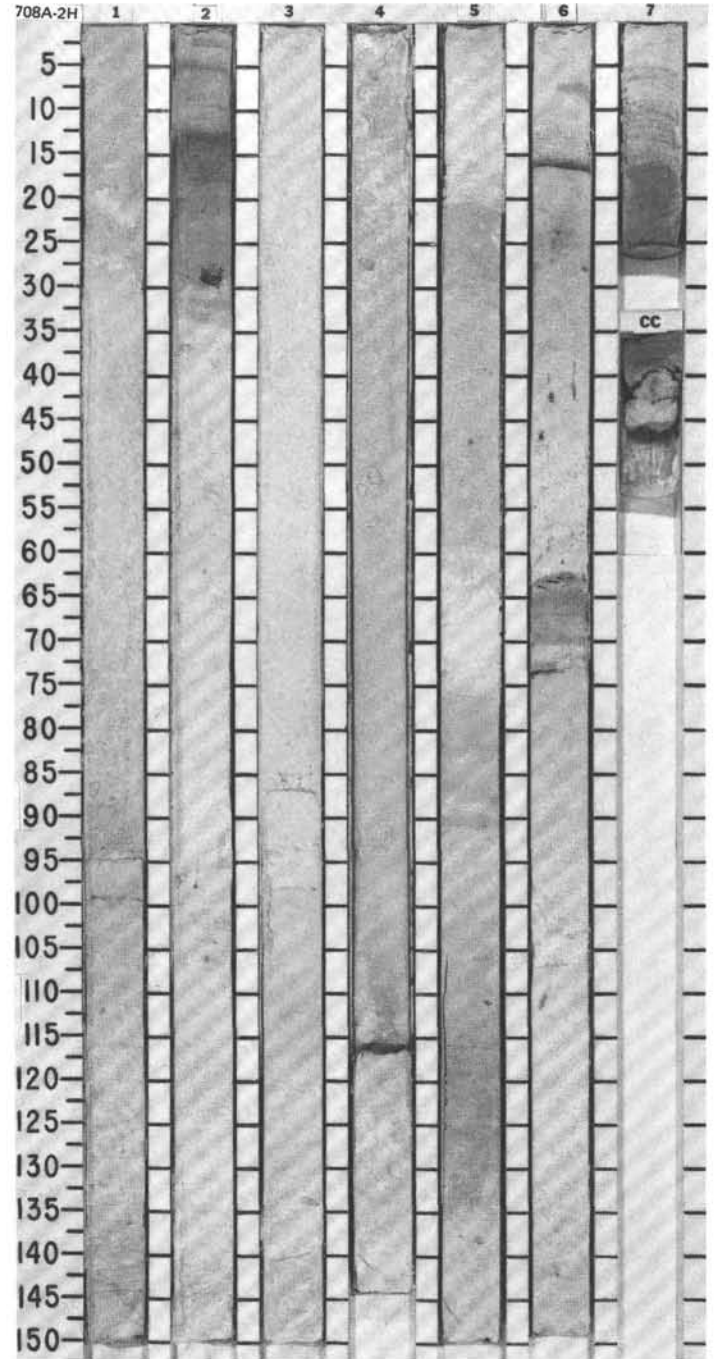


Figure 26. The *JOIDES Resolution* single-channel seismic (SCS), water-gun reflection profile over Site 708 shows the coherent appearance of internal reflectors in this basement-bounded basin. Abrupt impedance changes due to numerous turbidites seem to be the cause of this layering. See Figure 9 in "Underway Geophysics" chapter, this volume, for location of Site 708 track line.



SITE 708 HOLE A CORE 2H CORED INTERVAL 4105.5-4115.1 mbsl; 9.0-18.6 mbsf

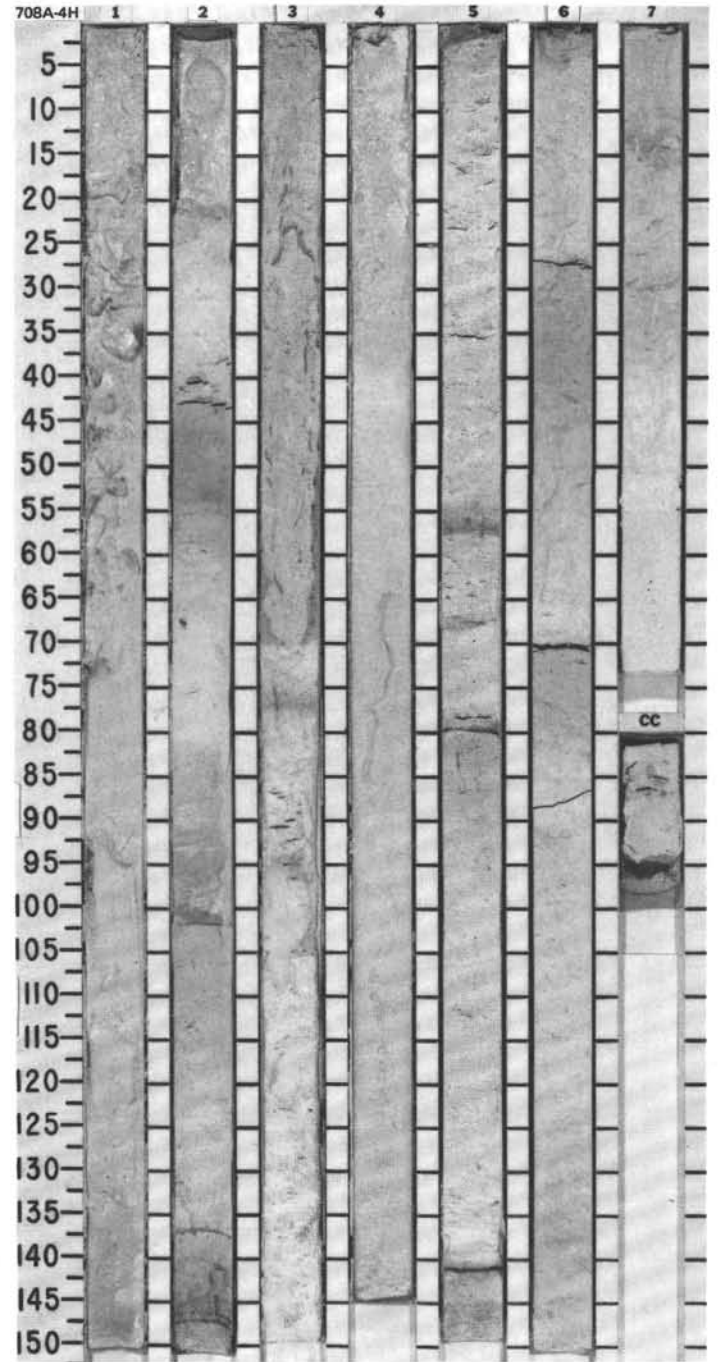
TIME - ROCK UNIT	BIOSTRAT. ZONE/ FOSSIL CHARACTER				PALEOMAGNETICS	PHYS. PROPERTIES	CHEMISTRY	SECTION	METERS	GRAPHIC LITHOLOGY	DRILLING DISTURB.	SED. STRUCTURES	SAMPLES	LITHOLOGIC DESCRIPTION																																																																																										
	FORAMINIFERS	NANNOFOSSILS	RADIOLARIANS	DIATOMS																																																																																																				
PLEISTOCENE	RP								0.5					<p><b>NANNOFOSSIL OOZE</b></p> <p>Major lithology: Nannofossil ooze, white (10YR 8/1, 5YR 8/1), light gray (5Y 7/1), light greenish gray (5GY 7/1), and light blue gray (5B 7/1).</p> <p>Minor lithologies: Nannofossil-bearing foraminiferal ooze, white (2.5Y 8/2, 5Y 8/1); nannofossil foraminiferal ooze, white (10YR 8/1); and diatom-bearing foraminifer-bearing nannofossil ooze, light greenish gray (5GY 5/1).</p> <p>Nine turbidites, 37% of core volume.</p> <p><b>SMEAR SLIDE SUMMARY (%):</b></p> <table border="1"> <thead> <tr> <th></th> <th>1, 65 D</th> <th>2, 62 D</th> <th>5, 48 D</th> <th>6, 68 D</th> <th>7, 20 M</th> </tr> </thead> <tbody> <tr> <td><b>TEXTURE:</b></td> <td></td> <td></td> <td></td> <td></td> <td></td> </tr> <tr> <td>Sand</td> <td>80</td> <td>2</td> <td>5</td> <td>40</td> <td>5</td> </tr> <tr> <td>Silt</td> <td>10</td> <td>40</td> <td>35</td> <td>30</td> <td>—</td> </tr> <tr> <td>Clay</td> <td>10</td> <td>68</td> <td>60</td> <td>30</td> <td>95</td> </tr> </tbody> </table> <p><b>COMPOSITION:</b></p> <table border="1"> <thead> <tr> <th></th> <th>85</th> <th>2</th> <th>2</th> <th>50</th> <th>20</th> </tr> </thead> <tbody> <tr> <td>Foraminifers</td> <td>85</td> <td>2</td> <td>2</td> <td>50</td> <td>20</td> </tr> <tr> <td>Nannofossils</td> <td>15</td> <td>91</td> <td>93</td> <td>18</td> <td>55</td> </tr> <tr> <td>Diatoms</td> <td>—</td> <td>2</td> <td>2</td> <td>—</td> <td>15</td> </tr> <tr> <td>Radiolarians</td> <td>—</td> <td>3</td> <td>3</td> <td>30</td> <td>5</td> </tr> <tr> <td>Sponge spicules</td> <td>—</td> <td>—</td> <td>—</td> <td>2</td> <td>5</td> </tr> <tr> <td>Intraclasts</td> <td>—</td> <td>2</td> <td>—</td> <td>—</td> <td>—</td> </tr> <tr> <td>Silicoflagellates</td> <td>—</td> <td>—</td> <td>—</td> <td>—</td> <td>Tr</td> </tr> <tr> <td>Volcanic glass</td> <td>—</td> <td>—</td> <td>—</td> <td>—</td> <td>—</td> </tr> <tr> <td>Chert</td> <td>—</td> <td>—</td> <td>—</td> <td>—</td> <td>1</td> </tr> </tbody> </table>		1, 65 D	2, 62 D	5, 48 D	6, 68 D	7, 20 M	<b>TEXTURE:</b>						Sand	80	2	5	40	5	Silt	10	40	35	30	—	Clay	10	68	60	30	95		85	2	2	50	20	Foraminifers	85	2	2	50	20	Nannofossils	15	91	93	18	55	Diatoms	—	2	2	—	15	Radiolarians	—	3	3	30	5	Sponge spicules	—	—	—	2	5	Intraclasts	—	2	—	—	—	Silicoflagellates	—	—	—	—	Tr	Volcanic glass	—	—	—	—	—	Chert	—	—	—	—	1
		1, 65 D	2, 62 D	5, 48 D	6, 68 D	7, 20 M																																																																																																		
	<b>TEXTURE:</b>																																																																																																							
	Sand	80	2	5	40	5																																																																																																		
	Silt	10	40	35	30	—																																																																																																		
	Clay	10	68	60	30	95																																																																																																		
		85	2	2	50	20																																																																																																		
Foraminifers	85	2	2	50	20																																																																																																			
Nannofossils	15	91	93	18	55																																																																																																			
Diatoms	—	2	2	—	15																																																																																																			
Radiolarians	—	3	3	30	5																																																																																																			
Sponge spicules	—	—	—	2	5																																																																																																			
Intraclasts	—	2	—	—	—																																																																																																			
Silicoflagellates	—	—	—	—	Tr																																																																																																			
Volcanic glass	—	—	—	—	—																																																																																																			
Chert	—	—	—	—	1																																																																																																			
								1.0																																																																																																





SITE 708 HOLE A CORE 4H CORED INTERVAL 4124.6-4134.1 mbsl; 28.1-37.6 ,bsf

TIME-ROCK UNIT	BIOSTRAT. ZONE/ FOSSIL CHARACTER				PALEOMAGNETICS	PHYS. PROPERTIES	CHEMISTRY	SECTION METERS	GRAPHIC LITHOLOGY	DRILLING DISTURB.	SED. STRUCTURES	LITHOLOGIC DESCRIPTION																																																							
	FORAMINIFERS	NANNOFOSSILS	RADIOLARIANS	DIATOMS																																																															
LATE PLIOGENE	RP	AM CN 12a (NN 18)										<p>NANNOFOSSIL OOZE and FORAMINIFER-NANNOFOSSIL OOZE</p> <p>Major lithologies: Nannofossil ooze, white (5Y 8/1), light gray (5Y 7/1), and light greenish gray (5GY 8/1). Foraminifer-nannofossil ooze, white (5Y 8/1, 10YR 8/2, N9).</p> <p>Minor lithologies: Nannofossil-foraminifer ooze, light gray (5Y 7/1) and white (10YR 7/2).</p> <p>Nine turbidites, 21% of core volume.</p> <p>SMEAR SLIDE SUMMARY (%):</p> <table border="1"> <thead> <tr> <th></th> <th>2, 100 D</th> <th>4, 100 D</th> <th>6, 100 D</th> <th>7, 65 D</th> </tr> </thead> <tbody> <tr> <td>Sand</td> <td>60</td> <td>25</td> <td>15</td> <td>10</td> </tr> <tr> <td>Silt</td> <td>15</td> <td>15</td> <td>10</td> <td>5</td> </tr> <tr> <td>Clay</td> <td>25</td> <td>60</td> <td>75</td> <td>85</td> </tr> </tbody> </table> <p>TEXTURE:</p> <p>COMPOSITION:</p> <table border="1"> <tbody> <tr> <td>Clay</td> <td>—</td> <td>—</td> <td>5</td> <td>5</td> </tr> <tr> <td>Foraminifers</td> <td>70</td> <td>35</td> <td>3</td> <td>3</td> </tr> <tr> <td>Nannofossils</td> <td>25</td> <td>60</td> <td>70</td> <td>80</td> </tr> <tr> <td>Diatoms</td> <td>1</td> <td>—</td> <td>5</td> <td>2</td> </tr> <tr> <td>Radiolarians</td> <td>2</td> <td>2</td> <td>15</td> <td>7</td> </tr> <tr> <td>Sponge spicules</td> <td>2</td> <td>1</td> <td>2</td> <td>2</td> </tr> <tr> <td>Mollusk fragments</td> <td>—</td> <td>2</td> <td>—</td> <td>1</td> </tr> </tbody> </table>		2, 100 D	4, 100 D	6, 100 D	7, 65 D	Sand	60	25	15	10	Silt	15	15	10	5	Clay	25	60	75	85	Clay	—	—	5	5	Foraminifers	70	35	3	3	Nannofossils	25	60	70	80	Diatoms	1	—	5	2	Radiolarians	2	2	15	7	Sponge spicules	2	1	2	2	Mollusk fragments	—	2	—	1
		2, 100 D	4, 100 D	6, 100 D	7, 65 D																																																														
Sand	60	25	15	10																																																															
Silt	15	15	10	5																																																															
Clay	25	60	75	85																																																															
Clay	—	—	5	5																																																															
Foraminifers	70	35	3	3																																																															
Nannofossils	25	60	70	80																																																															
Diatoms	1	—	5	2																																																															
Radiolarians	2	2	15	7																																																															
Sponge spicules	2	1	2	2																																																															
Mollusk fragments	—	2	—	1																																																															
PLEISTOCENE		CN 14a (NN 19)																																																																	
	FM	<i>Pterocanium prismatium</i>																																																																	
	RP	<i>R. praebergonii</i>																																																																	

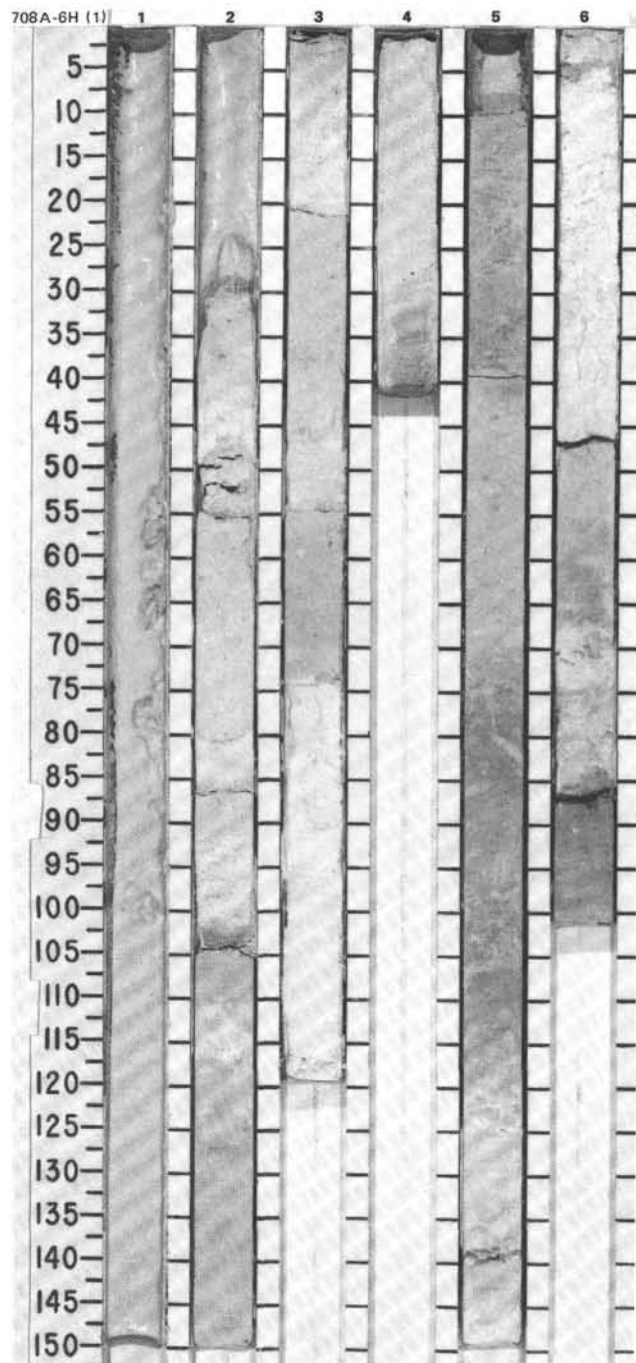




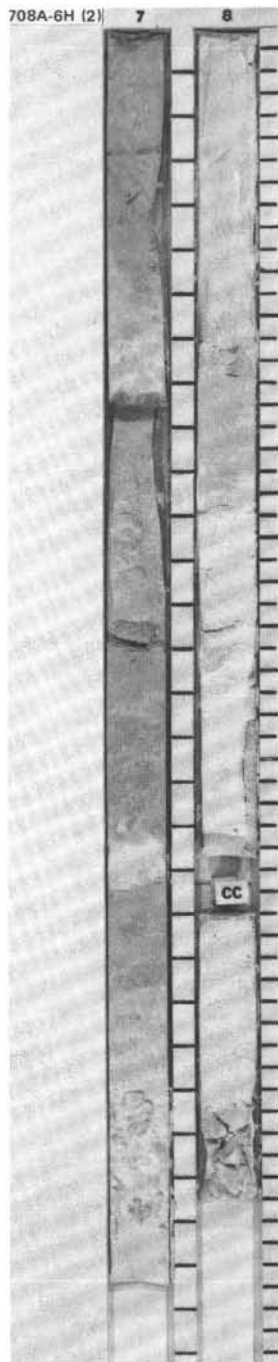
SITE 708 HOLE A CORE 6H CORED INTERVAL 4143.7-4153.3 mbsl; 47.2-56.8 mbsf

TIME-ROCK UNIT	BIOSTRAT. ZONE/ FOSSIL CHARACTER			PALEOMAGNETICS	PHYS. PROPERTIES	CHEMISTRY	SECTION	METERS	GRAPHIC LITHOLOGY	DRILLING DISTURB. BED. STRUCTURES	SAMPLES	LITHOLOGIC DESCRIPTION																																																																
	FORAMINIFERS	NANNOFOSSILS	RADIOLARIANS DIATOMS																																																																									
UPPER PLIOCENE	N 21	CN 12b+c						0.5 1.0				<p>FORAMINIFERAL NANNOFOSSIL OOZE and NANNOFOSSIL OOZE</p> <p>Major lithologies: Foraminiferal nannofossil ooze, light gray (5Y 7/1) and white (N8, N9). Nannofossil ooze, light gray (5GY 7/1).</p> <p>Minor lithologies: Nannofossil foraminiferal ooze, white (N9, 5Y 8/1), and foraminifer-bearing nannofossil ooze, white (N8) and light gray (N7).</p> <p>Thirteen turbidites, 56% of core volume.</p> <p>SMEAR SLIDE SUMMARY (%):</p> <table border="1"> <tr> <td></td> <td>3, 70</td> <td>6, 20</td> <td>7, 70</td> </tr> <tr> <td></td> <td>D</td> <td>D</td> <td>D</td> </tr> </table> <p>TEXTURE:</p> <table border="1"> <tr> <td>Sand</td> <td>10</td> <td>55</td> <td>10</td> </tr> <tr> <td>Silt</td> <td>15</td> <td>5</td> <td>10</td> </tr> <tr> <td>Clay</td> <td>75</td> <td>40</td> <td>80</td> </tr> </table> <p>COMPOSITION:</p> <table border="1"> <tr> <td>Quartz</td> <td>—</td> <td>Tr</td> <td>Tr</td> </tr> <tr> <td>Clay</td> <td>3</td> <td>5</td> <td>—</td> </tr> <tr> <td>Foraminifers</td> <td>5</td> <td>45</td> <td>3</td> </tr> <tr> <td>Nannofossils</td> <td>75</td> <td>40</td> <td>81</td> </tr> <tr> <td>Diatoms</td> <td>5</td> <td>1</td> <td>4</td> </tr> <tr> <td>Radiolarians</td> <td>8</td> <td>5</td> <td>8</td> </tr> <tr> <td>Sponge spicules</td> <td>2</td> <td>3</td> <td>2</td> </tr> <tr> <td>Silicoflagellates</td> <td>1</td> <td>1</td> <td>Tr</td> </tr> <tr> <td>Fish remains</td> <td>Tr</td> <td>Tr</td> <td>Tr</td> </tr> <tr> <td>Mollusk debris</td> <td>1</td> <td>—</td> <td>—</td> </tr> <tr> <td>Pyrite framboids</td> <td>—</td> <td>Tr</td> <td>—</td> </tr> </table>		3, 70	6, 20	7, 70		D	D	D	Sand	10	55	10	Silt	15	5	10	Clay	75	40	80	Quartz	—	Tr	Tr	Clay	3	5	—	Foraminifers	5	45	3	Nannofossils	75	40	81	Diatoms	5	1	4	Radiolarians	8	5	8	Sponge spicules	2	3	2	Silicoflagellates	1	1	Tr	Fish remains	Tr	Tr	Tr	Mollusk debris	1	—	—	Pyrite framboids	—	Tr	—
	3, 70	6, 20	7, 70																																																																									
	D	D	D																																																																									
Sand	10	55	10																																																																									
Silt	15	5	10																																																																									
Clay	75	40	80																																																																									
Quartz	—	Tr	Tr																																																																									
Clay	3	5	—																																																																									
Foraminifers	5	45	3																																																																									
Nannofossils	75	40	81																																																																									
Diatoms	5	1	4																																																																									
Radiolarians	8	5	8																																																																									
Sponge spicules	2	3	2																																																																									
Silicoflagellates	1	1	Tr																																																																									
Fish remains	Tr	Tr	Tr																																																																									
Mollusk debris	1	—	—																																																																									
Pyrite framboids	—	Tr	—																																																																									
							2																																																																					
							3																																																																					
							4	VOID																																																																				
							5																																																																					
							6	VOID																																																																				

Cont.

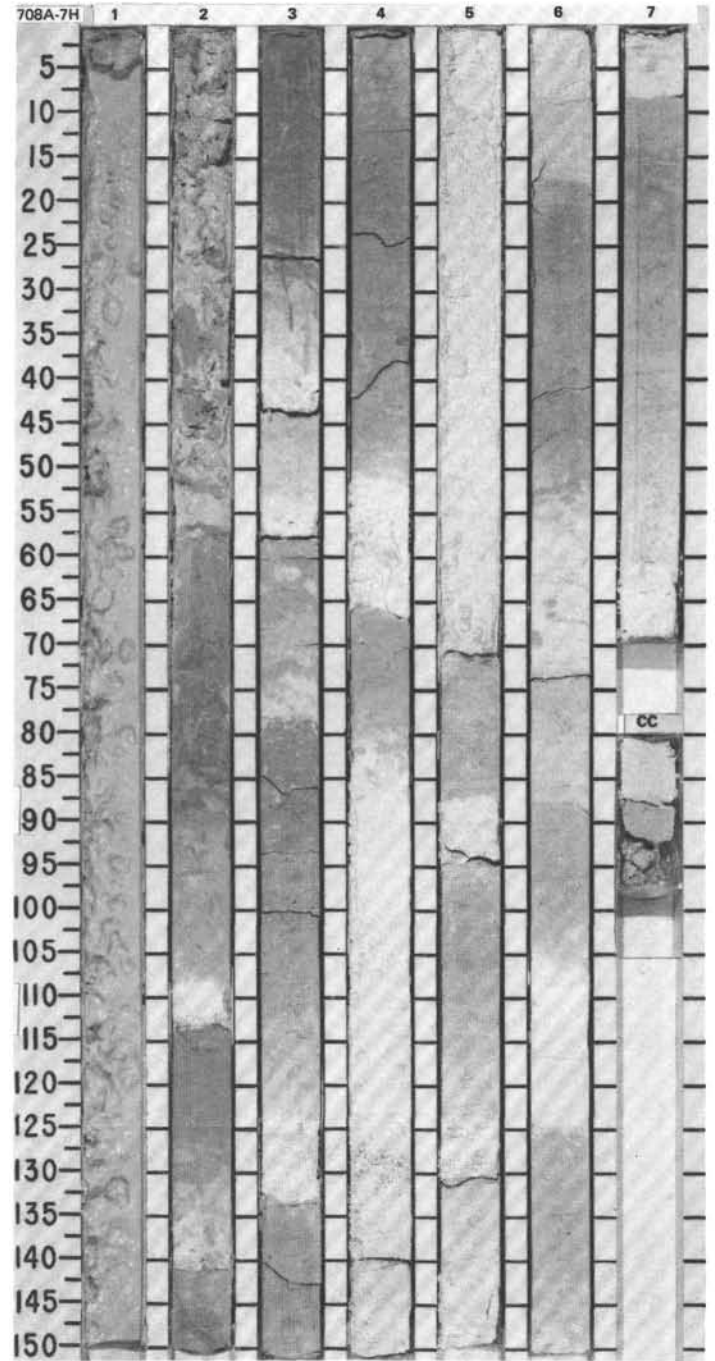


TIME-ROCK UNIT	BIOSTRAT. ZONE/ FOSSIL CHARACTER				PALEOMAGNETICS	PHYS. PROPERTIES	CHEMISTRY	SECTION	METERS	GRAPHIC LITHOLOGY	DRILLING DISTURB.	BED. STRUCTURES	SAMPLES	LITHOLOGIC DESCRIPTION
	FORAMINIFERS	NAKNOFOSSILS	RADIOLARIANS	DIATOMS										
FM									0.5					Cont.
AM								7						
GG								1.0						
RP								8						
								CC						

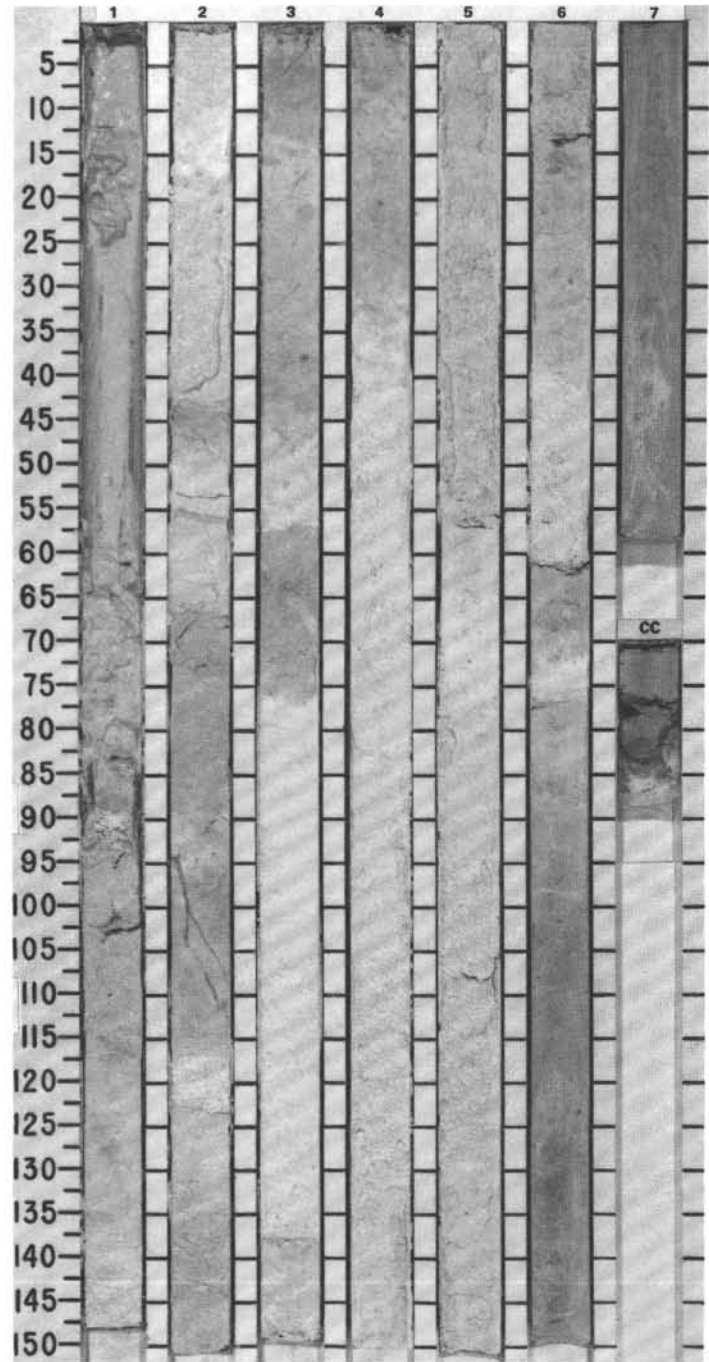


SITE 708 HOLE A CORE 7H CORED INTERVAL 4153.3-4162.9 mbsl; 56.8-66.4 mbsf

TIME-ROCK UNIT	BIOSTRAT. ZONE/ FOSSIL CHARACTER				PHYS. PROPERTIES CHEMISTRY	SECTION METERS	GRAPHIC LITHOLOGY	DRILLING DISTURB.	SED. STRUCTURES	SAMPLES	LITHOLOGIC DESCRIPTION																																										
	FORAMINIFERS	NANNOFOSSILS	RADIOLARIANS	DIATOMS																																																	
LOWER PLIOCENE	FM	AP	CG	CM							<p>NANNOFOSSIL OOZE and NANNOFOSSIL FORAMINIFERAL OOZE AND FORAMINIFERAL NANNOFOSSIL OOZE</p> <p>Major lithologies: Nannofossil ooze, light gray (5Y 7/1, 10YR 7/4) and white (10YR 8/2); nannofossil foraminiferal ooze and foraminiferal nannofossil ooze in alternating layers, white (N9, 10YR 9/1).</p> <p>Minor lithology: Foraminifer-bearing nannofossil ooze, white (N9), in Section 2, 0-58 cm.</p> <p>Sixteen turbidites, 50% of core volume.</p> <p>SMEAR SLIDE SUMMARY (%):</p> <table border="1"> <tr> <td></td> <td>3, 56</td> <td>3, 100</td> </tr> <tr> <td>D</td> <td></td> <td>D</td> </tr> </table> <p>TEXTURE:</p> <table border="1"> <tr> <td>Sand</td> <td>50</td> <td>12</td> </tr> <tr> <td>Silt</td> <td>10</td> <td>8</td> </tr> <tr> <td>Clay</td> <td>40</td> <td>80</td> </tr> </table> <p>COMPOSITION:</p> <table border="1"> <tr> <td>Quartz</td> <td>Tr</td> <td>—</td> </tr> <tr> <td>Clay</td> <td>5</td> <td>5</td> </tr> <tr> <td>Dolomite</td> <td>3</td> <td>—</td> </tr> <tr> <td>Foraminifers</td> <td>47</td> <td>5</td> </tr> <tr> <td>Nannofossils</td> <td>36</td> <td>80</td> </tr> <tr> <td>Diatoms</td> <td>1</td> <td>2</td> </tr> <tr> <td>Radiolarians</td> <td>5</td> <td>7</td> </tr> <tr> <td>Sponge spicules</td> <td>2</td> <td>1</td> </tr> <tr> <td>Mollusk debris</td> <td>1</td> <td>—</td> </tr> </table>		3, 56	3, 100	D		D	Sand	50	12	Silt	10	8	Clay	40	80	Quartz	Tr	—	Clay	5	5	Dolomite	3	—	Foraminifers	47	5	Nannofossils	36	80	Diatoms	1	2	Radiolarians	5	7	Sponge spicules	2	1	Mollusk debris	1	—
	3, 56	3, 100																																																			
D		D																																																			
Sand	50	12																																																			
Silt	10	8																																																			
Clay	40	80																																																			
Quartz	Tr	—																																																			
Clay	5	5																																																			
Dolomite	3	—																																																			
Foraminifers	47	5																																																			
Nannofossils	36	80																																																			
Diatoms	1	2																																																			
Radiolarians	5	7																																																			
Sponge spicules	2	1																																																			
Mollusk debris	1	—																																																			
	N 21				0.5																																																
	CN 11 - CN 12c (NN 13 - NN 15)				1.0																																																
	<i>S. pentas</i>																																																				
	<i>N. jouseae</i>																																																				
					2																																																
					3																																																
					4																																																
					5																																																
					6																																																
					7																																																



TIME-ROCK UNIT	BIOSTRAT. ZONE/ FOSSIL CHARACTER				PALEOMAGNETICS	PHYS. PROPERTIES	CHEMISTRY	SECTION	METERS	GRAPHIC LITHOLOGY	DRILLING DISTURB.	SED. STRUCTURES	SAMPLES	LITHOLOGIC DESCRIPTION																																																
	FORAMINIFERS	NANNOFOSSILS	RADIOLARIANS	DIATOMS																																																										
LOWER PLIOCENE	CN 10c - CN 11 (NN 13 - NN 15)							1	0.5					<p>NANNOFOSSIL FORAMINIFERAL OOZE and FORAMINIFER-BEARING NANNOFOSSIL OOZE</p> <p>Major lithologies: Nannofossil foraminiferal ooze, white (N9, 10YR 8/2). Foraminifer-bearing nannofossil ooze, light gray to greenish gray (5Y 7/1, 5GY 7/1).</p> <p>Minor lithologies: Clay-bearing, foraminifer-bearing nannofossil ooze, light gray (5Y 7/1), and nannofossil ooze, light gray (5Y 7/1).</p> <p>Nine turbidites, 44% of core volume.</p> <p>SMEAR SLIDE SUMMARY (%):</p> <table border="1"> <tr> <td></td> <td>1, 110</td> <td>5, 72</td> </tr> <tr> <td></td> <td>D</td> <td>D</td> </tr> </table> <p>TEXTURE:</p> <table border="1"> <tr> <td>Sand</td> <td>20</td> <td>22</td> </tr> <tr> <td>Clay</td> <td>80</td> <td>78</td> </tr> </table> <p>COMPOSITION:</p> <table border="1"> <tr> <td>Quartz</td> <td>—</td> <td>1</td> </tr> <tr> <td>Feldspar</td> <td>—</td> <td>Tr</td> </tr> <tr> <td>Clay</td> <td>10</td> <td>5</td> </tr> <tr> <td>Volcanic glass</td> <td>—</td> <td>Tr</td> </tr> <tr> <td>Accessory minerals:</td> <td></td> <td></td> </tr> <tr> <td>  Glauconite</td> <td>—</td> <td>Tr</td> </tr> <tr> <td>  Foraminifers</td> <td>15</td> <td>20</td> </tr> <tr> <td>  Nannofossils</td> <td>65</td> <td>72</td> </tr> <tr> <td>  Diatoms</td> <td>1</td> <td>—</td> </tr> <tr> <td>  Radiolarians</td> <td>5</td> <td>1</td> </tr> <tr> <td>  Sponge spicules</td> <td>2</td> <td>1</td> </tr> <tr> <td>  Silicoflagellates</td> <td>2</td> <td>—</td> </tr> </table>		1, 110	5, 72		D	D	Sand	20	22	Clay	80	78	Quartz	—	1	Feldspar	—	Tr	Clay	10	5	Volcanic glass	—	Tr	Accessory minerals:			Glauconite	—	Tr	Foraminifers	15	20	Nannofossils	65	72	Diatoms	1	—	Radiolarians	5	1	Sponge spicules	2	1	Silicoflagellates	2	—
	1, 110	5, 72																																																												
	D	D																																																												
Sand	20	22																																																												
Clay	80	78																																																												
Quartz	—	1																																																												
Feldspar	—	Tr																																																												
Clay	10	5																																																												
Volcanic glass	—	Tr																																																												
Accessory minerals:																																																														
Glauconite	—	Tr																																																												
Foraminifers	15	20																																																												
Nannofossils	65	72																																																												
Diatoms	1	—																																																												
Radiolarians	5	1																																																												
Sponge spicules	2	1																																																												
Silicoflagellates	2	—																																																												
FP	N 18 - N 19						2	1.0																																																						
AP	CN 10a+b (NN 12)						3																																																							
CG	<i>Stichocorys peregrina</i>						4																																																							
RP	<i>T. convexa</i>						5																																																							
							6																																																							
							7																																																							



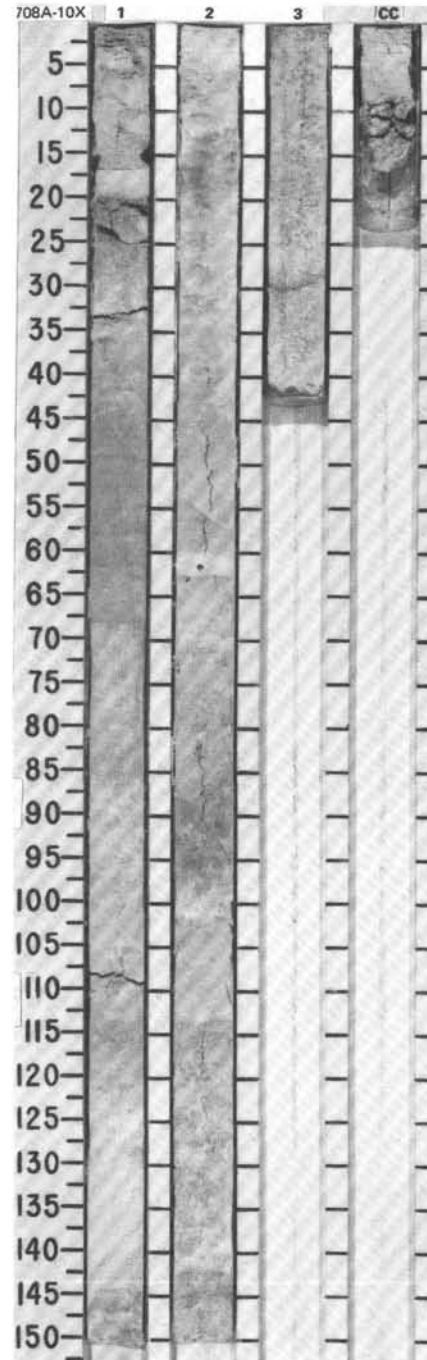


SITE 708 HOLE A CORE 10X CORED INTERVAL 4178.6-4188.2 mbsl; 82.1-91.7 mbsf

TIME-ROCK UNIT	BIOSTRAT. ZONE/ FOSSIL CHARACTER				PALEOMAGNETICS	PHYS. PROPERTIES	CHEMISTRY	SECTION	METERS	GRAPHIC LITHOLOGY	DRILLING DISTURB. SED. STRUCTURES	SAMPLES	LITHOLOGIC DESCRIPTION																																																																								
	FORAMINIFERS	NANNOFOSSILS	RADIOLARIANS	DIATOMS																																																																																	
UPPER MIOCENE	RP	AM	CG	CM					1				<p>NANNOFOSSIL OOZE and FORAMINIFER-BEARING NANNOFOSSIL OOZE</p> <p>Major lithologies: Nannofossil ooze, light gray to greenish gray (5Y 7/1, 5GY 7/1). Foraminifer-bearing nannofossil ooze, white (N9) and gray to light gray (N6, N7).</p> <p>Nine turbidites, 21% of core volume.</p> <p>SMEAR SLIDE SUMMARY (%):</p> <table border="1"> <tr> <td></td> <td>1, 46</td> <td>1, 143</td> <td>3, 20</td> </tr> <tr> <td>D</td> <td></td> <td></td> <td></td> </tr> </table> <p>TEXTURE:</p> <table border="1"> <tr> <td>Sand</td> <td>35</td> <td>12</td> <td>5</td> </tr> <tr> <td>Clay</td> <td>65</td> <td>88</td> <td>95</td> </tr> </table> <p>COMPOSITION:</p> <table border="1"> <tr> <td>Quartz</td> <td>Tr</td> <td>Tr</td> <td>Tr</td> </tr> <tr> <td>Mica</td> <td>—</td> <td>—</td> <td>Tr</td> </tr> <tr> <td>Volcanic glass</td> <td>Tr</td> <td>—</td> <td>Tr</td> </tr> <tr> <td>Dolomite</td> <td>—</td> <td>Tr</td> <td>—</td> </tr> <tr> <td>Accessory minerals:</td> <td></td> <td></td> <td></td> </tr> <tr> <td>  Zeolite(?)</td> <td>—</td> <td>Tr</td> <td>—</td> </tr> <tr> <td>Foraminifers</td> <td>35</td> <td>10</td> <td>—</td> </tr> <tr> <td>Nannofossils</td> <td>45</td> <td>88</td> <td>96</td> </tr> <tr> <td>Diatoms</td> <td>—</td> <td>Tr</td> <td>1</td> </tr> <tr> <td>Radiolarians</td> <td>—</td> <td>Tr</td> <td>2</td> </tr> <tr> <td>Sponge spicules</td> <td>Tr</td> <td>Tr</td> <td>1</td> </tr> <tr> <td>Silicoflagellates</td> <td>—</td> <td>Tr</td> <td>Tr</td> </tr> <tr> <td>Micrite</td> <td>20</td> <td>—</td> <td>—</td> </tr> <tr> <td></td> <td>—</td> <td>2</td> <td>—</td> </tr> </table>		1, 46	1, 143	3, 20	D				Sand	35	12	5	Clay	65	88	95	Quartz	Tr	Tr	Tr	Mica	—	—	Tr	Volcanic glass	Tr	—	Tr	Dolomite	—	Tr	—	Accessory minerals:				Zeolite(?)	—	Tr	—	Foraminifers	35	10	—	Nannofossils	45	88	96	Diatoms	—	Tr	1	Radiolarians	—	Tr	2	Sponge spicules	Tr	Tr	1	Silicoflagellates	—	Tr	Tr	Micrite	20	—	—		—	2	—
	1, 46	1, 143	3, 20																																																																																		
D																																																																																					
Sand	35	12	5																																																																																		
Clay	65	88	95																																																																																		
Quartz	Tr	Tr	Tr																																																																																		
Mica	—	—	Tr																																																																																		
Volcanic glass	Tr	—	Tr																																																																																		
Dolomite	—	Tr	—																																																																																		
Accessory minerals:																																																																																					
Zeolite(?)	—	Tr	—																																																																																		
Foraminifers	35	10	—																																																																																		
Nannofossils	45	88	96																																																																																		
Diatoms	—	Tr	1																																																																																		
Radiolarians	—	Tr	2																																																																																		
Sponge spicules	Tr	Tr	1																																																																																		
Silicoflagellates	—	Tr	Tr																																																																																		
Micrite	20	—	—																																																																																		
	—	2	—																																																																																		
								2																																																																													
								3																																																																													
								CC																																																																													

SITE 708 HOLE A CORE 11X CORED INTERVAL 4188.2-4197.9 mbsl; 91.7-101.4 mbsf

TIME-ROCK UNIT	BIOSTRAT. ZONE/ FOSSIL CHARACTER				PALEOMAGNETICS	PHYS. PROPERTIES	CHEMISTRY	SECTION	METERS	GRAPHIC LITHOLOGY	DRILLING DISTURB. SED. STRUCTURES	SAMPLES	LITHOLOGIC DESCRIPTION
	FORAMINIFERS	NANNOFOSSILS	RADIOLARIANS	DIATOMS									
UPPER MIOCENE	RP	AM	FM	RP									<p>FORAMINIFER-BEARING NANNOFOSSIL OOZE</p> <p>Major lithologies: Trace recovery of light gray (N7) foraminifer-bearing nannofossil ooze in CC. Foraminifer-bearing Nannofossil ooze.</p> <p>Coccolith date, from small sample in CC.</p>

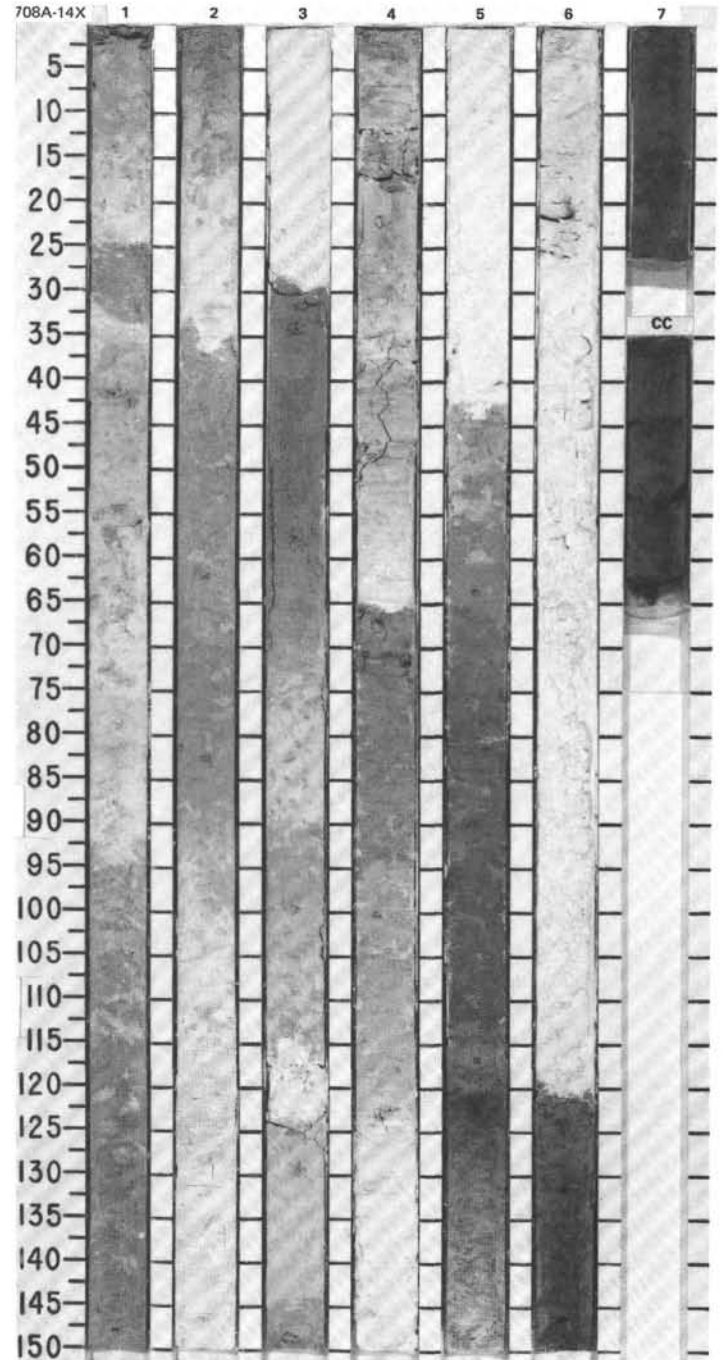






SITE 708 HOLE A CORE 14X CORED INTERVAL 4217.1-4226.8 mbsl; 120.6-130.3 mbsf

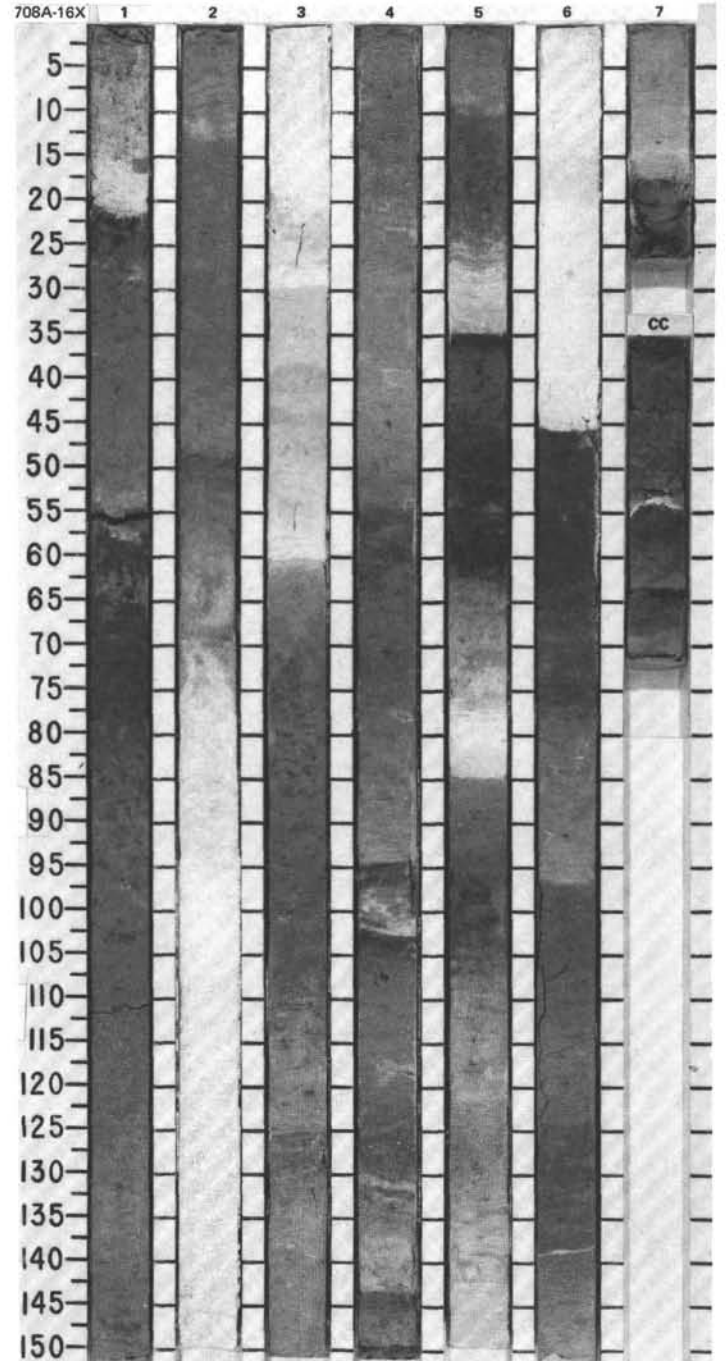
TIME-ROCK UNIT	BIOSTRAT. ZONE/ FOSSIL CHARACTER				PALEOMAGNETICS	PHYS. PROPERTIES	CHEMISTRY	SECTION METERS	GRAPHIC LITHOLOGY	DRILLING DISTURB.	SED. STRUCTURES	SAMPLES	LITHOLOGIC DESCRIPTION																																								
	FORAMINIFERS	NANNOFOSSILS	RADIOLARIANS	DIATOMS																																																	
UPPER MIOCENE	AM	CN 7b (NN 9)	AM	CN 7b (NN 9)				0.5 1.0					<p>CLAY-BEARING, FORAMINIFER-BEARING NANNOFOSSIL OOZE and FORAMINIFER-NANNOFOSSIL OOZE</p> <p>Major lithologies: Clay-bearing, foraminifer-bearing nannofossil ooze, pale brown (10YR 6/3), light yellowish brown (10YR 6/4), or brown (10YR 5/3). Foraminifer-nannofossil ooze, turbidite, white (10YR 8/2).</p> <p>The turbidites are recognized on the basis of lighter color. The pelagic sediments grade to darker brown toward top. The basal turbidite boundaries are sharp.</p> <p>Ten turbidites, 35% of core volume.</p> <p>SMEAR SLIDE SUMMARY (%):</p> <table border="1"> <tr> <td></td> <td>2, 62</td> <td>3, 55</td> <td>6, 17</td> </tr> <tr> <td>D</td> <td></td> <td>D</td> <td>D</td> </tr> </table> <p>TEXTURE:</p> <table border="1"> <tr> <td>Sand</td> <td>10</td> <td>—</td> <td>30</td> </tr> <tr> <td>Silt</td> <td>40</td> <td>5</td> <td>10</td> </tr> <tr> <td>Clay</td> <td>50</td> <td>95</td> <td>60</td> </tr> </table> <p>COMPOSITION:</p> <table border="1"> <tr> <td>Clay</td> <td>10</td> <td>95</td> <td>—</td> </tr> <tr> <td>Foraminifers</td> <td>10</td> <td>—</td> <td>35</td> </tr> <tr> <td>Nannofossils</td> <td>74</td> <td>Tr</td> <td>65</td> </tr> <tr> <td>Radiolarians</td> <td>5</td> <td>3</td> <td>2</td> </tr> <tr> <td>Sponge spicules</td> <td>1</td> <td>2</td> <td>1</td> </tr> </table>		2, 62	3, 55	6, 17	D		D	D	Sand	10	—	30	Silt	40	5	10	Clay	50	95	60	Clay	10	95	—	Foraminifers	10	—	35	Nannofossils	74	Tr	65	Radiolarians	5	3	2	Sponge spicules	1	2	1
		2, 62	3, 55	6, 17																																																	
D		D	D																																																		
Sand	10	—	30																																																		
Silt	40	5	10																																																		
Clay	50	95	60																																																		
Clay	10	95	—																																																		
Foraminifers	10	—	35																																																		
Nannofossils	74	Tr	65																																																		
Radiolarians	5	3	2																																																		
Sponge spicules	1	2	1																																																		
RP	Barren		AM	CN 7a																																																	
MIDDLE MIOCENE	RP	Barren	AM	CN 6 (NN 8)									<p>CC</p>																																								
	RP	Barren																																																			





SITE 708 HOLE A CORE 16X CORED INTERVAL 4236.5-4246.1 mbsl; 140.0-149.6 mbsf

TIME-ROCK UNIT	BIOSTRAT. ZONE/ FOSSIL CHARACTER				PALEOMAGNETICS	PHYS. PROPERTIES	CHEMISTRY	SECTION	METERS	GRAPHIC LITHOLOGY	DRILLING DISTURB.	SED. STRUCTURES	SAMPLES	LITHOLOGIC DESCRIPTION																																																																											
	FORAMINIFERS	NANNOFOSSILS	RADIOLARIANS	DIATOMS																																																																																					
MIDDLE MIOCENE	CN 4 (NN 5)							1	0.5					<p><b>NANNOFOSSIL OOZE</b></p> <p>Major lithology: Nannofossil ooze, light gray (10YR 7/2) and light yellowish brown (10YR 6/4) to pale yellow (2.5Y 7/4), with dark greenish brown (10YR 4/2) mottled clay.</p> <p>Minor lithology: Light gray foraminifer-nannofossil ooze (10YR 7/2), Section 7, 0-15 cm, turbidite.</p> <p>Ten white (10YR 8/2) turbidites, 20% of total core volume.</p> <p><b>SMEAR SLIDE SUMMARY (%)</b></p> <table border="1"> <thead> <tr> <th></th> <th>1, 74</th> <th>2, 34</th> <th>3, 33</th> <th>7, 13</th> </tr> <tr> <th></th> <th>M</th> <th>D</th> <th>D</th> <th>D</th> </tr> </thead> <tbody> <tr> <td>Sand</td> <td>5</td> <td>—</td> <td>1</td> <td>25</td> </tr> <tr> <td>Silt</td> <td>20</td> <td>1</td> <td>—</td> <td>25</td> </tr> <tr> <td>Clay</td> <td>75</td> <td>99</td> <td>99</td> <td>50</td> </tr> </tbody> </table> <p><b>TEXTURE:</b></p> <table border="1"> <tbody> <tr> <td>Sand</td> <td>5</td> <td>—</td> <td>1</td> <td>25</td> </tr> <tr> <td>Silt</td> <td>20</td> <td>1</td> <td>—</td> <td>25</td> </tr> <tr> <td>Clay</td> <td>75</td> <td>99</td> <td>99</td> <td>50</td> </tr> </tbody> </table> <p><b>COMPOSITION:</b></p> <table border="1"> <tbody> <tr> <td>Quartz</td> <td>Tr</td> <td>—</td> <td>—</td> <td>—</td> </tr> <tr> <td>Rock fragments</td> <td>5</td> <td>1</td> <td>Tr</td> <td>—</td> </tr> <tr> <td>Clay</td> <td>92</td> <td>—</td> <td>—</td> <td>—</td> </tr> <tr> <td>Volcanic glass</td> <td>—</td> <td>Tr</td> <td>—</td> <td>Tr</td> </tr> <tr> <td>Foraminifers</td> <td>—</td> <td>—</td> <td>1</td> <td>30</td> </tr> <tr> <td>Nannofossils</td> <td>3</td> <td>99</td> <td>99</td> <td>70</td> </tr> <tr> <td>Sponge spicules</td> <td>Tr</td> <td>—</td> <td>—</td> <td>—</td> </tr> </tbody> </table>		1, 74	2, 34	3, 33	7, 13		M	D	D	D	Sand	5	—	1	25	Silt	20	1	—	25	Clay	75	99	99	50	Sand	5	—	1	25	Silt	20	1	—	25	Clay	75	99	99	50	Quartz	Tr	—	—	—	Rock fragments	5	1	Tr	—	Clay	92	—	—	—	Volcanic glass	—	Tr	—	Tr	Foraminifers	—	—	1	30	Nannofossils	3	99	99	70	Sponge spicules	Tr	—	—	—
	1, 74	2, 34	3, 33	7, 13																																																																																					
	M	D	D	D																																																																																					
Sand	5	—	1	25																																																																																					
Silt	20	1	—	25																																																																																					
Clay	75	99	99	50																																																																																					
Sand	5	—	1	25																																																																																					
Silt	20	1	—	25																																																																																					
Clay	75	99	99	50																																																																																					
Quartz	Tr	—	—	—																																																																																					
Rock fragments	5	1	Tr	—																																																																																					
Clay	92	—	—	—																																																																																					
Volcanic glass	—	Tr	—	Tr																																																																																					
Foraminifers	—	—	1	30																																																																																					
Nannofossils	3	99	99	70																																																																																					
Sponge spicules	Tr	—	—	—																																																																																					
							2	1.0																																																																																	
							3																																																																																		
							4																																																																																		
							5																																																																																		
							6																																																																																		
LOWER MIOCENE	CN 3 (NN 4)						7																																																																																		
							CC																																																																																		



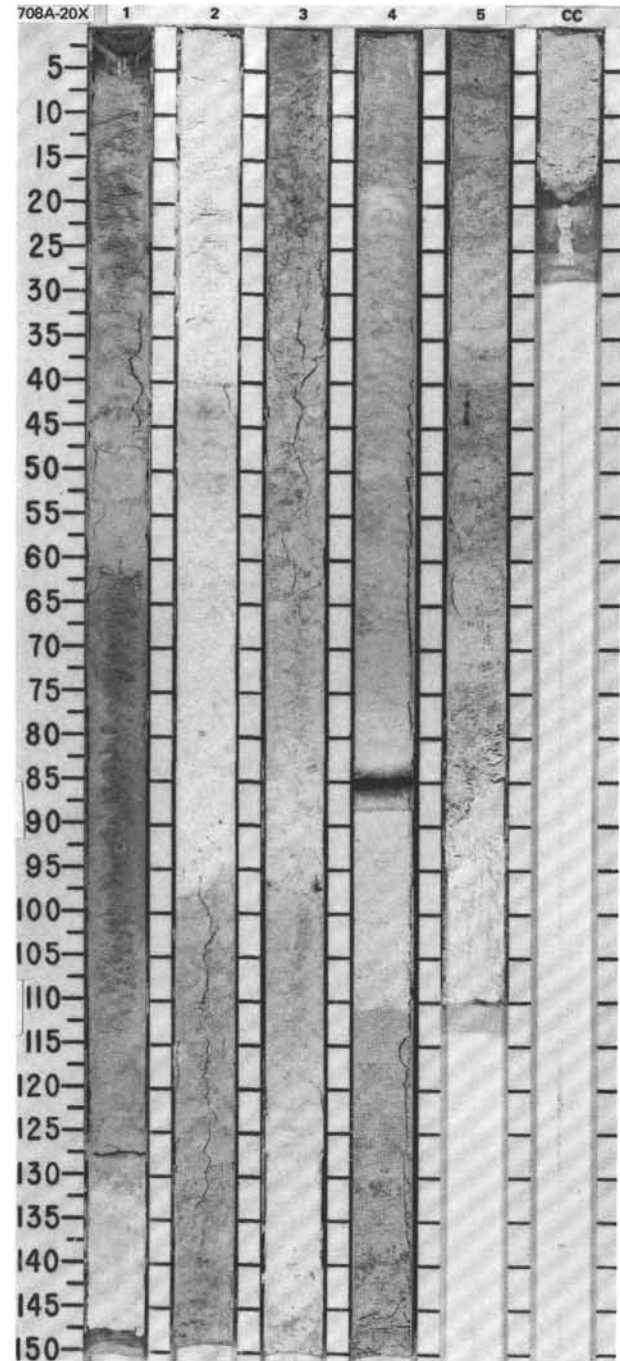






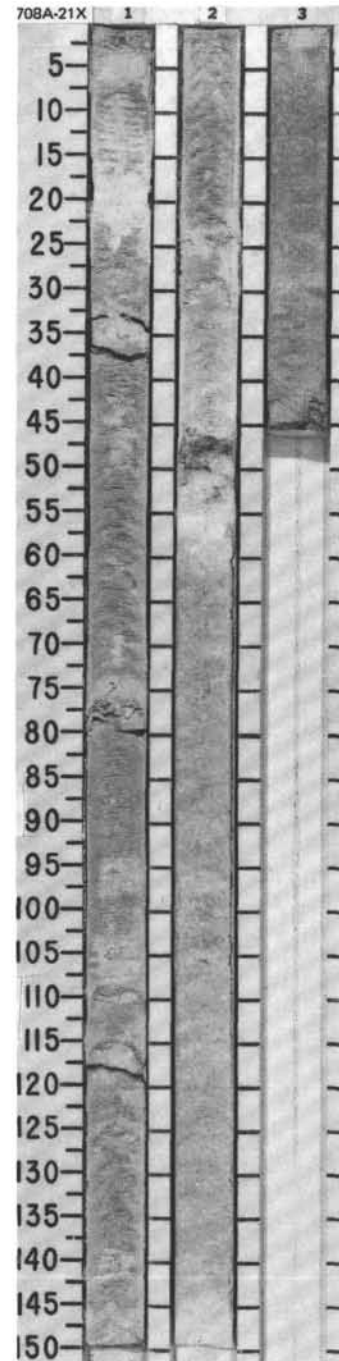
SITE 708 HOLE A CORE 20X CORED INTERVAL 4274.7-4284.4 mbsl; 178.2-187.9 mbsf

TIME-ROCK UNIT	BIOSTRAT. ZONE/ FOSSIL CHARACTER				PALEOMAGNETICS	PHYS. PROPERTIES	CHEMISTRY	SECTION	METERS	GRAPHIC LITHOLOGY	DRILLING DISTURB.	SED. STRUCTURES	SAMPLES	LITHOLOGIC DESCRIPTION																																																								
	FORAMINIFERS	NANNOFOSSILS	RADIOLARIANS	DIATOMS																																																																		
LOWER MIOCENE	(1	NN)	1	CN				1	0.5		...	*		<p>NANNOFOSSIL OOZE</p> <p>Major lithology: Nannofossil ooze, very pale brown (10YR 8/3) and white (10YR 8/2).</p> <p>Minor lithology: Foraminifer-nannofossil ooze, very pale brown (10YR 8/3) and white (10YR 8/2).</p> <p>Ten turbidites, 28% of core volume.</p> <p>SMEAR SLIDE SUMMARY (%):</p> <table border="1"> <tr> <td></td> <td>1, 80</td> <td>2, 95</td> <td>4, 83</td> </tr> <tr> <td></td> <td>D</td> <td>M</td> <td>D</td> </tr> </table> <p>TEXTURE:</p> <table border="1"> <tr> <td>Sand</td> <td>10</td> <td>40</td> <td>60</td> </tr> <tr> <td>Silt</td> <td>—</td> <td>5</td> <td>10</td> </tr> <tr> <td>Clay</td> <td>90</td> <td>55</td> <td>30</td> </tr> </table> <p>COMPOSITION:</p> <table border="1"> <tr> <td>Quartz</td> <td>Tr</td> <td>1</td> <td>—</td> </tr> <tr> <td>Clay</td> <td>5</td> <td>5</td> <td>8</td> </tr> <tr> <td>Volcanic glass</td> <td>—</td> <td>—</td> <td>54</td> </tr> <tr> <td>Dolomite</td> <td>—</td> <td>Tr</td> <td>—</td> </tr> <tr> <td>Foraminifers</td> <td>8</td> <td>40</td> <td>5</td> </tr> <tr> <td>Nannofossils</td> <td>86</td> <td>50</td> <td>25</td> </tr> <tr> <td>Diatoms</td> <td>Tr</td> <td>—</td> <td>—</td> </tr> <tr> <td>Radiolarians</td> <td>1</td> <td>3</td> <td>5</td> </tr> <tr> <td>Sponge spicules</td> <td>Tr</td> <td>1</td> <td>3</td> </tr> </table>		1, 80	2, 95	4, 83		D	M	D	Sand	10	40	60	Silt	—	5	10	Clay	90	55	30	Quartz	Tr	1	—	Clay	5	5	8	Volcanic glass	—	—	54	Dolomite	—	Tr	—	Foraminifers	8	40	5	Nannofossils	86	50	25	Diatoms	Tr	—	—	Radiolarians	1	3	5	Sponge spicules	Tr	1	3
	1, 80	2, 95	4, 83																																																																			
	D	M	D																																																																			
Sand	10	40	60																																																																			
Silt	—	5	10																																																																			
Clay	90	55	30																																																																			
Quartz	Tr	1	—																																																																			
Clay	5	5	8																																																																			
Volcanic glass	—	—	54																																																																			
Dolomite	—	Tr	—																																																																			
Foraminifers	8	40	5																																																																			
Nannofossils	86	50	25																																																																			
Diatoms	Tr	—	—																																																																			
Radiolarians	1	3	5																																																																			
Sponge spicules	Tr	1	3																																																																			
UPPER OLILOCENE	RP							2	1.0		...	*																																																										
UPPER OLILOCENE	AM	CP 19b (NP 25)						3			...	*																																																										
	FP	<i>D. atouchus</i>						4			...	*																																																										
		Barren						5			...	*																																																										
								CC			...	*																																																										



SITE 708 HOLE A CORE 21X CORED INTERVAL 4284.4-4294.0 mbsf; 187.9-197.5 mbsf

TIME-ROCK UNIT	BIOSTRAT. ZONE/ FOSSIL CHARACTER				PALEOMAGNETICS	PHYS. PROPERTIES	CHEMISTRY	SECTION	METERS	GRAPHIC LITHOLOGY	DRILLING DISTURB.	SED. STRUCTURES	SAMPLES	LITHOLOGIC DESCRIPTION																																				
	FORAMINIFERS	NANNOFOSSILS	RADIOLARIANS	DIATOMS																																														
UPPER OLIGOCENE																																																		
RP P22	AM	CP 19b (NP 25)	FP	<i>Doreadapsyris atuechus</i>				1	0.5 1.0				*	<p><b>NANNOFOSSIL OOZE and NANNOFOSSIL CHALK</b></p> <p>Major lithology: Nannofossil ooze, white (10YR 8/2). Nannofossil chalk occurs in lumps, e.g., Section 1, 75-80, 110-112, and 115-120 cm.</p> <p>Minor lithology: Foraminifer-bearing nannofossil chalk, white (10YR 5/3), Section 1, 15-20 cm; and altered ash(?), brown (10YR 5/3), Section 2, 45-50 cm.</p> <p><b>SMEAR SLIDE SUMMARY (%):</b></p> <table border="1"> <tr> <td></td> <td>1, 20</td> <td>1, 60</td> </tr> <tr> <td></td> <td>M</td> <td>D</td> </tr> </table> <p><b>TEXTURE:</b></p> <table border="1"> <tr> <td>Sand</td> <td>10</td> <td>7</td> </tr> <tr> <td>Silt</td> <td>10</td> <td>3</td> </tr> <tr> <td>Clay</td> <td>80</td> <td>90</td> </tr> </table> <p><b>COMPOSITION:</b></p> <table border="1"> <tr> <td>Clay</td> <td>5</td> <td>5</td> </tr> <tr> <td>Foraminifers</td> <td>12</td> <td>5</td> </tr> <tr> <td>Nannofossils</td> <td>74</td> <td>85</td> </tr> <tr> <td>Diatoms</td> <td>1</td> <td>—</td> </tr> <tr> <td>Radiolarians</td> <td>5</td> <td>3</td> </tr> <tr> <td>Sponge spicules</td> <td>3</td> <td>2</td> </tr> <tr> <td>Silicoflagellates</td> <td>—</td> <td>Tr</td> </tr> </table>		1, 20	1, 60		M	D	Sand	10	7	Silt	10	3	Clay	80	90	Clay	5	5	Foraminifers	12	5	Nannofossils	74	85	Diatoms	1	—	Radiolarians	5	3	Sponge spicules	3	2	Silicoflagellates	—	Tr
	1, 20	1, 60																																																
	M	D																																																
Sand	10	7																																																
Silt	10	3																																																
Clay	80	90																																																
Clay	5	5																																																
Foraminifers	12	5																																																
Nannofossils	74	85																																																
Diatoms	1	—																																																
Radiolarians	5	3																																																
Sponge spicules	3	2																																																
Silicoflagellates	—	Tr																																																
							2																																											
							3																																											





TIME-ROCK UNIT		BIOSTRAT. ZONE/ FOSSIL CHARACTER	PALEOMAGNETICS	PHYS. PROPERTIES	CHEMISTRY	SECTION METERS	GRAPHIC LITHOLOGY	DRILLING DISTURB.	SED. STRUCTURES	SAMPLES	LITHOLOGIC DESCRIPTION																																							
FORAMINIFERS	NANNOFOSSILS																																																	
UPPER OLIGOCENE											<p>* NANNOFOSSIL OOZE and FORAMINIFER-NANNOFOSSIL OOZE</p> <p>Major lithologies: Nannofossil ooze, very pale brown (10YR 8/3). Foraminifer-nannofossil ooze, white (10YR 9/2), occurs in turbidites.</p> <p>Minor lithologies: Foraminiferal ooze, white (10YR 9/2), occurs in turbidites; and volcanic glass, fresh, gray (N6), Section 4, 130-138 cm.</p> <p>Three turbidites, one of which is 280 cm thick between Sections 1, 120-150 cm, and Section 3, 0-100 cm. The total volume of turbidites is 48%.</p> <p>SMEAR SLIDE SUMMARY (%):</p> <table border="1"> <tr> <td></td> <td>1, 20</td> <td>4, 135</td> </tr> <tr> <td></td> <td>D</td> <td>M</td> </tr> </table> <p>TEXTURE:</p> <table border="1"> <tr> <td>Sand</td> <td>5</td> <td>60</td> </tr> <tr> <td>Silt</td> <td>5</td> <td>10</td> </tr> <tr> <td>Clay</td> <td>90</td> <td>30</td> </tr> </table> <p>COMPOSITION:</p> <table border="1"> <tr> <td>Quartz</td> <td>Tr</td> <td>—</td> </tr> <tr> <td>Clay</td> <td>5</td> <td>8</td> </tr> <tr> <td>Volcanic glass</td> <td>—</td> <td>60</td> </tr> <tr> <td>Foraminifers</td> <td>5</td> <td>5</td> </tr> <tr> <td>Nannofossils</td> <td>86</td> <td>20</td> </tr> <tr> <td>Radiolarians</td> <td>2</td> <td>5</td> </tr> <tr> <td>Sponge spicules</td> <td>2</td> <td>2</td> </tr> <tr> <td>Silicoflagellates</td> <td>—</td> <td>Tr</td> </tr> </table>		1, 20	4, 135		D	M	Sand	5	60	Silt	5	10	Clay	90	30	Quartz	Tr	—	Clay	5	8	Volcanic glass	—	60	Foraminifers	5	5	Nannofossils	86	20	Radiolarians	2	5	Sponge spicules	2	2	Silicoflagellates	—	Tr
	1, 20	4, 135																																																
	D	M																																																
Sand	5	60																																																
Silt	5	10																																																
Clay	90	30																																																
Quartz	Tr	—																																																
Clay	5	8																																																
Volcanic glass	—	60																																																
Foraminifers	5	5																																																
Nannofossils	86	20																																																
Radiolarians	2	5																																																
Sponge spicules	2	2																																																
Silicoflagellates	—	Tr																																																
CP P20	P 21	CP 19a (NP 24)				1																																												
AG		<i>Dorcadospyrus atleuchus</i>				2																																												
FP		Barten				3																																												
						4																																												
						5																																												
						6																																												

